Marine and Petroleum Geology 177 (2025) 107385

Contents lists available at ScienceDirect

Marine and Petroleum Geology

journal homepage: www.elsevier.com/locate/marpetgeo

Campanian-Maastrichtian evolution of sedimentary systems during the final stages of an epeiric sea —La Luna Sea— in eastern Colombia: Processes, spatio-temporal variability, and depositional controls

Carlos A. Giraldo-Villegas [a,b,*], Francisco J. Rodríguez-Tovar [a], Sergio A. Celis [a,b], Andrés Pardo-Trujillo [b,c]

[a] Departamento de Estratigrafía y Paleontología, Universidad de Granada, Av. Fuente Nueva s/n, 18071, Granada, Spain
[b] Instituto de Investigaciones en Estratigrafía-IIES, Grupo de Investigación en Estratigrafía y Vulcanología (GIEV) Cumanday, Universidad de Caldas, Calle 65 No 26-10, 170004, Manizales, Colombia
[c] Departamento de Ciencias Geológicas, Universidad de Caldas, Calle 65 No 26-10, 170004, Manizales, Colombia

ARTICLE INFO

Keywords:
La Luna Sea
Cretaceous
Sedimentary parameters
Depositional settings
Macrobenthic communities
Allogenic and autogenic controls
South America

ABSTRACT

Epeiric seas were widespread during the Cretaceous, associated with global sea-level rise. Their stratigraphic record, controlled mainly by eustasy, tectonic and climatic factors, resulted in the accumulation of important hydrocarbon source and reservoir rocks. In the NW of South America-Colombia, an epeiric sea established in the Early Cretaceous—knows as La Luna Sea in the Late Cretaceous—, bounded by a volcanic arc to the western side and by the Amazonian Craton to the east, was progressively filled during the Campanian-Maastrichtian, being these latest Cretaceous deposits important hydrocarbon reservoirs for conventional petroleum systems. In the Campanian-early Maastrichtian period the western side and the central part of the basin had a normal shoreface profile, dominated by pelagic and wave sedimentation processes, while a delta profile dominated by fluvial processes characterized the eastern side. During the late Maastrichtian, directly related to the accretion of western Caribbean terranes, transitional and continental environments dominated by fluvial processes were established on both sides of the basin, suggesting changes in geomorphological-topographic and drainage system characteristics of the emerged areas, leading to the filling of the epeiric basin. The distribution of the deposits was controlled by allogenic processes: tectonism associated with the growth of the proto-Central Cordillera, the global eustatic level, and in minor degree by autogenic processes such as channel avulsion, bottom and longshore currents, and high productivity events. These processes and their variable temporal and spatial influence were responsible for the different types of deposits on either side of the basin, which had a direct impact on the establishment of macrobenthic communities, also providing new exploration ideas related to the reservoirs.

Comparisons suggest that the size of the receiving and emerged zones plays an important role in the distribution and arrangement of deposits along and across the basin, related to the nature of the internal processes involved in sediment redistribution.

1. Introduction

An epeiric sea develops when cratons are flooded during sea-level rise (Johnson and Baldwin, 1996; Pratt and Holmden, 2008). This type of sea has been widely documented in the geologic past, showing great variability due to the diversity of processes and factors involved in its origin, evolution and filling —e.g., tectonic setting, connection to adjacent oceans, sediment composition, water-column fluctuations, hydrological configuration, climatic and oceanographic variables— (Erlich et al., 2003; Schwarz et al., 2022; Ferreira et al., 2025). In these shallow seas, important factors and/or processes to estimate are how the siliciclastic material arrived and was distributed in the basin (e.g., Orton and Reading, 1993; Nittrouer and Wright, 1994; Wright and Nittrouer, 1995; Walsh and Nittrouer, 2009; Schwarz et al., 2022). Arrival depends on external basin factors that include the distribution, extent and topography of emerged areas, erosion rate, transport mechanism, and sediment paths. Distribution is controlled by internal basin factors, including waves, storms, tides, bottom and longshore currents,

* Corresponding author. Departamento de Estratigrafía y Paleontología, Universidad de Granada, Av. Fuente Nueva s/n, 18071, Granada, Spain.
E-mail address: carlosgiraldo@correo.ugr.es (C.A. Giraldo-Villegas).

https://doi.org/10.1016/j.marpetgeo.2025.107385
Received 16 July 2024; Received in revised form 12 March 2025; Accepted 13 March 2025
Available online 19 March 2025

hypopycnal river plumes, paleobathymetric barriers and submarine gravity flows (Johnson and Baldwin, 1996; Erlich et al., 2000; Schieber, 2016). These processes and factors behind sediment arrival and its subsequent distribution in the epeiric basin affect parameters such as salinity, productivity, oxygenation and food supply, hence determining the existence, evolution, and distribution of macrobenthic communities in the depositional setting. The combination of external and internal factors, as well as physical and biological parameters, would therefore condition the origin, development, and subsequent evolution of elements of the petroleum system in hydrocarbon-producing basins.

The Cretaceous was a highly dynamic period in which diverse geologic and biologic processes occurred: important eustatic changes generating epicontinental seas, the formation of large igneous provinces (LIPs), the occurrence of Oceanic Anoxic Events (OAEs), a geographic expansion of carbonate platforms, collision of terrains, global warming and cooling, and mass extinctions (Scotese et al., 2024 and references therein). Although the imprint of all these events is recorded in the sedimentary deposits, their detection and differentiation is not an easy task and requires very detailed work that integrates different analytical tools.

In the northwestern margin of South America, especially in Colombia and Ecuador, the Cretaceous was characterized by a simultaneous occurrence of several of the aforementioned complex geologic processes (e.g., accretion of oceanic terranes, vulcanism, magmatism, eustatic sea-level fluctuations, rifting, OAEs), making it challenging to understand the geologic evolution of this region (Villamil, 1998; Villamil et al., 1999; Pindell and Kennan, 2009; Zapata et al., 2019; Paez-Reyes et al., 2021; Zapata-Villada et al., 2021). The rocks that preserve the record of these processes currently crop out in the western and eastern domains of Colombia, separated by the Romeral Fault System (RFS) acting as the tectonic boundary between these domains (Moreno-Sánchez and Pardo-Trujillo, 2002; Vinasco, 2019; Restrepo and Toussaint, 2020; Toussaint and Restrepo, 2020, Fig. 1). The co-existence during the Late Cretaceous of contractional processes in the western allochthonous margin related to the Caribbean Plate evolution, and extensional processes in the eastern autochthonous margin related to the South American Plate, were the dominant tectonic processes that controlled sedimentary dynamics and basin evolution of this region (Bayona, 2018; Sarmiento-Rojas, 2019; Pardo-Trujillo et al., 2020; Botero-Garcia et al., 2023; León et al., 2023). The western domain exhibits a discontinuous Cretaceous sedimentary record, with mainly Santonian-Maastrichtian deposits accumulated in deep marine environments associated with the proto-Pacific Ocean (Pardo-Trujillo et al., 2020; Giraldo-Villegas et al., 2023 and references therein), while the eastern domain has a record of shallow marine deposits associated with the development of an epeiric sea connected to the proto-Atlantic Ocean during most of the Cretaceous, and finally filled during the Campanian-Maastrichtian (Villamil et al., 1999; Erlich et al., 2000, 2003; Sarmiento-Rojas et al., 2006; Bayona, 2018; Sarmiento-Rojas, 2019; Bayona et al., 2021; Paez-Reyes et al., 2021).

The sedimentary basins associated with the eastern domain have been extensively studied due to their hydrocarbon potential, as they host significant global oil source rocks, commonly known as the La Luna Fm, now Salada, Pujamana, Galembo and La Renta formations (Terraza, 2019; Pastor-Chacón et al., 2023; De la Parra et al., 2024) and the Campanian-Maastrichtian reservoirs that are the focus of this work. The fine-grained source rocks were deposited during the Cenomanian-Campanian in an epeiric sea called the La Luna Sea (Erlich et al., 2000; Paez-Reyes et al., 2021), dominated by oxygen-deficient and highly productive environments that allowed the accumulation of large amounts of organic carbon (Villamil et al., 1999; Erlich et al., 2003; Terraza, 2019). Posteriorly, during the Campanian-Maastrichtian the uplift of the proto-Central Cordillera driven by the collision of the Caribbean Plate with the NW margin of South America, led to the deposition of coarse-grained deposits (Guadalupe Group, La Tabla Fm, Cimarrona Fm; Guerrero, 2002; Gómez et al., 2003, 2005; Sarmiento-Rojas, 2019; Giraldo-Villegas et al., 2024), which constitute important producing reservoirs in the basin (e.g., Guando, Guaduas, Colon, Cusiana oil fields). Since the Campanian-Maastrichtian deposits were also accumulated under marine influence and mark the final stages of the epeiric sea before it became a continental basin, we use the term La Luna Sea to refer to the epeiric basin developed in the northwestern of South America from the Cenomanian to the Maastrichtian.

Despite extensive research on the Cretaceous sedimentary basins of the eastern domain in Colombia, significant gaps remain in understanding of the depositional processes (physical and ecological) and spatio-temporal variability of sedimentary environments associated with the depositional controls (autogenic and allogenic) that governed the final stages of the La Luna Sea. Previous studies have primarily focused on broader stratigraphic, paleontologic and tectono-structural aspects, often emphasizing the Cenozoic, rather than Mesozoic deposits (e.g., Bayona et al., 2006, 2008, 2013, 2021; Parra et al., 2010; Mora et al., 2013, 2015a, 2015b; Bayona, 2018; Caballero et al., 2020), and recently, important works have focused on the study of the change from calcareous to siliciclastic sedimentation that occurred during the Late Campanian (Patarroyo et al., 2017; Bayona, 2018; Etayo-Serna, 2019; Patarroyo et al., 2022).

Our research, therefore, provides a detailed process-based sedimentologic and ichnologic analysis of the Campanian-Maastrichtian deposits. By integrating depositional environments and their spatio-temporal variability, this study provides for a comprehensive understanding of the physical and ecological processes involved in the sediment accumulation, controlling factors and the regional distribution of hydrocarbon reservoirs. This contribution is essential for refining regional geological models and enhancing our knowledge of the sedimentary dynamics in this region, thus offering valuable insights for future explorations and study of similar epeiric systems.

This work aims to understand the evolution of sedimentary systems during the final stages of the central part of the Late Cretaceous La Luna epeiric sea in Colombia, specifically seeking to elucidate the processes and factors that controlled the spatial and stratigraphic distribution of deposits and influenced the evolution of the macrobenthic fauna on the seafloor. Through sedimentologic, ichnologic, and paleogeographic evidence, this research furthermore provides a comprehensive understanding of the regional stratigraphic architecture and sedimentary dynamics, offering valuable insights into basin evolution, reservoir potential, and paleoenvironmental conditions in hydrocarbon-producing epeiric basins.

2. Geologic setting and stratigraphic framework

The Cretaceous geologic evolution of the NW corner of South America was controlled by the interaction among the Caribbean, Nazca-Farallon, and South American plates (Pindell and Kennan, 2009; Montes et al., 2019; Mora-Páez et al., 2019; González et al., 2023). This interplay during the Cretaceous divided the region into two distinct geologic domains separated by the RFS —a western allochthonous domain and an eastern autochthonous domain (Moreno-Sánchez and Pardo-Trujillo, 2003; Vinasco, 2019; Toussaint and Restrepo, 2020). This plate interaction has likewise controlled the development of orogens and sedimentary basins from Mesozoic to recent times (Fig. 1). Several sedimentary basins linked to this interaction developed in the eastern domain of Colombia, over the South American Plate, during the Cretaceous. Today, remnants of this basins in Colombia are mainly found in outcrops of the Upper Magdalena Valley (UMVB), Middle Magdalena Valley (MMVB), Eastern Cordillera (ECB), Cesar-Ranchería (CR) and Catatumbo (CA) basins, and wells of the Eastern Llanos Basin, UMVB and MMVB (Villamil et al., 1999; Gómez et al., 2003, 2005; Sarmiento-Rojas, 2019), all currently significant hydrocarbon-producing basins (Cediel et al., 2011). This study focuses on the central part of the epeiric basin, encompassing the UMVB, MMVB and ECB (Fig. 1).

These present-day sedimentary basins formed a single one during the

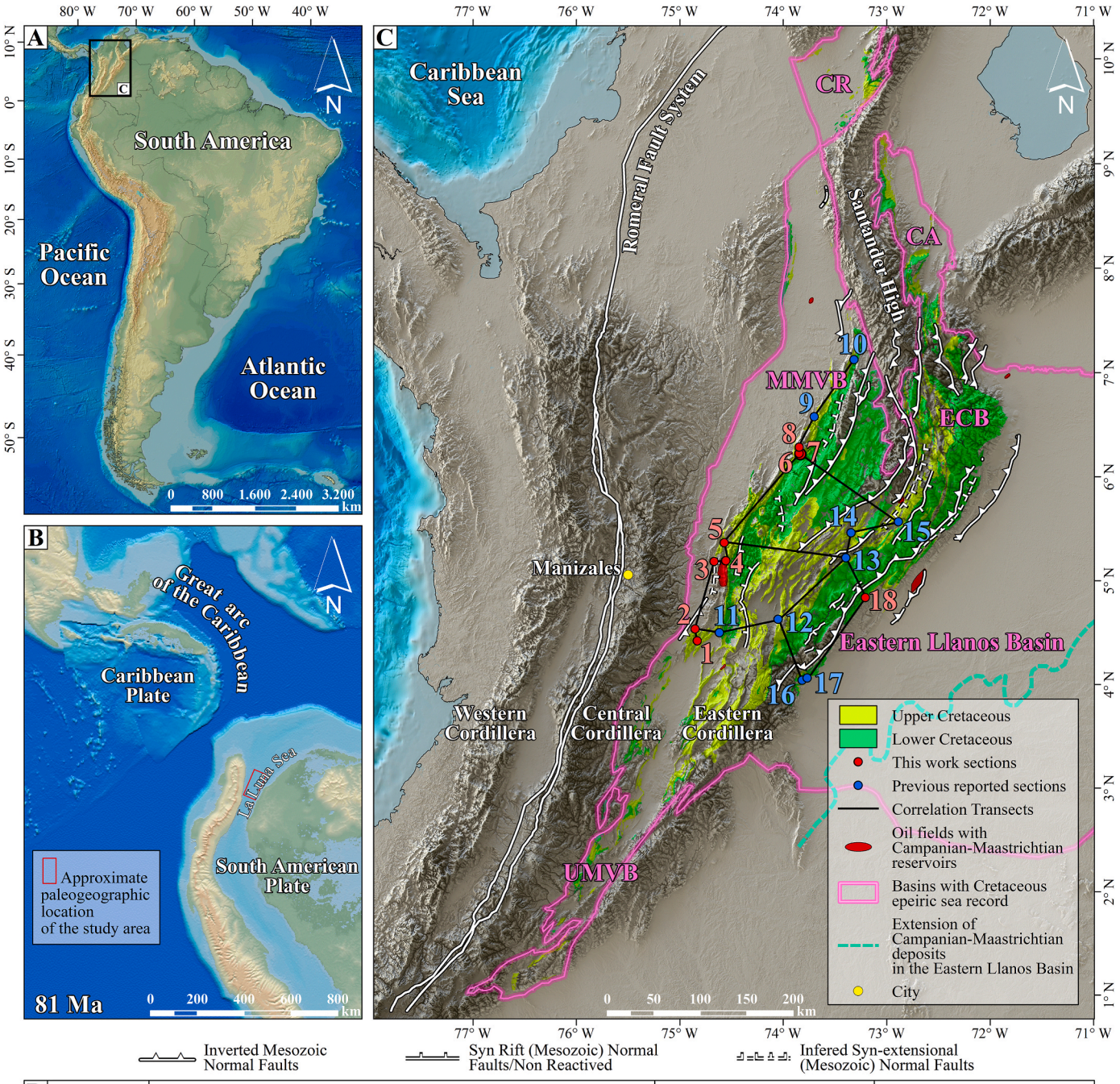

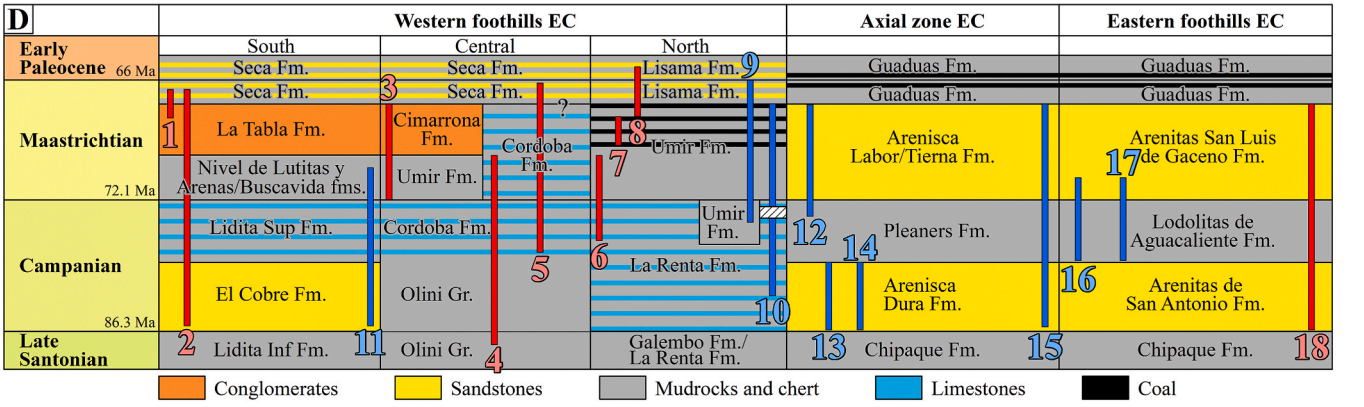

(caption on next page)

Fig. 1. A-C. Location maps. Green marks the remnant surface outcrops of Cretaceous epeiric sea deposits in different sedimentary basins (pink polygon). CA: Catatumbo Basin; CR: Cesar-Ranchería Basin; ECB: Eastern Cordillera Basin; MMVB: Middle Magdalena Valley Basin; UMVB: Upper Magdalena Valley Basin. In red are the stratigraphic sections of this work and in blue the stratigraphic sections of Vergara and Rodriguez (1997), Garzón et al. (2012), Montaño et al. (2016), Terraza (2019), and Carvajal-Torres et al. (2022). The black lines correspond to stratigraphic correlation transects. **B.** Paleogeographic map of the northwestern corner of South America at 81 Ma, showing the La Luna epeiric sea and the approximate location of the study area (from Salles et al., 2022). **D.** Lithostratigraphic nomenclature for the Campanian-Maastrichtian deposits according to their position in the sedimentary basins and the corresponding studied sections (red bars for this study and blue bars for previously reported sections) with the age interval according to Petters (1955), De Porta (1966), Pérez and Salazar (1978). Föllmi et al. (1992), Tchegliakova (1993, 1995, 1996), Rodríguez and Ulloa (1994), Guerrero and Sarmiento (1996), Tchegliakova et al. (1997), Vergara (1997), Vergara and Rodriguez (1997), Guerrero et al. (2000), Sarmiento and Guerrero (2000), Tchegliakova and Mojica (2001), Montaño et al. (2016), Etayo-Serna (2019), Terraza (2019), Patarroyo et al. (2022, 2023), De la Parra et al. (2024). Faults taken from Tesón et al. (2013). (For interpretation of the references to color in this figure legend, the reader is referred to the Web version of this article.)

Jurassic-Cretaceous and part of the Cenozoic (Fig. 1). It was an elongated NNE-SSW basin, with maximum widths of ~400–500 km, bounded by a volcanic arc (proto-Central Cordillera) to the west which was partially flooded during the Turonian-Santonian and later reemerged during the Campanian-Maastrichtian, and the Amazonian Craton to the east, as indicated by the compositional provenance of the deposits in both the eastern and western domains (Guerrero et al., 2000, 2020; Sarmiento-Rojas et al., 2006; Horton et al., 2010, 2015, 2020; Bayona, 2018; Zapata et al., 2019; Pardo-Trujillo et al., 2020; Valencia-Gómez et al., 2020; Botero-Garcia et al., 2023; Reyes et al., 2024). The origin of the former Early Cretaceous extensional basins has been linked to a rifting phase associated with the breakup of Pangaea and/or back arc extension between the Triassic and Early Cretaceous (Etayo-Serna et al., 1983; Maze, 1984; Cooper et al., 1995; Sarmiento-Rojas, 2001, 2019; Cediel et al., 2003; Gómez et al., 2003, 2005; Sarmiento-Rojas et al., 2006; Spikings et al., 2015; Leal-Mejía et al., 2019; Guerrero et al., 2020; Bayona et al., 2021). The sedimentary fill is a mixture of siliciclastic and carbonate deposits, related to the development of carbonate platforms overlain by mixed and siliciclastic shelves. During the Jurassic-Lower Cretaceous (syn-rift phase), ~3 km thick red beds and pyroclastic deposits were deposited (Etayo-Serna et al., 1983; Sarmiento-Rojas, 2001; Gómez et al., 2005; Bayona et al., 2020; Jiménez et al., 2021; Osorio-Afanador and Velandia, 2021). Subsequently, an Early Cretaceous marine transgression allowed the development of an interior sea connected with the proto-Atlantic Ocean, depositing marine rocks ~7 km thick (Cooper et al., 1995; Villamil and Pindell, 1998; Sarmiento-Rojas, 2001, 2019; Gómez et al., 2003; Sarmiento et al., 2015; Paez-Reyes et al., 2021). Variations in deposit thicknesses along the basin suggest tectonic activity during deposition. At the end of the Cretaceous, the focus of this study, the collision of allochthonous terrains in western Colombia, combined with a global sea-level fall, led to the retreat of the sea, and the accumulation of fine- and coarse-grained deposits, that now constitute important hydrocarbon sources and reservoirs in the basin. This event marked a shift in depositional systems, transitioning from marine deposition during the Latest Cretaceous to continental accumulation during the early Paleocene (Cooper et al., 1995; Sarmiento-Rojas et al., 2006; Bayona, 2018; Sarmiento-Rojas, 2019). The terrain collision is evidenced in the sedimentary record by the local deposition of coarse-grained clastic wedges near the uplifted mountain ranges (Gómez et al., 2003; Bayona et al., 2021; Giraldo-Villegas et al., 2024).

The current structural configuration of the UMVB, MMVB and ECB basins is related to a Cenozoic double vergent orogen caused by tectonic inversion processes (Cooper et al., 1995; Mora et al., 2015a, 2015b; Siravo et al., 2019). Tectonic inversion occurred through major faults on the western (La Salina Fault) and eastern (Guaicaramo Fault) boundaries, along with associated transfer faults (e.g., El Carmen, Tesalia, Pajarito; Cooper et al., 1995; Mora et al., 2013; Jiménez et al., 2022); the most positive relief zone roughly coincides with the zone of maximum subsidence during the Early Cretaceous (Casero et al., 1997; Mora et al., 2006, 2013; Sarmiento-Rojas et al., 2006).

The Cretaceous deposits of these basins have different lithostratigraphic nomenclatures owing to their wide and complex lithological variations, both vertically and laterally, in terms of depositional settings, ages and geographic locations. For the Campanian-Maastrichtian deposits in the study area, dividing the basins in three along-strike transects (western, central and eastern), the nomenclature from south to north and from west to east is as shown in Fig. 1.

The sedimentary record throughout the epeiric basin is not continuous, and some unevenly distributed unconformities have been identified in the uppermost Cretaceous deposits. North of the MMVB and in the UMVB, late Campanian-early Maastrichtian and Maastrichtian unconformities have been reported, separating La Renta and Umir, and Monserrate and San Francisco formations, respectively (Veloza et al., 2008; Mora et al., 2010; Bayona, 2018; Etayo-Serna, 2019; Guerrero et al., 2021; Carvajal-Torres et al., 2022; Pastor-Chacón et al., 2023; De la Parra et al., 2024).

2.1. *Biostratigraphic considerations*

Various micropaleontological analyses have been conducted on Campanian-Maastrichtian deposits in the UMVB, MMVB and the Eastern Cordillera basins, to study marine (foraminifers, calcareous nannofossils, ostracods) and continental (palynomorphs, ostracods) fossil groups. Recent research (e.g., UCaldas-ANH, 2021; Patarroyo et al., 2023) has focused on establishing a robust biostratigraphic framework for the selected outcrop sections for this work (Fig. 1; Supplementary file 1). However, the resolution of these data prevents the recognition of time gaps (unconformities). Our study involved 18 stratigraphic sections. From south to north along the western foothills of the central part of the Eastern Cordillera, Section 1 shows middle Campanian-late Maastrichtian ages between 4.3 and 5.9 m based on the presence of calcareous nannofossils. However, by correlation it is considered late Maastrichtian. In Section 2, ages range from the Campanian-Maastrichtian (109–218 m) to Maastrichtian (218–363 m) as identified through the integration of palynomorphs, foraminifers, ostracods, and calcareous nannofossils. Previous work reports early to late Campanian ages for this stratigraphic section based on foraminifers and ammonites (Guerrero et al., 2000; Tchegliakova and Mojica, 2001; Patarroyo et al., 2010). Section 3 reveals a Maastrichtian age based on the integration of palynomorphs, foraminifers, ostracods and calcareous nannofossils. Middle to upper Maastrichtian ages have been previously attributed to this section based on foraminifers (Tchegliakova, 1996). Section 4 has Santonian-Campanian (31.5–72 m) and Campanian-Maastrichtian (72–185.5 m) ages, while 5 exhibits late Campanian-Maastrichtian (0–76 m) and Maastrichtian ages (76–150 m) based on the integration of palynomorphs, foraminifers and calcareous nannofossils. Section 6 shows Campanian-Maastrichtian (1.5–6 m) and Maastrichtian (6–19.5 m) ages derived from the integration of palynomorphs, foraminifers and calcareous nannofossils. Maastrichtian ages are reported for Section 7 based on palynomorphs. Maastrichtian-Paleocene ages are obtained from palynomorphs for Section 8. In Section 9, late Campanian-Maastrichtian ages are reported based on palynomorphs (Montaño et al., 2016). Patarroyo et al. (2023) assign Campanian to late Maastrichtian ages for Section 10 according to the integration of foraminifers and calcareous nannofossils and Section 11 records deposits accumulated between the Campanian and lower Maastrichtian suggested by the palynomorphs (Garzón et al., 2012).

In the axial zone of the central segment of the Eastern Cordillera,

Late Campanian-Maastrichtian ages indicated by palynomorphs are reported for section 12 (Vergara and Rodriguez, 1997). Likewise based on palynomorphs, Vergara and Rodriguez (1997) report Campanian ages for Sections 13 and 14, in agreement with those reported by Pérez and Salazar (1978) and Föllmi et al. (1992). Lower Campanian to upper Maastrichtian deposits are preserved in Section 15, as indicated by the record of palynomorphs (Vergara and Rodriguez, 1997). Along the eastern foothills of the central segment of the Eastern Cordillera, the palynomorphs in Sections 16 and 17 points to the late Campanian-early Maastrichtian (Vergara and Rodriguez, 1997; Carvajal-Torres et al., 2022), while in Section 18, early Campanian-early Maastrichtian ages are suggested by Guerrero and Sarmiento (1996), also derived from the palynomorph record.

3. Methodology

An outcrop-based facies analysis was conducted, entailing the description of nine Campanian-Maastrichtian stratigraphic sections situated along the current outcropping eastern and western foothills of the central portion of the Eastern Cordillera Basin, which can be associated paleogeographically with the eastern and western sides of the central part of the La Luna Sea: eight located on the western foothills (Sections 1 to 8) and one on eastern foothills (Section 18). Nine previously studied and well-dated Campanian-Maastrichtian stratigraphic sections were included for comparison, integration, regional stratigraphic correlation and paleogeographic interpretations: three on the western (Sections 9 to 11), two on the eastern (Sections 16 and 17), and four in the axial part (Sections 12 to 15, Fig. 1). The first preliminary field descriptions of the western zone sections were developed under the 220–2021 project contract 220–2021 developed between the ANH and the University of Caldas (UCaldas-ANH, 2021). The same field sections were subsequently revisited to perform and refine the descriptions and interpretations.

Lithological and paleontological features such as bed geometry and thickness, grain size, sorting, sedimentary structures, trace fossils and fossil distribution were recorded in each section. We use the term "mudrock" to refer to lithologies with grain sizes smaller than 63 μm and having similar proportions of silt and clay. Ichnologic analysis encompassed the identification of ichnogenera considering qualitative and quantitative properties (following the ichnotaxobases of Bromley, 1996; Bertling et al., 2006, 2022). The abundance of bioturbation (bioturbation index, BI) was assessed following Taylor and Goldring (1993), ranging from no bioturbation (BI = 0) to complete bioturbation (BI = 6). Bed thickness characterization followed the proposal of Ingram (1954): laminae (<1 cm), very thin (1–3 cm), thin (3–10 cm), medium (10–30 cm), thick (30–100 cm) and very thick (>100 cm). Sedimentary facies were defined according to sedimentologic and ichnologic signatures and grouped in facies associations (FA) based on their relationships, vertical and spatial distribution, and stacking patterns, allowing for the interpretation of depositional settings, specific physical and ecological sedimentary parameters, and the overall paleoenvironmental and paleogeographic evolution.

To assess and understand the evolution of the sedimentary systems over time and space, six correlation transects were performed, including three along-strike and three cross-strike transects of the depositional system. Although paleomagnetic research concludes that the inverted rift shares similar structural trends with the exposed compressional structures (Jiménez et al., 2014), it should be noted that even though these successions are currently located towards the basin sides, their positioning does not always correspond directly to these edges due to the evolution of the basin in its inversion process. In some cases, especially in the north-south transects, different tectonic thrust sheets may be involved.

4. Results

4.1. Facies and facies associations

The integration of sedimentologic, ichnologic, and paleontologic (micro and macro) data allowed for the definition of seven facies associations (FA) in the western zone (from FA1w to FA7w), two in the central part (FA1c and FA2c), and three in the eastern zone (from FA1e to FA3e). These combinations of facies are genetically related to specific depositional environments (see Table 1). The FA are organized by location related to the Eastern Cordillera Basin (western foothills, axial zone, and eastern foothills), thus by regional location within the sedimentary epeiric basin (western side, central part, and eastern side) and arranged from the most distal (deeper) to the most proximal (shallower) with respect to the coastline. Shallow marine sedimentary environments dominated by pelagic settling, waves and local tides were interpreted for the western and central parts, along with a fan delta complex and fluvial deposits. In contrast, deltaic environments dominated by hyperpycnal processes were interpreted along the eastern side.

4.1.1. Western foothills

This western side of the basin includes Sections 1, 2, 3, 4, 5, 6, 7 and 8. Integrated additionally are Sections 9 of Montaño et al. (2016), 10 of Terraza (2019), and 11 of Garzón et al. (2012).

4.1.1.1. FA1w: mixed to carbonate shelf. Description: FA1w is recorded in the Campanian and Maastrichtian deposits of Sections 2, 4, 5, 6, 10 and 11, being predominant in the Campanian. It shows aggradational trends (up to ~ 200 m thick; Fig. 2A) of thin to thick tabular beds of limestones (mainly mudstones, occasionally wackestones and packstones, according to Dunham, 1962) in some cases silicified, with horizontal lamination and occasional asymmetric ripple cross-lamination, both highlighted by foraminifers alignment (Fig. 2B–C), as well as structureless chert with concoid fracture (Fig. 2D). The lamination in limestones is laterally continuous, with lenticular sheets of segregated grains (foraminifers). In addition, thick tabular beds of horizontally laminated marls and mudrocks are observed, interbedded with black shales (Fig. 2E–F). Thin to very thin beds of phosphorites are also recorded separating the limestones layers. These lithologies sporadically show macro- and microfossils such as ammonites, bivalves, foraminifers, fish scraps, and indeterminate mollusk fragments. Scattered medium to thin tabular beds of fine-to very fine-grained bioclastic sandstones with horizontal lamination are seen. Bioturbation is not observed in these lithologies (BI = 0). Some levels with calcareous concretions up to 1.5 m in diameter are locally recorded. Layers of granular phosphorites are also reported by Terraza (2019) in Section10. These successions are underlain by shoreface deposits (FA3w) and overlain by offshore deposits (FA2w).

Interpretation: The domain of mixed fine-grained lithologies (mudrocks and limestones) with foraminifers suggests pelagic settling from suspension in low-energy environments below the storm-wave base in a mixed shelf environment (Reading, 1996; Nichols, 2009; Flügel, 2010). The horizontal and asymmetric ripple cross-lamination indicates weak suspension currents (Potter et al., 2005; Stow and Smillie, 2020) or bedload transport related to weak bottom currents (Schieber et al., 2007; Yawar and Schieber, 2017). The bioclastic sandstones and granular phosphorites may be considered as distal tempestites linked to storm events that caused sediment remobilization (Kidwell, 1991; Glenn et al., 1994; Myrow and Southard, 1996). The high abundance of organic matter reflected in the dark colors of the rock, and the lack of bioturbation indicate high productivity and a poorly oxygenated seafloors (Ekdale and Mason, 1988; Savrda and Bottjer, 1991; Tyson and Pearson, 1991), which could be linked to upwelling (Föllmi et al., 1992; Villamil et al., 1999; Spalletti et al., 2001). However, the discrete level with fossils suggests a macrobenthic community tolerant of

Table 1
Description and interpretation of facies associations identified in the last stages of the central part of the La Luna epeiric sea during the Campanian-Maastrichtian.

Region	Facies association	Stratigraphic section	Lithology	Sedimentary structures	Trace fossils and fossils	Thickness	Depositional setting
Western	Mixed to carbonate shelf (FA1w)	2, 4, 5, 6, 10, 11	Tabular beds of limestones (mudstones, wackestones, packstones), marls, cherts, mudrocks, shales, and bioclastic sandstones.	Fissility, structureless, horizontal lamination, asymmetric ripples.	Barren in trace fossils (BI 0); foraminifers, ammonites, bivalves, fish scraps, mollusk fragments.	~600 m thick	Pelagic settling from suspension in low energy, poorly oxygenated environments, with influence of bottom currents and local storms. Mixed shelf.
	Offshore (FA2w)	2, 3, 5	Tabular beds of mudrocks, muddy sandstones, sandstones, and locally marls.	Horizontal lamination, heterolithic bedding (lenticular, wavy, flaser), symmetric ripples, structureless	*Asterosoma*, *Chondrites*, *Ophiomorpha*, *Palaeophycus*, *Planolites*, *Schaubcylindrichnus*, *Scolicia*, *Taenidium*, *Teichichnus*, *Thalassinoides* (BI 3 to 4); ammonites, fish scraps, inoceramids, mollusk fragments.	~80 m thick	Alternation of settling from suspension and high energy storm events in well-oxygenated settings. *Cruziana* ichnofacies. Offshore.
	Shoreface (FA3w)	2	Amalgamated tabular beds of very fine- to fine-grained sandstones and sandy siltstones. Locally mudrocks.	Ripple lamination, heterolithic bedding (flaser, wavy), horizontal lamination.	*Thalassinoides* (BI 1); foraminifers, carbonized wood fragments.	~120 m thick	High-energy environments controlled by wave oscillatory processes and storms. Shoreface.
	Fan delta (FA4w)	1, 2, 3	Amalgamated cuneiform-lenticular- and tabular-shape medium to very thick beds of clast- and matrix-supported granule- to cobble-size conglomerates, pebble- and granule-size conglomeratic sandstones, fine- to very coarse-grained sandstones, mudrocks.	Structureless, planar and trough cross-bedding, horizontal bedding, normal grading, heterolithic bedding (wavy).	*Arenicolites*, *Dactyloidites*, *Ophiomorpha*, *Taenidium*, *Thalassinoides* (BI = 2); bivalves, gastropods, carbonized wood fragments.	~100 m thick	High-energy environments and sediment source relatively close to the receiving basin. Subaerial cohesionless debris and sheet flow deposits typical of alluvial fan environments. Intervals with fining- and thinning-upward trends are interpreted as channel filling, which would be arriving at the coast. The occasional presence of marine fossils and trace fossils is indicative of marine influence in the system. Fan delta complex.
	Tidal flat (FA5w)	1, 2, 8	Irregular concave-up and tabular beds of very fine- to medium-grained sandstones interbedded with mudrocks. Very thin beds of mudrocks follow the tangential cross-strata foresets.	Macro-heterolithic bedding, symmetric and asymmetric ripples, flaser and wavy bedding, trough cross-bedding, bi-directional cross-bedding reactivation surfaces, structureless.	*Arenicolites*, *Rhizocorallium*, *Thalassinoides* (BI 1).	~50 m thick	The physical sedimentary structures (heterolithic bedding) reflect increase and decrease in the speed and energy of flows, sandy material deposited during high-energy episodes (tidal flood) and muddy material in low-energy periods (tidal ebb). Bidirectional trough cross-bedding and mud drapes associated with trough cross-bedding, forming bundled cross-bedding, are clearly indicative of tidal processes. Tidal flat.
	Swamp-lagoon (FA6w)	7, 9	Tabular beds of mudrocks, carbonaceous mudrocks and coal, and tabular to lenticular beds of very fine- to medium-grained sandstones.	Structureless, horizontal lamination, symmetric and combined-flow ripples, flaser and wavy bedding.	?*Gyrolithes*, *Taenidium*, *Thalassinoides* (BI 0 to 1); mangrove palynomorphs.	~450 m thick	High amount of organic matter linked to mudrocks and coals is indicative of large accumulations of organic matter and areas near the continent. The dominant fine-grained lithologies are indicative of low-energy settings, e.g., lagoon or protected coastal plains.
	Fluvial (FA7w)	3, 5	Amalgamated tabular to cuneiform-shaped beds of fine- to medium-grained	Structureless, horizontal lamination, trough and	?*Taenidium* (BI 1); agglutinated foraminifers.	~40 m thick	Fining upward trends from erosional-base sandstones to mudrocks

(*continued on next page*)

Table 1 (*continued*)

Region	Facies association	Stratigraphic section	Lithology	Sedimentary structures	Trace fossils and fossils	Thickness	Depositional setting
			sandstones, and tabular beds of siltstones and mudrocks.	planar cross-bedding, scour marks.			are characteristic of channel-floodplain deposits. Mixed- or suspended-load anastomosing river systems
Central	Offshore (FA1c)	12, 15	Tabular beds of cherts, shales, siltstones, claystones, very fine- to fine-grained sandstones.	Horizontal lamination, wavy and lenticular bedding, ripples, convolute lamination.	Indeterminate bioturbation (BI not reported); foraminifers, fish scraps.	~60 m thick	Offshore.
	Shoreface (FA2c)	12, 13, 14, 15	Tabular beds of medium- to very fine-grained sandstones, mudrocks, cherts.	Horizontal lamination, heterolithic bedding (flaser and wavy), planar and trough cross-bedding, hummocky and swaley cross-bedding, ripples.	Indeterminate bioturbation (BI not reported); fish scraps, foraminifers, bivalves.	~200 m thick	Shoreface.
Eastern	Fluvial-dominated prodelta (FA1e)	18	Tabular beds of mudrocks, siltstones, very fine-to fine-grained sandstones.	Structureless, horizontal lamination, flaser, wavy and lenticular bedding, scour marks.	*Thalassinoides* (BI 0 to 1); carbonaceous sheets.	~100 m thick	High amounts of carbonaceous material indicate significant terrestrial supply. This, combined with features such as internal scours, tractive and massive structures related fine-grained lithologies, may suggest traction transport or fall-out processes from turbulent flows associated with hyperpycnal and hypopycnal flows in prodelta settings.
	Fluvial-dominated delta front (FA2e)	17, 18	Tabular and lenticular beds of fine- to coarse-grained sandstones, tabular beds of mudrocks and lenticular beds or pockets of granule- to pebble-size conglomerates.	Discontinuous horizontal lamination, structureless, symmetric and combined flow ripples, trough cross-bedding, convolute lamination, normal grading.	*Conichnus*, *Ophiomorpha*, *Palaeophycus*, *Planolites*, *Rhizocorallium*, *Skolithos*, *Taenidium*, *Teichichnus* and *Thalassinoides* (BI 2 to 4); bivalves. Carbonaceous sheets.	~250 m thick	This facies association shows products related to high energy settings linked to oscillatory and combined flows, like those recorded in shoreface-foreshore environments. However, in contrast to shoreface settings, these successions are regarded as delta front deposits based on the abundant amount of carbonaceous material, suggesting phytodetrital pulses from fluvial discharges.
	Shoreface (FA3e)	16	Tabular beds of fine- to medium-grained sandstones and mudrocks, with phosphahtic peloids and mud intraclasts.	Structureless, horizontal lamination, wavy and lenticular bedding.	Indeterminate bioturbation (BI no reported), plant remains.	~260 m thick	Shoreface.

oxygen-deficient environments. The origin of the chert is considered diagenetic in other parts of the basin, such as the Upper Magdalena Valley Basin, where it was derived from mudstones and wackestones that were later intensely silicified (Terraza, 2003). These silicified beds, also called "liditas", are considered regional lithological markers (Mora et al., 2010).

4.1.1.2. FA2w: offshore. Description: FA2w is observed in the Maastrichtian of Sections 2, 3 and 5. It is characterized by mudrocks, and discrete marls, sandstones and muddy sandstones, interbedded in an aggradational arrangement, resulting in successions up to ~80 m thick (Fig. 3A–C). The mudrock beds are medium to very thick, with tabular geometry, showing horizontal and lenticular (heterolithic) bedding. The sandstones and muddy sandstones beds are sharp-based, medium to very thick, tabular in geometry, fine-to very fine-grained, with horizontal lamination, symmetric ripple cross-lamination (Fig. 3D), flaser and wavy bedding, and locally structureless (Fig. 3B–E). The thick to very thick tabular beds of marls show horizontal lamination. Occasionally, intervals up to 2 m thick of amalgamated massive sandstones are present (Fig. 3A–B). Ammonites, fish remains, inoceramids and mollusk fragments are recorded mainly in the sandy beds. Fallen blocks exposed at the base of the some of these exposed outcrops exhibit a moderate to abundant (BI = 3, 4) and diverse ichnoassemblage composed of *Asterosoma*, *Chondrites*, *Ophiomorpha*, *Palaeophycus*, *Planolites*, *Schaubcylindrichnus*, *Scolicia*, *Taenidium*, *Teichichnus*, and *Thalassinoides* (Fig. 3F–H). These successions are underlain and overlain by mixed shelf (FA1w) and fan delta/fluvial deposits (FA4w and FA7w), respectively.

Interpretation: The high occurrence of mudrocks represents suspended fall-out deposition in low-energy offshore environments (Stow, 1985; Stow and Tabrez, 1998). Sandstones bearing broken fossils and

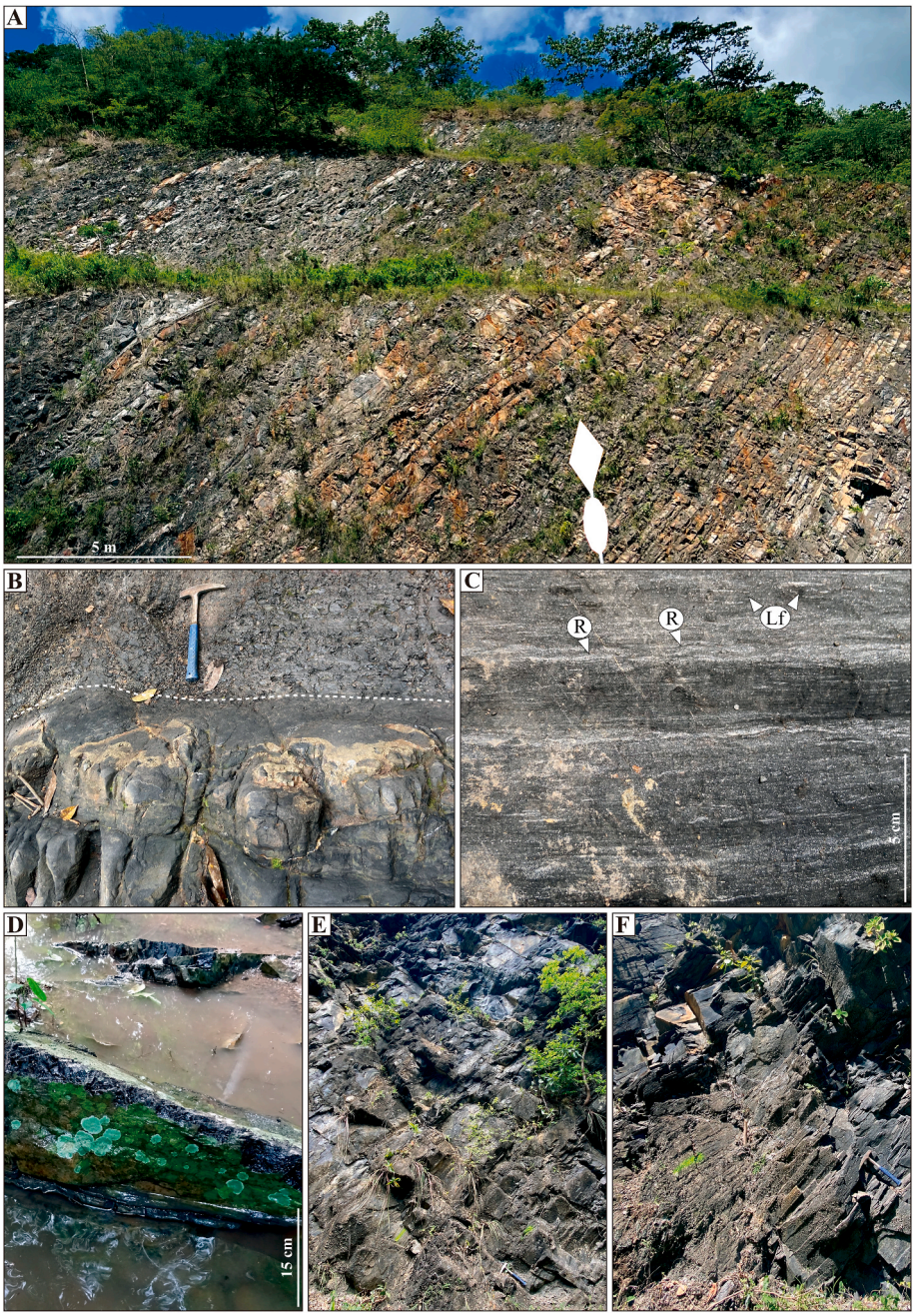

Fig. 2. Mixed to carbonate shelf FA1w. **A.** General outcrop view of Section 5. **B.** Sharp contact between limestones (base) and mudrocks (top) in Section 6. **C.** Detail of horizontal and ripple (R) lamination, and lenticular sheets of foraminifers (Lf) in wackestones and packstones of section 6. **D.** Lenticular chert bed in Section 2. **E, F.** Mudrocks-shales interlayered in Section 4.

horizontal lamination and subordinate amalgamated massive beds may be the response to high-energy storm-related events (Walker and Plint, 1992; Myrow and Southard, 1996), whereas the symmetric ripple cross-lamination and heterolithic bedding probably formed by the action of oscillatory flows (Dumas et al., 2005). This is supported by the trace fossil assemblage, interpreted as the *Cruziana* ichnofacies, associated with lower shoreface-offshore environments, between storm-wave base and fair-weather-wave base (MacEachern et al., 2007; MacEachern and Bann, 2008). The abundant and diverse trace fossil assemblage indicates a well-oxygenated seafloor, with benthic food available for a macrobenthic tracemaker community. In this scenario, the siliciclastic supply was high enough to dilute the calcium carbonate, avoiding limestone deposition.

4.1.1.3. FA3w: shoreface. Description: FA3w is recorded in the Campanian of Section 2. Towards the base of this section, a succession up to ~120 m thick comprises amalgamated thick to very thick tabular beds of very fine-to fine-grained sandstones and sandy siltstones, locally fossiliferous (foraminifers), with symmetric ripple and horizontal lamination (Fig. 4A–C). Sporadic mudrocks forming heterolithic bedding (flaser and wavy with symmetric and asymmetric ripple cross-lamination) (Fig. 4D–E), show aggradational and progradational arrangements. Occasional glauconite grains, foraminifers, charred wood fragments and *Thalassinoides* (BI = 1) are observed. These successions are underlain and overlain by mixed to carbonate shelf deposits (FA1w).

Interpretation: The record of amalgamated sandstone bedsets with ripple cross-lamination, glauconite, and occasional foraminifers suggests a relatively moderate-energy environment controlled by

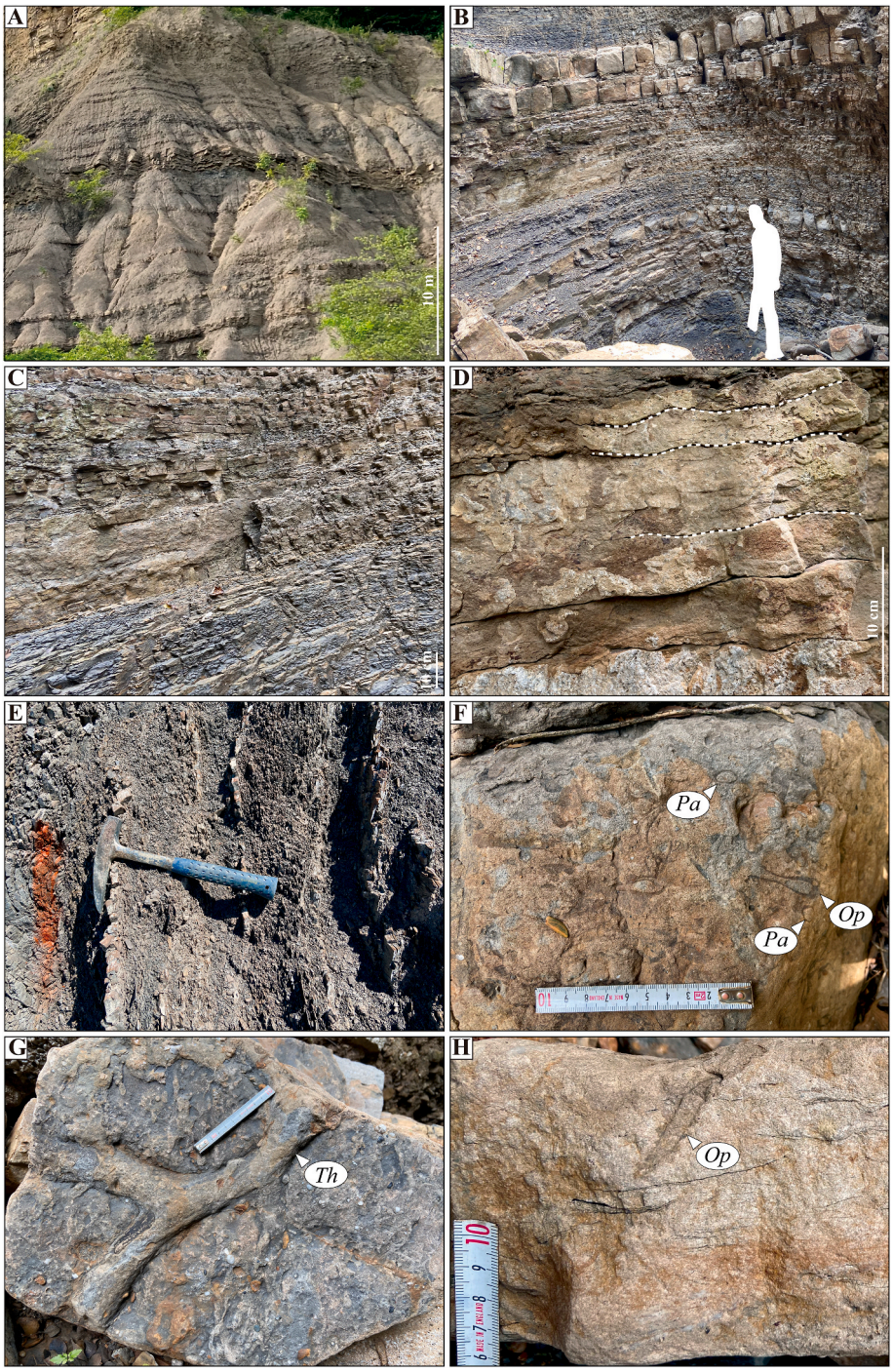

Fig. 3. Offshore FA2w. **A, B.** General outcrop views of Section 3. **C.** Mudrock-fine-grained sandstone interbedding in Section 3. **D.** Fine-grained sandstone with symmetric ripple cross-lamination in Section 3. **E.** Mudrocks interbedded with fine-grained sandstone in Section 5. **F, G, H.** Trace fossils in fallen blocks of Section 3. *Op: Ophiomorpha, Pa: Palaeophycus, Th: Thalassinoides.*

oscillatory wave processes in shoreface and probably some variations to foreshore settings (Reading, 1996; Einsele, 2000). The high energy caused by prolonged wave action removes mud from the seafloor, except where the local occurrence of mudrocks forming heterolites suggests a decrease in energy relative to sandstones-dominated areas (Weimer et al., 1982; Brenchley et al., 1993; Reading, 1996). The horizontal lamination can be linked to high-energy events generated by combined flows, e.g. storms (Arnott, 1993; Perillo et al., 2014). The scarce mudrock record suggests deposition above the fair-weather-wave base. The low bioturbation is indicative of a high-energy unstable environment that inhibits the establishment of a macrobenthic community. Charred wood remains indicate a nearby terrestrial source.

4.1.1.4. FA4w: fan delta. Description: FA4w occurs in the Maastrichtian of Sections 1, 2 and 3. Successions up to ~100 m thick show aggradational, progradational, and retrogradational patterns, characterized by amalgamated cuneiform- lenticular- and tabular-shaped medium to very thick beds of clast- and matrix-supported granule-to cobble-size conglomerates, pebble- and granule-size conglomeratic sandstones, and medium-to very coarse-grained sandstones with irregular and planar sharp bases (Fig. 5A). The dominant sedimentary structures of these

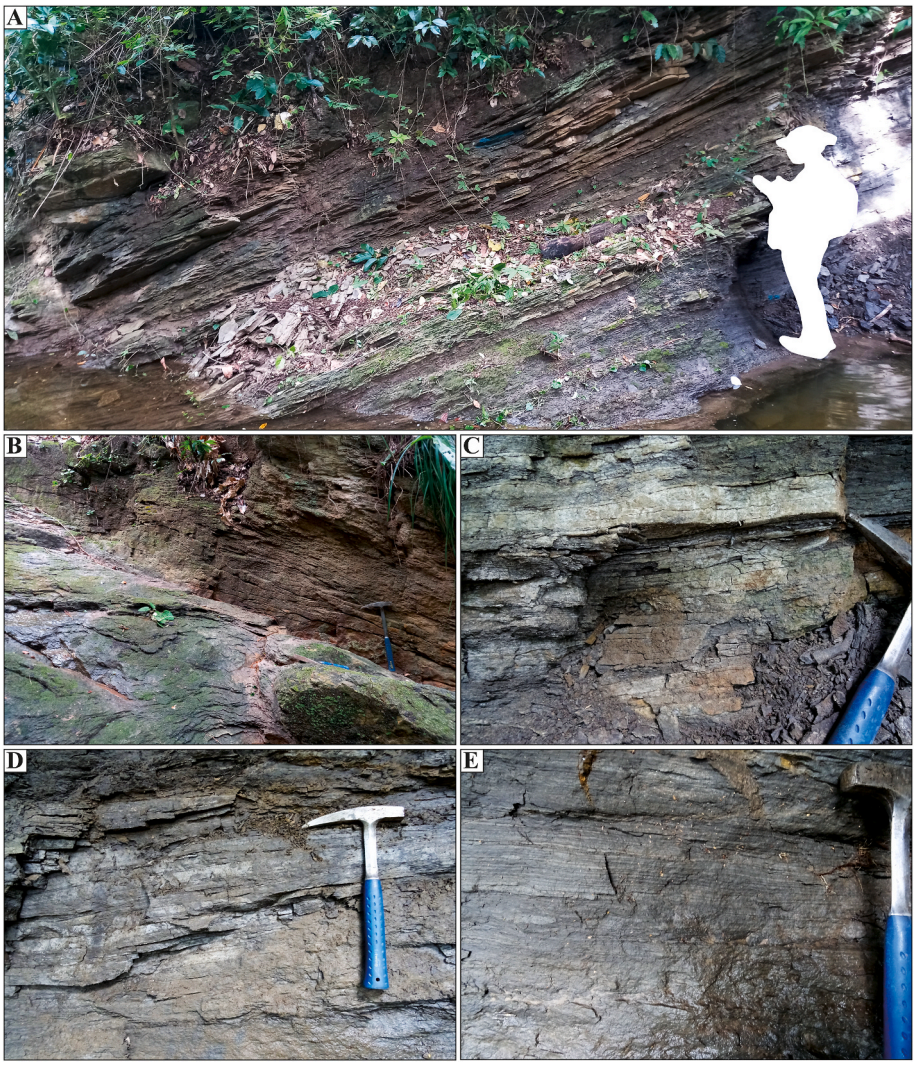

Fig. 4. Shoreface FA3w in Section 2. **A.** General outcrop view composed of amalgamated sandstones with wavy bedding. **B, C.** Medium-grained sandstone with ripple cross-lamination. **D-E.** General and detailed views of fine-to medium-grained sandstones and sandy siltstones with wavy lamination.

lithologies are massive, planar and trough cross-, as well as horizontal-bedding, and normal grading. The sedimentary structures in the gravelly sandstones are often highlighted by granule- and pebble-sized clasts (Fig. 5B–E). The matrix varies between fine-to coarse-grained sandy material. Lateral outcrop variations in thickness are associated with the cuneiform-lenticular geometry of beds. Some fining- and thinning-upward trends are observed, from cuneiform-shape beds of massive conglomerates to medium-grained sandstones with tractional structures. The clasts are poorly-to well-sorted, showing subangular to rounded and highly spherical morphologies, and mostly quartz composition. Calcareous concretions and muddy intraclasts are common features. Locally, some intercalations of fine-grained sandstones and mudrocks forming heterolithic (wavy) bedding are found overlying gravelly beds with molluscan shell fragments (bivalves and gastropods) (Fig. 5F). In addition, charred wood fragments and *Ophiomorpha* occur in in-situ outcrops (Fig. 5G), and *Arenicolites*, *Dactyloidites*, *Taenidium* and *Thalassinoides* are recorded in fallen blocks (BI = 2). These successions are underlain and overlain by offshore (FA2w), and tidal (FA5w) and fluvial (FA7w) deposits, respectively.

Interpretation: The dominance of coarse-grained lithologies suggests high-energy environments and a sediment source relatively close to the basin (Nemec and Steel, 1988). The occasional presence of marine fossils and trace fossils is indicative of marine influence in the system (Giraldo-Villegas et al., 2024). Intervals of structureless conglomerates, along with horizontally stratified and normally graded conglomeratic beds, suggest subaerial cohesionless debris and sheet flows deposits typical of alluvial fan environments (Nemec and Steel, 1988; Blair, 1999; Sohn et al., 1999; García-García, 2004; Boggs, 2014). Conglomerates and sandstones with *Ophiomorpha* and mollusk shell fragments are associated with mouth bar deposits reworked by marine processes, representing a seaward migration of the sedimentary system (Lowe, 1982; Kleinspehn et al., 1984; Nemec and Steel, 1984; Ainsworth et al., 2016; van Yperen et al., 2020; Giraldo-Villegas et al., 2024). Intervals with fining- and thinning-upward trends are interpreted as channels that would have reached the coast (Miall, 1996; Einsele, 2000; Longhitano, 2008; Yeste et al., 2020). Structureless conglomerates represent the bedload or channel-floor lag deposits transported by the river during the peak flood, while the cross-bedding features attest to gradual filling of active channels related to the migration of bedforms (2D and 3D dunes or megaripples) (Lowe, 1982; Nemec and Postma, 1993; Miall, 1996; Reading, 1996). The horizontal lamination associated with these successions may reflect the development of longitudinal bar bedforms in the channels (Hein and Walker, 1977; Miall, 1996), or else could be related to short-lived increases in channel energy or stream velocity (Flemming, 2000; Yeste et al., 2019). Some thin beds of mudrocks and fine-grained sandstones associated with these channel successions may correspond to floodplains in the fluvial system (Miall, 1996). The amalgamated cuneiform- and lenticular-shaped beds of coarse-grained sandstones and

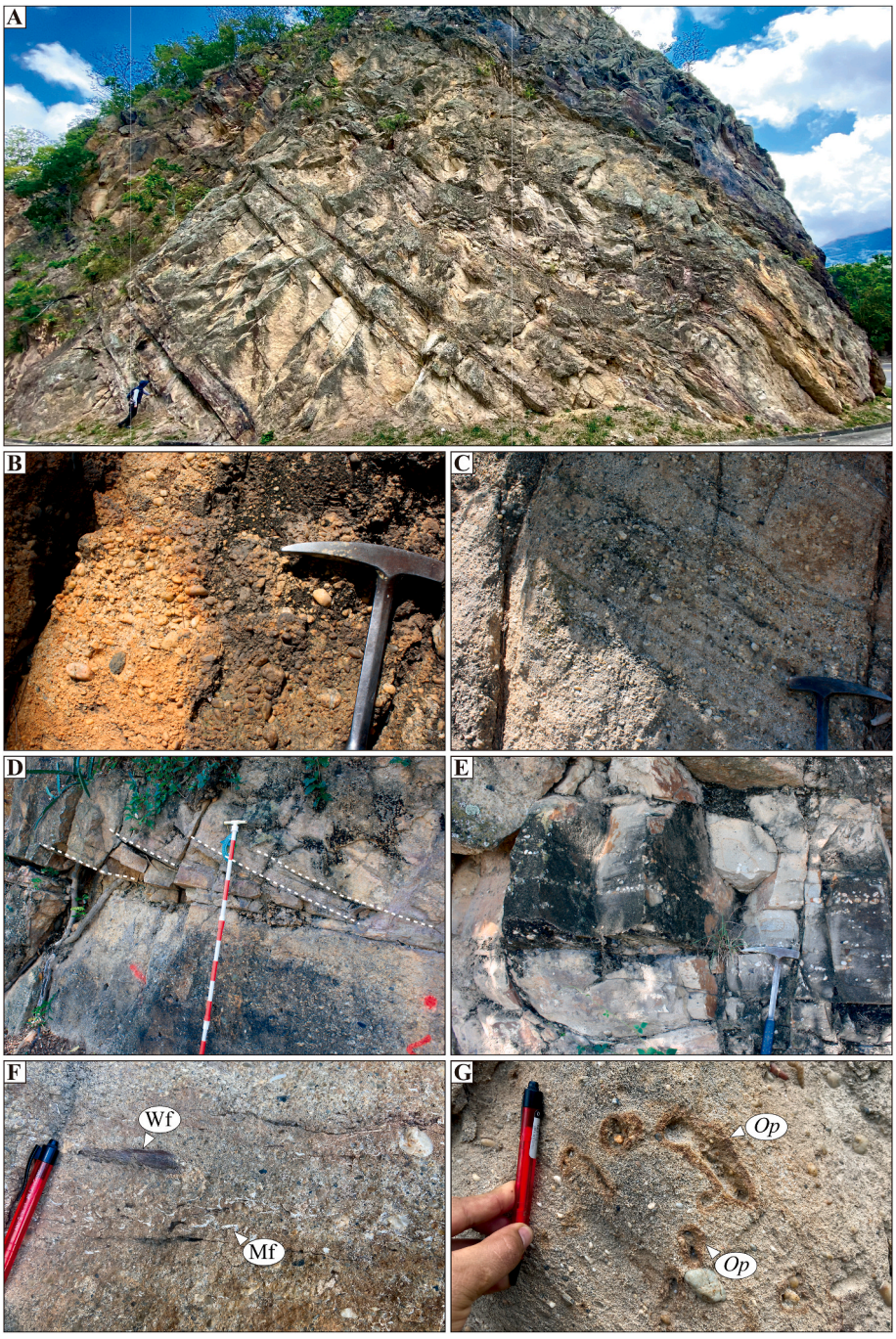

Fig. 5. Fan delta FA4w in section 3. **A.** General outcrop view. **B.** Massive clast-supported conglomerate dominated by quartz. **C.** Granule-size conglomerate with planar cross-bedding. **D.** Conglomeratic sandstones with trough cross-bedding. **E.** Conglomeratic sandstone with horizontal lamination. **F.** Conglomeratic sandstone with mollusk shell fragments (Mf) and charred wood fragments (Wf). **G.** *Ophiomorpha* (*Op*) in conglomeratic sandstone.

conglomerates are interpreted as multi-storey channels or as the result of rapid runoff during or after sudden rainstorms on the alluvial fans (Siggerud and Steel, 1999; Scherer et al., 2015; Varejão et al., 2021). Furthermore, the heterolithic intervals overlying the coarse-grained marine influenced deposits indicate wave and tidal activity in the more distal parts of the system (e.g., Ainsworth et al., 2016). This relationship between alluvial, fluvial and marine processes and the resulting deposits signals a fan delta complex setting (Gómez and Pedraza, 1994; Nemec and Steel, 1988; Giraldo-Villegas et al., 2024). The establishment of these prevailing marine processes in the fluvial-dominated sedimentary system could indicate upstream avulsion of fluvial channels, or relative sea-level variations.

4.1.1.5. FA5w: tidal flat. Description: FA5w is recorded in the Maastrichtian of Sections 1, 2 and 8. It occurs as sandstones interbedded with mudrocks (Fig. 6A), generating in some cases macro-heterolithic bedding (Fig. 6B) that forms aggradational trends, resulting in successions up to ~50 m thick. Irregular concave-up and tabular beds of sandstones are recorded, ranging from thin-to thick, very fine-to medium-grained, with asymmetric, and locally symmetric ripples, flaser and wavy bedding (Fig. 6C–E). Intervals of medium- and fine-to very fine-grained sandstone sheets are interbedded, forming a type of "horizontal lamination" that is locally interrupted by massive sandstones (Fig. 6F). Thick stacked sets of trough cross-bedding with reactivation surfaces and locally bidirectional cross-bedding are also present,

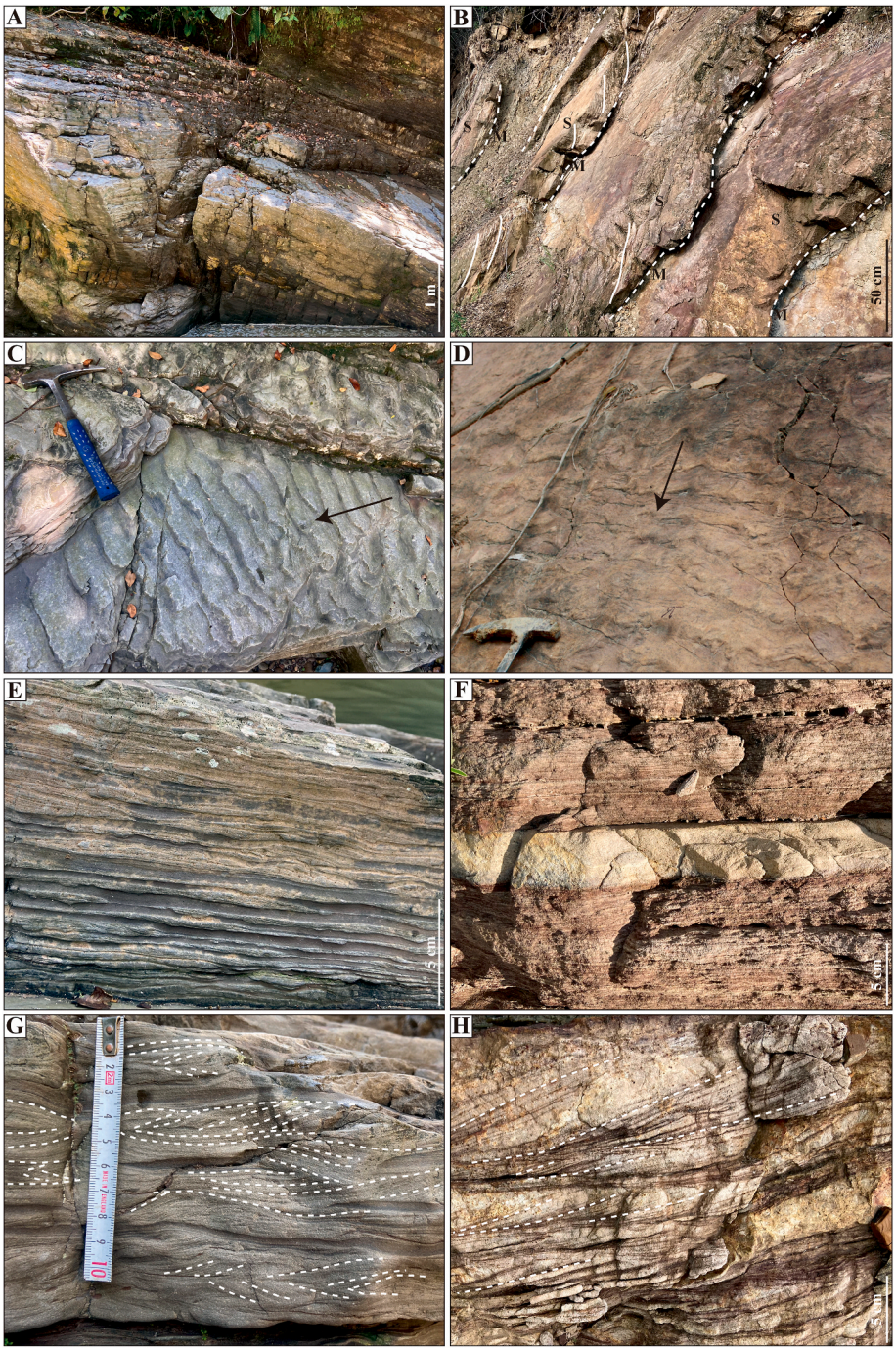

Fig. 6. Tidal flat FA5w. **A.** General outcrop view of Section 8, with interbedded mudrocks and sandstones forming heterolithic bedding. **B.** Macro-heterolithic flaser bedding in Section 1 (S: sandstone, M: mudrocks). Note the irregularly-shaped beds and the mudrocks filling the concave-up bed morphologies. **C, D.** Asymmetric ripples in Sections 8 and 2, respectively. Arrows indicate flow direction. **E.** Wavy heterolithic bedding in Section 8. **F.** Medium-to very fine-grained sheet sandstones forming horizontal lamination in Section 1. **G.** Fine-grained sandstones with bi-directional trough cross-lamination in Section8. **H.** Fine-grained sandstone with trough cross-bedding and mud drapes following the foresets in Section 2 (bundled cross-bedding).

occasionally with very thin beds of mudrocks following the tangential cross-strata foresets (mud drapes; Fig. 6G–H). The mudrock beds are thin to thick, structureless, found filling the concave-up morphology of sandstone beds. Trace fossils such as *Arenicolites*, *Rhizocorallium* and *Thalassinoides* are registered in the sandstone beds (BI = 1). A mixture of marine (dinoflagellates and foraminiferal linings) and continental (pollen and spores) elements are found in these deposits (UCaldas-ANH, 2021). These successions are respectively underlain and overlain by fan delta (FA4w) and fluvial (FA7w) deposits.

Interpretation: Physical sedimentary structures (heterolithic bedding) reflect changes (increase/decrease) in the velocity and energy of flows, sandy material being deposited during high-energy episodes (tidal flood) and muddy material during low-energy periods (tidal ebb) in marine settings, as indicated by the marine trace fossil assemblage (Reineck and Singh, 1973; Allen, 1982; Davis and Dalrymple, 2012). Features such as bidirectional trough cross-bedding and the mud drapes associated with trough cross-bedding, forming bundled cross-bedding, are evidence of tidal processes (Davis and Dalrymple, 2012; Longhitano et al., 2012; Steel et al., 2012). Sandstone beds with sets of trough cross-bedding can be linked to tidal dune bedforms (Longhitano and

Nemec, 2005; Davis and Dalrymple, 2012) and the sandstone sheets showing horizontal lamination may indicate the development of tidal rhythmites. Additionally, some thick structureless sandstone layers could potentially reflect the influence of storm events (Archer, 1991, 1995; Dalrymple, 1992; Longhitano et al., 2012). The scarce and scattered bioturbation suggests unfavorable marine habitats for macrobenthic communities, perhaps related to unstable substrates. Symmetrically-rippled sandstones point to a local influence of wave processes (Dumas et al., 2005).

4.1.1.6. FA6w: swamp-lagoon. Description: FA6w occurs in the Maastrichtian of Sections 7 and 9. It is characterized by mudrocks, carbonaceous mudrocks, coals and sandstones in aggradational successions up to ~450 m thick (Fig. 7A). Thin to medium tabular mudrock beds show horizontal lamination. Coal beds of massive structure and typical concoid fracture show tabular geometries with thicknesses ranging from medium to thick. The sandstone beds range from thin to thick, fine-to medium-grained, featuring tabular and lenticular geometries, and having asymmetric and combined-flow ripples and flaser and wavy bedding (Fig. 7B–F). Punctual records of ?*Gyrolithes*, *Taenidium*, and *Thalassinoides* (BI = 1) are observed (Fig. 7G–H). These deposits contain low records of marine elements (dinoflagellates and foraminiferal linings) and high abundances of continental palynomorphs (pollen and spores; UCaldas-ANH, 2021). Montaño et al. (2016) report beds

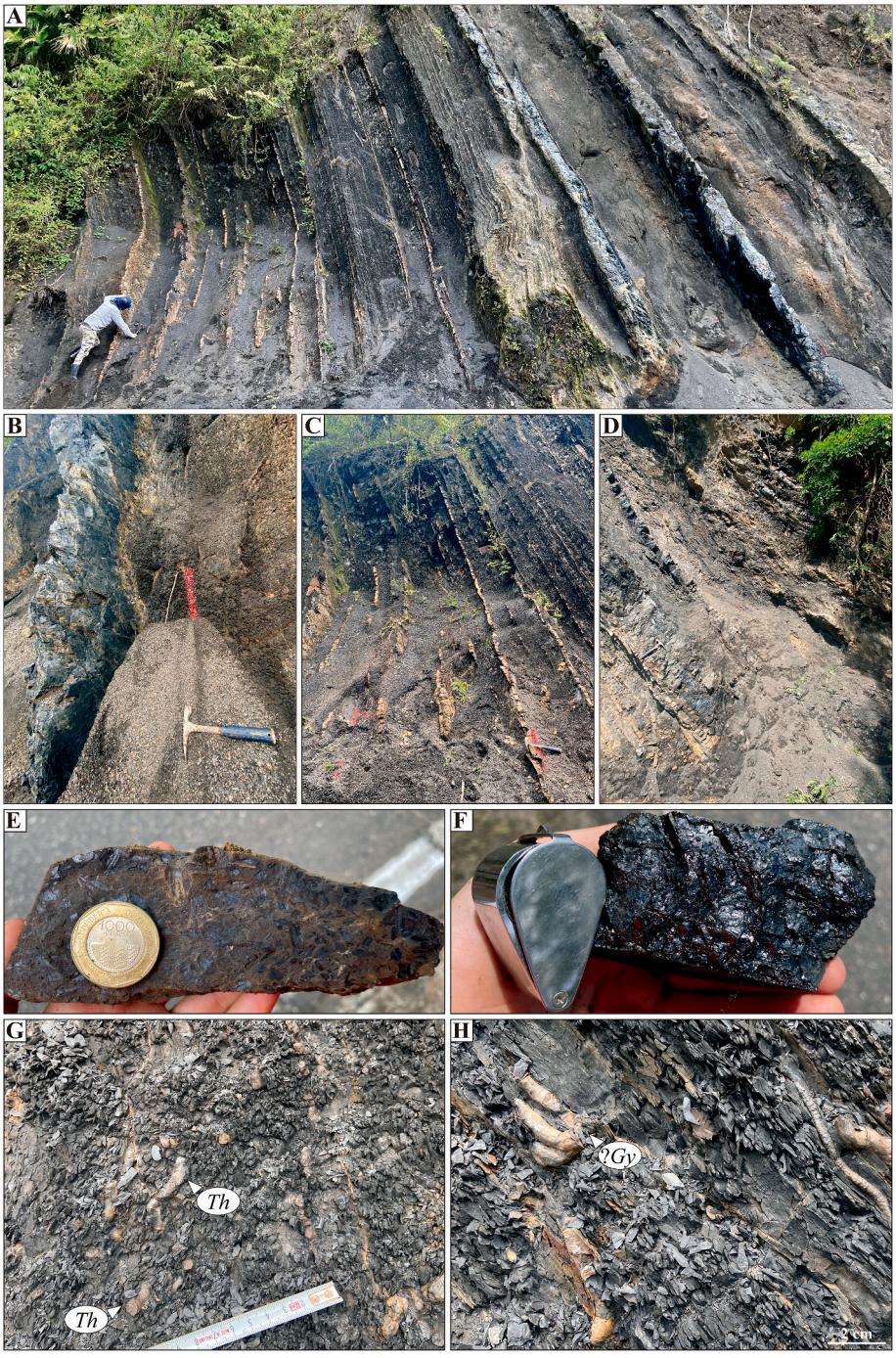

Fig. 7. Swamp-lagoon FA6w in Section 7. **A.** General outcrop view. **B, C, D.** Interbedding of carbonaceous mudrocks and coal beds. **E.** Detail of carbonaceous mudrock with high amount of fossilized organic matter. **F.** Detail of coal with concoid fracture. **G.** *Thalassinoides* (*Th*). **H.** ?*Gyrolites* (?*Gy*).

with marine and mangrove palynomorphs in Section 9. These successions are underlain and overlain by shelf (FA1w) and tidal deposits (FA5w), respectively.

Interpretation: High amounts of organic matter associated with mudrocks and coals indicate large accumulations of continental origin. However, the weak marine influence evidenced in the record of marine trace fossils and of mangrove and marine palynomorphs (Montaño et al., 2016) suggests that the accumulation occurs in continental areas locally flooded by the sea. The dominant fine-grained deposits suggests low-energy environments, such as lagoons or protected coastal plains. Heterolithic bedding may be related to local tidal and/or wave influence in the system.

4.1.1.7. FA7w: fluvial. Description: FA 7w is present in the Maastrichtian of Sections 3 and 5. It consists of tabular beds of mudrocks and claystones, either structureless or displaying horizontal lamination (Fig. 8A–B). These beds are occasionally interbedded with tabular and cuneiform sandstone beds, which may be structureless or exhibit horizontal lamination, as well as trough and planar cross-bedding, occasionally highlighted by granule-size clasts (Fig. 8C–F). The sandy levels show fining-upward trends, transitioning from thick amalgamated

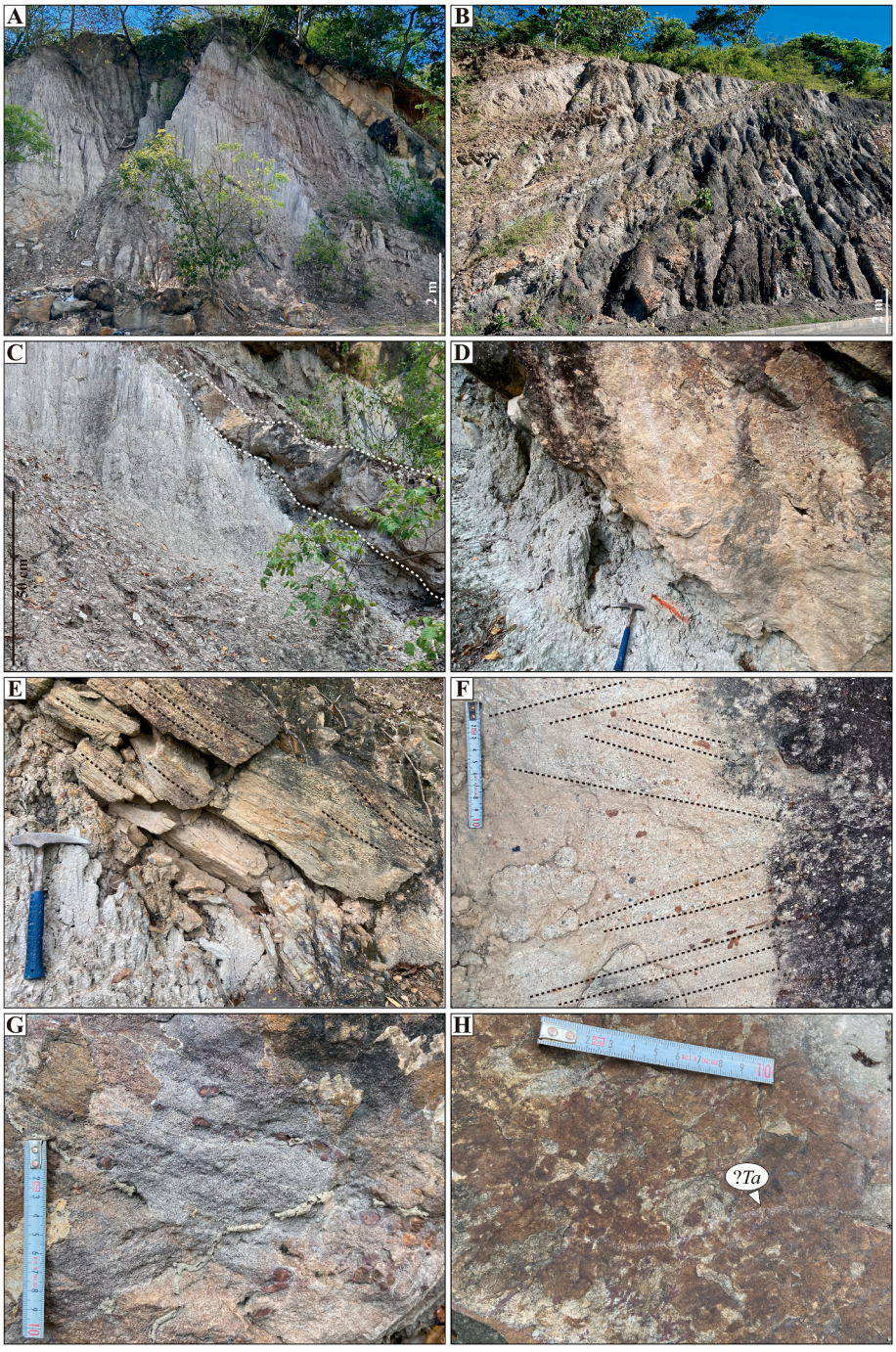

Fig. 8. Fluvial FA7w. **A, B.** General outcrop views of Sections 3 and 5. **C.** Cuneiform-shaped bed of fine-to medium grained sandstones interbedded with claystones and mudrocks in Section 3. **D.** Sharp irregular contact between massive mudrocks and medium-grained sandstones with trough cross-bedding in Section 3. Note scour marks at the base of the sandstone. **E, F.** Fine-to medium-grained sandstones with planar and trough cross-bedding in Section 3. **G.** Oxidized mud intraclast in sandstone. **H.** ?*Taenidium* (?*Ta*).

medium-grained sandstones to thin fine-to medium-grained beds and mudrocks, forming successions up to ~5 m thick, before reverting to a dominance of mudrocks. Scour marks are locally recorded at the mudrock and sandstone contacts (Fig. 8C). ?*Taenidium* (BI = 1) and oxidized mud intraclasts are rarely observed (Fig. 8G–H). Continental palynomorphs (pollen and spores) are abundant in these successions, while discrete agglutinated foraminifers are recorded in Section 3 (UCaldas-ANH, 2021). These successions reach thicknesses up to 40 m and are underlain by fan delta (FA4w) and tidal (FA5w) deposits.

Interpretation: The domain of mudrocks and claystones suggests relatively low-energy conditions, likely associated with extensive floodplains situated at a considerable distance from the main channel (e.g., Makaske, 2001). The scarce beds of sandstones with fining-upward trends and tractional structures such as planar and trough cross-bedding, would represent the action of unidirectional currents in fluvial channels. The mudrock-sandstone interbedding indicate sedimentation under varying hydrodynamic conditions, marked by periodical channel activity and the deposition of facies associated with small channels or crevasse splay deposits reaching the floodplain, such as those caused by levee breaches or overflows (Einsele, 2000; Yeste et al., 2020; Varejão et al., 2021). The fine-grained nature and the record of deposits associated with floodplains suggest mixed- or suspended-load anastomosing river systems (Reading, 1996; Makaske, 2001). The continental palynomorphs suggest the dominance of terrestrial environments, whereas foraminifers may indicate reworked material or a local rise in relative sea-level, reaching the mouths of river systems in coastal plain settings (e.g., Oboh-Ikuenobe et al., 2008).

4.1.2. Axial zone

This central part of the basin includes from south to north stratigraphic Sections 12, 13, 14 and 15 described by Vergara and Rodriguez (1997) along the axial part of the Eastern Cordillera Basin.

4.1.2.1. FA1c: offshore. Description: FA1c is recorded in the Campanian of Section 12 and in the Campanian-Maastrichtian of Section 15. It is dominated by aggradational and retrogradational trends forming successions up to ~60 m thick of cherts and black shales, locally with nodular phosphates and horizontal lamination (Vergara and Rodriguez, 1997). Siltstones, claystones and subordinate very fine-to fine-grained sandstones are also common, showing horizontal and convolute lamination, wavy and lenticular bedding, normal and inverse grading, and ripples. Foraminifers, fish scraps and indeterminate scarce bioturbation are also recorded. These successions are underlain and overlain by shoreface deposits.

Interpretation: FA1c is interpreted as an offshore marine environment with high primary productivity (Vergara and Rodriguez, 1997).

4.1.2.2. FA2c: shoreface. Description: FA2c is reported in the Campanian of Sections 13, 14 and 15, and in the Maastrichtian of Sections 12 and 15. It is characterized by progradational and aggradational trends in successions up to ~200 m thick containing tabular and cuneiform beds of fine-to very fine-grained (mainly in the Campanian) and medium-to very coarse-grained bioturbated sandstones (mainly in the Maastrichtian), and locally mudrocks and diagenetic cherts (only in the Campanian). The sandstone beds show tabular geometry, with horizontal lamination, lenticular and wavy bedding, planar and trough cross-bedding, hummocky and swaley cross-bedding, normal and inverse grading, locally symmetric and asymmetric ripples, and massive structures. In addition, glauconite, fish remains, foraminifers, bivalves, and indeterminate bioturbation are reported. Scattered phosphatic peloids, reactivation surfaces, and mud intraclasts are also recorded. These successions are respectively underlain and overlain by offshore and tidal/marsh deposits.

Interpretation: These deposits have been interpreted as accumulated in shoreface environments (Vergara and Rodriguez, 1997).

4.1.3. Eastern foothills

This eastern side of the basin includes Section 16 of Vergara and Rodriguez (1997), Section 17 of Carvajal-Torres et al. (2022), and Section 18 of this work complemented with information of Guerrero and Sarmiento (1996).

4.1.3.1. FA1e fluvial-dominated prodelta. Description: FA1e is recorded in the upper Campanian of Section 18. It is mainly characterized by very thin-to medium-thick tabular- and lenticular-shaped beds of mudrocks, siltstones and very fine-to medium-grained sandstones in aggradational trends, resulting in successions up to ~100 m thick (Fig. 9A–B). The mudrocks exhibit sharp bases, horizontal lamination and massive structures, and high organic matter content. They are interbedded with very thin beds of siltstones and sandstones having internal scours, load and flame structures, lenticular and wavy bedding (with symmetric and asymmetric ripple cross-lamination) (Fig. 9C). Predominantly muddy successions (Fig. 9A) alternate with intervals dominated by tabular sharp-based very fine-to medium-grained sandstones (Fig. 9B) with some phosphatic fragments and showing discontinuous subhorizontal lamination marked by muddy carbonaceous material, asymmetric ripple lamination, and local intercalations of mudrocks forming flaser bedding (Fig. 9D–E). These deposits are unbioturbated (BI = 0) to slightly bioturbated (BI = 1), with some *Thalassinoides* in the muddy beds (Fig. 9F). These successions are underlain and overlain by delta front deposits.

Interpretation: High amounts of carbonaceous material indicate significant terrestrial supply. This, combined with features such as internal scours, tractive and massive structures related fine-grained lithologies, may suggest traction transport or fall-out processes from turbulent flows associated with hyperpycnal currents (Sumner et al., 2008; Zavala et al., 2012; Wilson and Schieber, 2014; Zavala and Pan, 2018; Irastorza et al., 2021). The scarce or absent bioturbation may be related to stress conditions, probably salinity fluctuations in response to the freshwater input and water turbidity, or to high sedimentation rates, or soupground substrates having a low preservation potential (MacEachern et al., 2005; Bhattacharya and MacEachern, 2009; MacEachern and Bann, 2023). The massive mudrocks may be the result of flocculation processes from hypopycnal plumes, producing fluid mud deposits (MacEachern et al., 2005; Bhattacharya and MacEachern, 2009; Ponce et al., 2022), or could represent low-energy episodes with normal marine suspended sediment fall-out deposition (Potter et al., 2005). Relative variations in pollen vs. dinoflagellate content —with proportions of up to 70 % pollen vs. 30 % dinoflagellates in some beds— indicate high continental input (Guerrero and Sarmiento, 1996). These processes are interpreted as being responsible for the fluvial-dominated character of this prodelta environment. In addition, some intervals with horizontally laminated sandstones with phosphatic grains are interpreted as deposited from high-energy flows related to combined flows such as storms (Arnott, 1993; Glenn et al., 1994; Perillo et al., 2014). The rare occurrence of *Thalassinoides* suggests episodes of colonization between fluvial-dominated events (Buatois et al., 2011).

4.1.3.2. FA2e fluvial-dominated delta front. Description: FA2e occurs in the lower Campanian and Maastrichtian of Sections 17 and 18. It is characterized by progradational arrangements of thin to medium tabular beds of mudrocks interbedded with thin to thick tabular and lenticular beds of amalgamated sandstones, and subordinate lenticular beds or pockets of conglomerates, resulting in successions up to ~250 m thick. The sandstones are sharp- and irregular-based, fine-to coarse-grained, with discontinuous horizontal lamination highlighted by muddy carbonaceous material, massive, symmetric and asymmetric ripple cross-lamination, trough cross-bedding, and convolute lamination structures (Fig. 10A–C). Mud intraclast concentrations and bivalve fragments are rarely observed, while the phosphatic fragments are abundant. The mudrocks show horizontal lamination and are generally associated with sandstones forming heterolithic bedding (flaser and

Fig. 9. Fluvial-dominated prodelta FA1e in Section18. **A, B.** General outcrop views showing muddy- and sandy-dominated intervals, respectively. **C.** Interbedded mudrocks and siltstones. Note the scour marks (yellow arrows) and load structures (white arrows) at the base of the siltstone beds. **D.** Fine-grained sandstone with discontinuous horizontal and asymmetric ripple cross-lamination highlighted by muddy carbonaceous material. **E.** Mudrocks and sandstones interbedded, forming wavy bedding. **F.** Mudrocks bioturbated by *Thalassinoides* (*Th*). (For interpretation of the references to color in this figure legend, the reader is referred to the Web version of this article.)

wavy). In some intervals, centimeter-thick beds of highly bioturbated sandstones interbedded with bioturbated carbonaceous mudrocks are evidenced (Fig. 10D–E). Load and flame structures are also common in these intervals. The erosional-based conglomerates are granule-to pebble-grained, structureless, with subrounded and poorly sorted muddy clasts (Fig. 10F). Normal grading is occasionally observed between pebble-size conglomerates and medium-to coarse-grained sandstones. Toward the top of the succession, carbonaceous muddy and sandy-muddy beds up to 80 cm thick, with high amounts of organic matter, are registered (Fig. 10A–D). These beds have sharp and erosional bases and transitional irregular tops, horizontal lamination, and exhibit bioturbation represented almost exclusively by *Thalassinoides* and sporadically *Teichichnus* (BI = 2, 4), with diameters up to 6 cm. These levels are overlain by sandy beds that also show a high content of organic matter as sheets, organized forming a subtle horizontal lamination. A diverse and abundant (BI = 2, 4) trace fossil assemblage, composed of *Conichnus*, *Palaeophycus*, *Planolites*, *Rhizocorallium*, *Skolithos, Taenidium*, *Teichichnus* and *Thalassinoides*, characterizes these beds. A less abundant (BI = 1, 2) and diverse ichnoassemblage composed of *Ophiomorpha*, *Palaeophycus*, *Planolites* and *Thalassinoides* is observed throughout the succession, mainly associated with sandstones. Bed bases colonized exclusively by *Rhizocorallium* and *Thalassinoides* are recorded in the lower part of the succession (BI = 4) (Fig. 10G–H). Amalgamated fine-grained sandstone beds forming successions up to 6.5 m thick, colonized almost exclusively by *Ophiomorpha* and in a minor proportion *Palaeophycus* and *Planolites* are also recorded at the base of the section. These successions are underlain and overlain by swamp/coastal lagoons, and marsh/estuarine deposits, respectively.

Interpretation: This facies association may be related in a general context to high-energy environments associated with oscillatory and

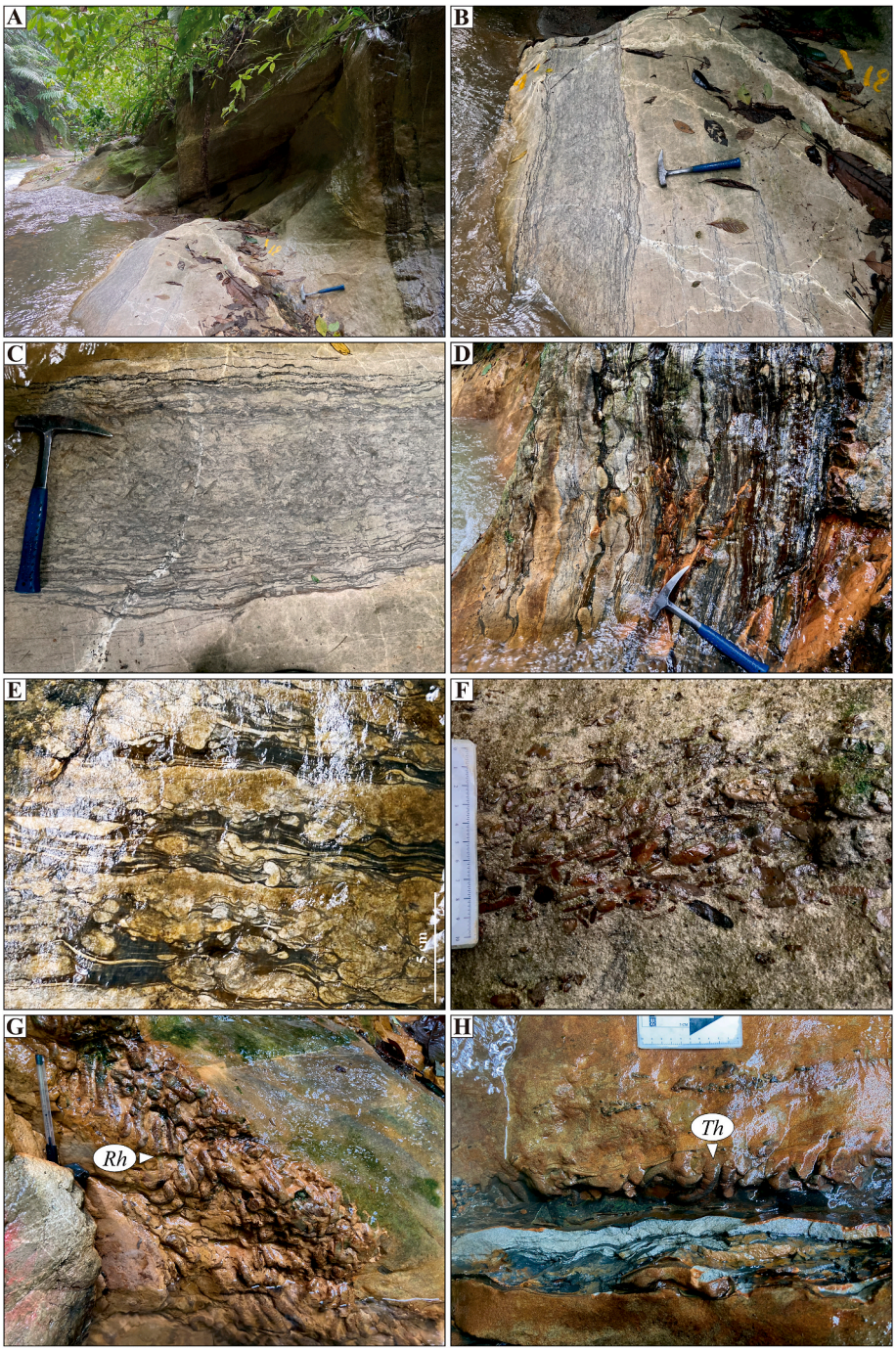

Fig. 10. Fluvial-dominated delta front FA2e in Section 18. **A.** General outcrop view. **B, C.** Sandy beds with subtle horizontal lamination highlighted by sheets of organic matter. Note abundant bioturbation. **D, E.** Medium-grained sandstones beds alternating with dark mudrocks drapes. Note the bioturbation associated mainly with sandstones. **F.** Pebble-size conglomerates grading into a coarse-grained sandstone. **G, H.** Base of a sandstone bed bioturbated exclusively by *Rhizocorallium* (*Rh*) and *Thalassinoides* (*Th*).

combined flows, like those recorded in shoreface-foreshore environments, within which some energy fluctuations may also be recorded. Yet in contrast to shoreface settings, these successions are considered as delta front deposits due to the abundance of carbonaceous material, suggesting phytodetrital pulses from fluvial discharges (MacEachern et al., 2005; MacEachern and Bann, 2023). In addition, these deltaic environments feature the occurrence of soft-sediment deformation structures related to sedimentary loading along steep slopes (MacEachern et al., 2005; Buatois et al., 2012). These structures may also be associated with deformation related to external factors such as earthquakes (e.g., seismites; Seilacher, 1969). The erosive conglomerate beds or pockets are interpreted as bedload arriving at the delta front linked to mouth bar deposits (van Yperen et al., 2020; Ponce et al., 2022). Intervals of massive (by bioturbation) sandstones interbedded with carbonaceous bioturbated mudrocks (colonized from the top down; Fig. 10E) suggest fluctuations in hydrodynamic energy; high-energy periods accumulating sandy beds alternate with the fall-out deposition of muddy beds. These muddy beds are considered as mudrock drapes, related to deposition by flocculation from hypopycnal plumes (MacEachern and Bann, 2023). The high bioturbation in sandy layers indicates the establishment of a well-developed macrobenthic trace-maker community between river flood events (mudstone drapes) under

normal, favorable marine conditions. Similar interpretations are suggested for the organic-rich muddy and sandy-muddy beds overlain by highly bioturbated sandstones that occur toward the top of the succession. These organic-rich beds would mark hyperpycnal deposits, linked to sudden fluvial flows arriving at the delta front, supported by the erosive bases and the record of *Thalassinoides* and *Taenidium* alone, possibly linked to brackish, less favorable conditions. The abundant bioturbation assigned to the *Cruziana* ichnofacies in the overlying sandstones could reveal wave-dominated periods, after fluvial discharges. The low record of trace fossils associated with suspension-feeders, as opposed to deposit-feeders, can be interpreted as a scarcity of suspension food, or high turbidity, suggesting that organic matter was transported mainly by hyperpycnal flows (MacEachern et al., 2005; MacEachern and Bann, 2023). The scarce levels with bivalve and phosphate fragments are considered as the result of storm events remobilizing material from distal areas (Glenn et al., 1994; Myrow and Southard, 1996). This difference between marine-dominated and those fluvial-dominated deposits is supported by the pollen vs. dinoflagellate record, which is 95 %–5 % in some cases and 70 %–30 % in others (Guerrero and Sarmiento, 1996).

4.1.3.3. FA3e shoreface. Description: FA3e is recorded in the Campanian and lower Maastrichtian of Section 16. A succession of ~260 m thick of sandstones and subordinate mudrocks arranged in progradational and aggradational trends characterizes these deposits. The tabular beds of fine-to medium-grained sandstones show massive, wavy bedding structures, while the mudrocks form tabular beds having horizontal lamination and lenticular bedding. Plant remains, phosphatic peloids, mud intraclasts and indeterminate bioturbation are common. These successions are respectively underlain and overlain by swamp/coastal lagoons and swamp/estuarine deposits.

Interpretation: Shoreface environments are interpreted for these deposits (Vergara and Rodriguez, 1997).

4.2. *Depositional model: spatial distribution and stratigraphic evolution of sedimentary deposits and processes*

The stratigraphic correlation of well-dated successions allows us to observe the distribution and evolution along-strike (Figs. 11 and 12) and cross-strike (Fig. 13) of depositional sedimentary systems during the Campanian-Maastrichtian. The vertical (stratigraphic) and lateral (spatial) relationship between calcareous, mixed (shelf) and siliciclastic (offshore, shoreface, fan delta, delta front, prodelta, tidal, swamp, fluvial) facies associations and sedimentary environments provide insight into the dominant sedimentary processes and depositional conditions in the final stages of the epeiric La Luna Sea during the Campanian-Maastrichtian. Two distinct phases are recognized in the basin during this period: one characterized by marine processes during the Campanian and early Maastrichtian, the other by marginal/transitional and continental processes during the late Maastrichtian (Figs. 14 and 15). At the marine phase, two different sedimentary systems are distinguished: a normal shoreface-basin profile that includes shelf, offshore, and shoreface-foreshore environments towards the western and central parts; and a delta profile in the eastern part, consisting of delta front to prodelta settings. These are respectively overlain by fan delta complex, tidal and fluvial deposits, and swamp and estuarine deposits, associated with the marginal-continental phase.

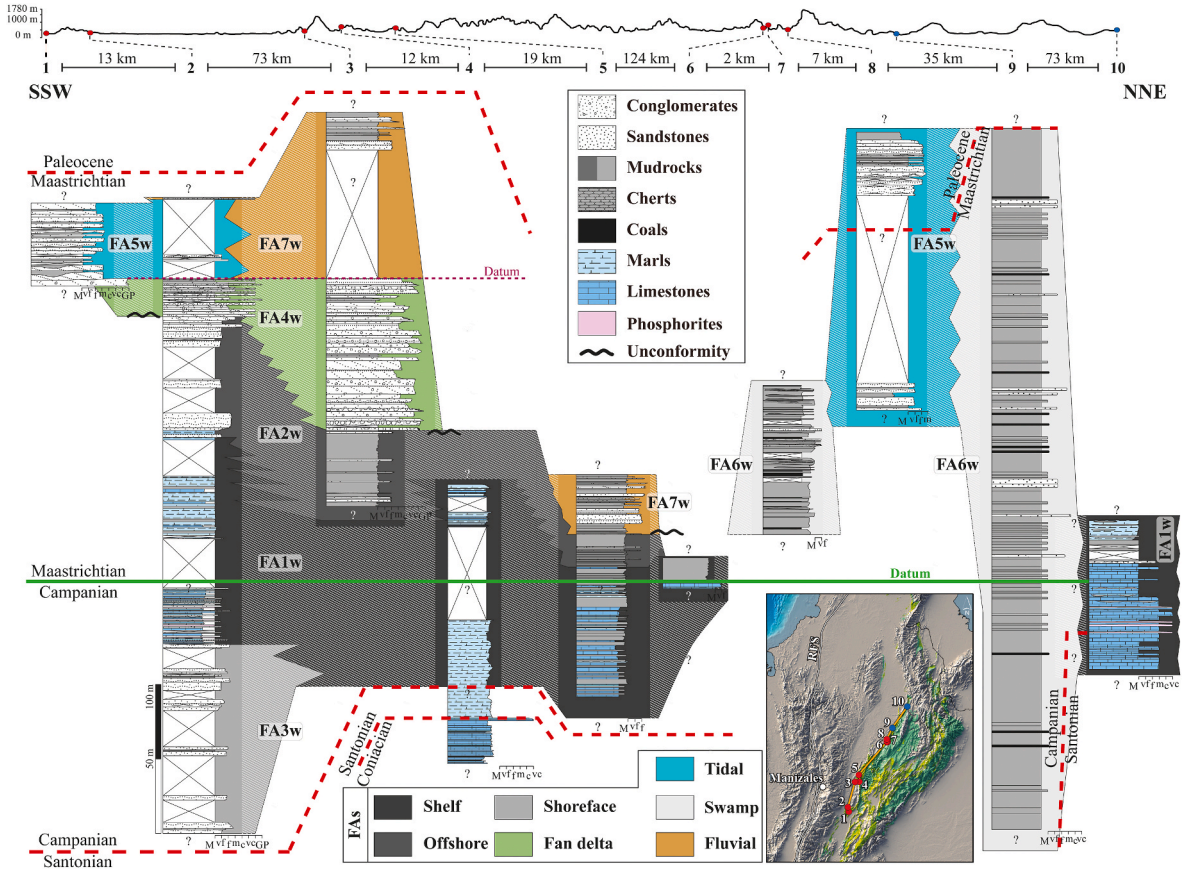

Fig. 11. Western along-strike correlation transect. The topographic profile shows the current location of the studied sections. Datum: approximate Campanian-Maastrichtian boundary and the top of fan delta deposits. Light areas with steep lines represent uncertainty in the stratigraphic correlation of the depositional settings.

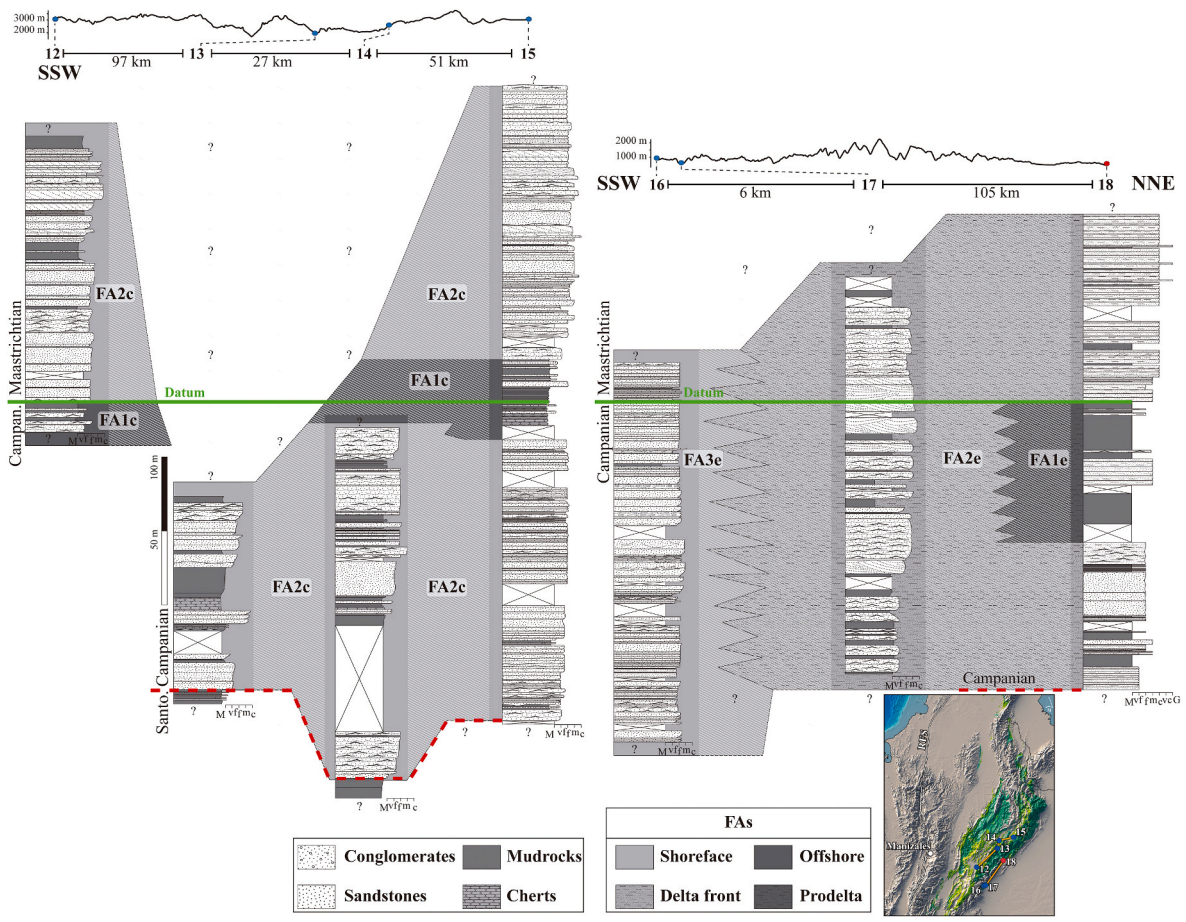

Fig. 12. Central and eastern along-strike correlation transects. The topographic profile shows the current location of the studied sections. Datum: approximate Campanian-Maastrichtian boundary. Light areas with steep lines represent uncertainty in the stratigraphic correlation of depositional settings.

4.2.1. Along- and cross-strike depositional trends and processes

4.2.1.1. Western zone. In the southwestern area, shoreface deposits overlie Santonian siliciclastic shelf deposits, associated with a progradational trend due to relative sea-level fall (Guerrero et al., 2000; Guerrero, 2002). They represent the onset of Campanian siliciclastic sedimentation in this sector of the basin (Section 2), while towards more northerly sectors (Sections 4 and 10), the deposition continues in carbonate and mixed shelf environments (Fig. 11). Thus, lower Campanian sedimentation in this region was dominated by high energy processes related to wave activity in shoreface environments, influenced by sporadic storm events (FA3w) and by suspended fall-out in shelf settings. These environments were unfavorable for the establishment of a macrobenthic tracemaker community, as indicated by the record of scarce or no bioturbation. However, a high abundance of benthic foraminifers has been reported (Guerrero et al., 2000), suggesting favorable habitats for microorganisms.

Above the shoreface deposits, during the late Campanian, shelf environments (FA1w) expanded and were also developed and distributed along the southwestern zone of the basin (Figs. 11 and 14), associated with a retrogradational trend due to relative sea-level rise (Guerrero et al., 2000; Guerrero, 2002). These shelf deposits, marking the deepest part of the basin for this epoch, were characterized by suspended fall-out deposition of calcareous and siliciclastic material, with a local influence of weak bottom currents, and an absence of significant seafloor colonization by macrobenthic tracemaker organisms, reflected in the rare or absent record of bioturbation. This might suggest depositional settings characterized by low oxygenation or nutrients availability. However, amounts of total organic carbon between 3 % and 7 % have been reported in these rocks, associated with upwelling processes (Föllmi et al., 1992; Villamil et al., 1999; Martínez, 2003; Patarroyo et al., 2017, 2021), ruling out this possibility. Thus, a low oxygenated environment can be interpreted, as supported by geochemical and micropaleontological analysis (Martínez, 2003; Patarroyo et al., 2023), as the main parameter controlling the colonization by macrobenthic tracemakers.

A marked change from calcareous-dominated to mixed- or siliciclastic dominated shelf and offshore deposits is evidenced in this basin area between the late Campanian and early Maastrichtian (Fig. 11). This change in mud composition (termed xenoconformity; Carroll, 2017) has been associated with freshwater input and an increase in the terrigenous sediment supply, linked to a regressive phase and tectonic activity generated by the accretion of western allochthonous terranes (Villamil et al., 1999; Guerrero et al., 2000; Guerrero, 2002; Bayona, 2018; Montes et al., 2019; Patarroyo et al., 2017, 2023). Different authors hold that the end of calcareous sedimentation occurred at the end of the Santonian and/or Campanian (Cooper et al., 1995; Ayala-Calvo et al., 2009; Bayona, 2018; Sarmiento-Rojas, 2019; Terraza, 2019; Pastor-Chacón et al., 2023). Section 6 shows the change in the approximate Campanian-Maastrichtian boundary, but Sections 2, 4, 5, and 10 show calcareous and mixed deposits even in the Maastrichtian (Fig. 11). The present stratigraphic correlation suggests that this change is diachronic throughout the basin, and its distribution is not only associated with an unconformity in certain areas but could be geographically controlled (location within the basin) in places where the sedimentation is continuous (Figs. 11, 13 and 14). Therefore, it is possible to infer that the areas where the change occurred first were those close to emerged areas or directly connected to the systems that transported the siliciclastic material through continental runoff, while areas where carbonate

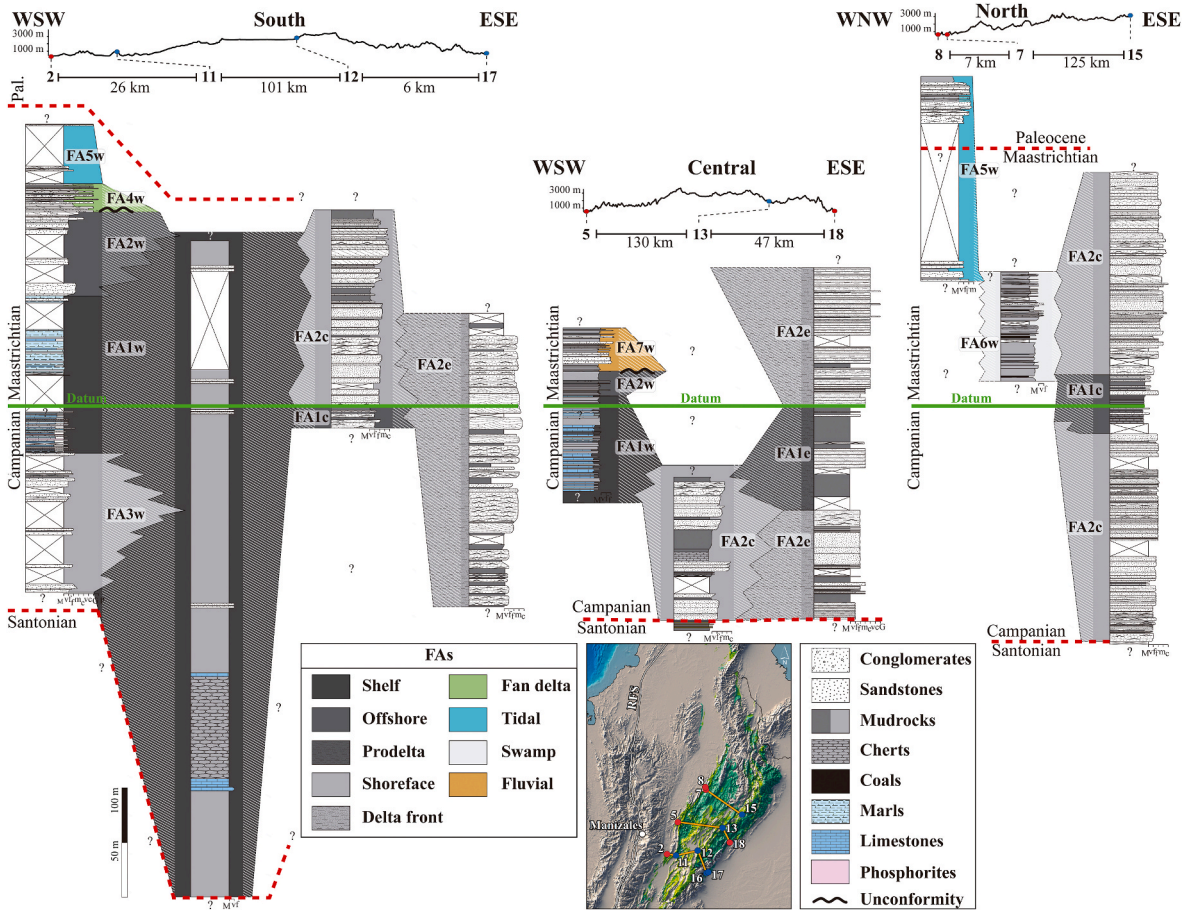

Fig. 13. South, central and north cross-strike correlation transects. The topographic profile shows the current location of the studied sections. Datum: approximate Campanian-Maastrichtian boundary. Light areas with steep lines represent uncertainty in the stratigraphic correlation of the depositional settings.

sedimentation continued were most likely protected areas or distant from continental systems. Intra-basin uplift blocks further to the southeast that occurred in the late Campanian may also have influenced these changes in sediment composition and distribution, and/or be associated with the development of the unconformity (Carvajal-Torres et al., 2022).

The siliciclastic/mixed/carbonate shelf evolved towards the SW part to deposits interpreted as offshore settings in the early Maastrichtian (FA2W; Fig. 11). The accumulation of these deposits was dominated by suspension settling and the influence of storms. Benthic conditions improved in these deposits, allowing in some cases the establishment of diverse and abundant macrobenthic tracemaker communities belonging to the *Cruziana* ichnofacies. The favorable conditions are further evidenced by geochemistry and micropaleontology, which indicate eutrophication and better oxygenation of the bottom waters in Section 10 (Patarroyo et al., 2023).

The most important change in deposits, and therefore in the depositional processes, took place in the southwestern zone of the central (this work) and south (Upper Magdalena Valley Basin) parts of the basin during the late Maastrichtian, associated with the transition from marine to marginal-continental phase, indicating rapid and significant changes in sedimentary dynamics (emerged vs catchment areas) (Figs. 11 and 14). The offshore deposits (FA2w) are overlain by coarse-grained fan delta complex deposits (FA4w) to the south and central parts (Section 1 and 3), and by fluvial deposits (FA7w) to the north (Section 5), representing the progradation of the marginal and continental sedimentary systems (Figs. 11 and 14). Although micropaleontological studies provide no evidence of missing time, this marked change represents an erosional unconformity in the sedimentary record (e.g., Veloza et al., 2008; Mora et al., 2010).

The conglomerate-dominated deposits —comprising the Cimarrona Formation— indicate very energetic processes during their accumulation, associated with channel deposits whose characteristics suggest a braided fluvial system (Gómez and Pedraza, 1994; Miall, 1996; Einsele, 2000; Giraldo-Villegas et al., 2024). These channels drained alluvial fans coming from the proto-Central Cordillera, according to detrital signals and paleocurrents (Gómez and Pedraza, 1994; Guerrero et al., 2020; Valencia-Gómez et al., 2020), and reached the coastal plain, forming mouth bar deposits and fan delta complexes where a scarce macrobenthic tracemaker community was established, due to the high erosive power and constant supply of fresh water (Giraldo-Villegas et al., 2024). Towards the eastern side, coeval coarse-grained deposits are not reported thus far (see below). The thickness of these deposits increases to the north, reaching up to ~100 m in Section 3 (Fig. 11), suggesting the location of a depocenter or arrival of the major channel systems. The fact that lateral expressions are not evidenced in our WSW-ESE correlations (Figs. 13 and 14), would indicate local extension or strong reworking by waves towards the central part of the basin. Accordingly, this sedimentary record provides direct evidence of the growth of the proto-Central Cordillera, and the development of an important sediment source relief.

Tidal (FA5w) to the south, and fluvial environments in the central part, overlie the coarse-grained sedimentation; again they represent a reaccommodation of sedimentary systems and a decrease in hydrodynamic energy as compared to the underlying deposits. The tidal deposits contain the record of flooding and ebbing. Because these marginal depositional settings are influenced by freshwater input and the arrival of sediments, the resulting environment is unfavorable for colonization

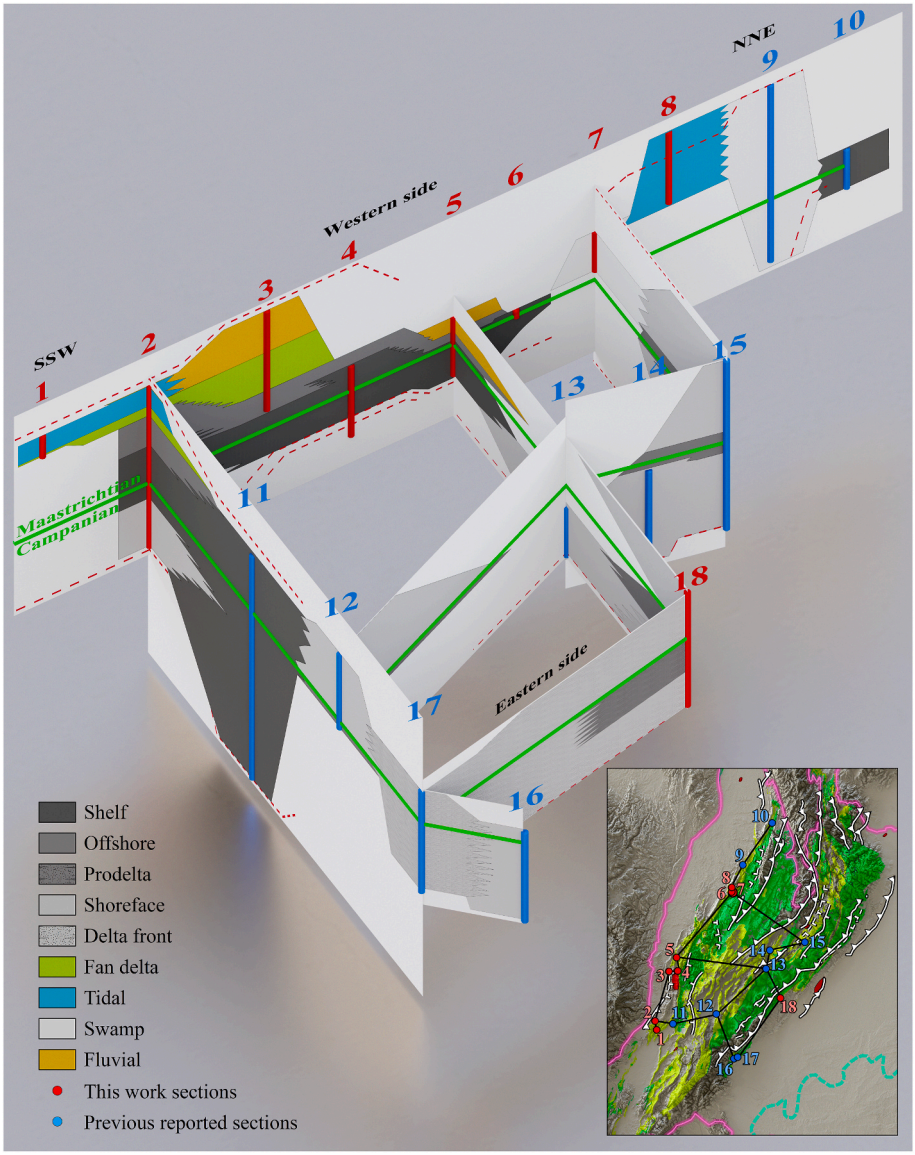

Fig. 14. 3D diagram (not to scale) showing the correlation between SSW-NNE and WSW-ESE transects and the distribution of sedimentary environments.

by a marine macrobenthic tracemaker community, as reflected by the scattered and sparse bioturbation recorded. The tidal environments change laterally to the north, to fluvial deposits of a fine-grained nature, with associated floodplains and crevasse splays, common features of anastomosed and/or meandering fluvial systems (Miall, 1996). The change in grain size (from the coarse-grained fan delta complex to the fine-grained tidal and fluvial deposits) reflects a marked change in hydrodynamic parameters possibly linked to the geomorphological/topographical configuration or differential erosion of emerged areas. The coarse-grained facies formed relatively close to the coast, implying less transport and considerable relief, associated with the development of alluvial fans in the most proximal parts and fluvial and fan delta deposits in the most distal positions, while still preserving their gravelly nature. In contrast, the fine-grained fluvial successions are associated with extensive, relatively flat areas that transported sediment over long distances. This change in depositional processes occurred over a relatively short period of time and space, suggesting important and rapid topographic or geomorphological changes in the western border. In Section 5, fluvial deposits overlie offshore successions, suggesting an unconformity.

In the northwesternmost part of the basin, the late Campanian is represented by two different depositional systems. One is associated with the calcareous shelf systems (Section 10), similar to those of the SW part, and the other related to marsh (Section 9) (Figs. 11 and 14). The late Campanian swamp settings (FA6w) are observed only in this area, implying that singular depositional parameters (compared to the general shelf context of most of the basin) prevailed locally during this period. The shallower near-continent areas point to an irregular basin border, providing high amounts of organic matter of terrestrial origin, hence favoring the accumulation of these successions. Moreover, these settings had a direct connection with the sea, evidenced by the presence of ?*Gyrolithes*, and several levels with marine palynomorphs (Montaño et al., 2016).

Swamp sedimentation continued in this area during the Maastrichtian (Sections 7 and 9), with some lateral variation to tidal deposits (Section 8) (Figs. 11 and 14). Tidal settings are correlated with the SW part (Sections 1 and 2), showing similar features, plus an absence of trace fossils suggesting unfavorable environments for the macrobenthic tracemaker community.

4.2.1.2. Axial zone. The central part of the basin was dominated by shallower depositional settings than the western zone (Figs. 12–14), and

environments that were slightly more distal or similar to those at the eastern area suggesting an off-axis basin. The Campanian sedimentation in this sector also overlies fine-grained deposits accumulated in estuarine to shelf environments, dominated by wave and storm processes (Vergara and Rodriguez, 1997). The lower Campanian deposits begin with shoreface successions (FA2c), indicating a regressive event as in the western side of the basin. These environments were dominated by waves and storms, and locally by tidal processes, providing favorable benthic conditions according to bioturbation. An abundant and diverse ichnoassemblage composed of *Arenicolites*, *Arthrophycus*, *Crossopodia*, *Cylindrichnus*, *Gordia*, *Laevicyclus*, *Planolites*, *Protovirgularia*, *Rhizocorallium*, *Scolicia* and *Thalassinoides* is reported by Pérez and Salazar (1978) for these deposits, and of *Arenicolites*, *Asterosoma*, *Diplocraterion*, *Helminthopsis*, *Ophiomorpha*, *Phycodes*, *Planolites*, *Rhizocorallium*, *Rosselia*, *Skolithos*, *Teichichnus*, *Thalassinoides*, and *Zoophycos* in southern deposits of the Guando oil field (Leckie et al., 2003), reflecting the development of a permanent macrobenthic community, in contrast to the westward coeval deposits. Offshore deposits (FA1c) that overlie these successions evidence a relative deepening of the sedimentary systems during the late Campanian-early Maastrichtian, as seen for the western and eastern sides (Figs. 12 and 13). In these environments suspension sedimentation prevailed, with a local influence of storm deposits. Scarce bioturbation suggests unfavorable benthic conditions for the tracemaker community. Overlying these deposits, shoreface environments were reestablished during the early to late Maastrichtian, when wave processes constituted the predominant sedimentation mechanism (Figs. 12 and 13). The ichnoassemblage composed of *Arenicolites*, *Cylindrichnus*, *Fraena*, *Gordia, Planolites*, *Protovirgularia*, *Rhizocorallium*, *Scolicia*, and *Thalassinoides* (Pérez and Salazar, 1978) indicates a weak influence of stress conditions (i.e., low oxygenation, brackish conditions, high sedimentation rate) during the accumulation of these deposits. This bioturbation is mainly associated with the contacts between shoreface sandy bodies and disappears again when paleoenvironmental conditions change in the overlying units (Pérez and Salazar, 1978; Sarmiento, 1992).

4.2.1.3. Eastern zone. The eastern segment of the basin is represented by deltaic deposits. As in the western and central parts, they overlie fine-grained deposits accumulated under estuarine to shelf environments, meaning a regressive event occurred at the end of the Santonian (Guerrero and Sarmiento, 1996). The early Campanian sedimentation begins with fluvial-dominated delta front successions (FA2e) having high continental organic content. Still, features such as storm beds and the trace fossil assemblage suggest that these sandy seafloors were locally reworked by wave activity. Similar to the shoreface deposits of the central part, these deltaic successions are bioturbated by an abundant and diverse ichnoassemblage belonging to *Cruziana* ichnofacies, so that habitats were suitable for the tracemaker community during wave-dominated periods of the system. These systems stratigraphically evolve into upper Campanian-lower Maastrichtian prodelta deposits (FA1e) that were dominated by fall-out and tractional transport processes from hyperpycnal flows and hypopycnal plumes, sporadically influenced by storm events. Altogether, the high amount of carbonaceous debris along with sparse bioturbation indicates a significant terrestrial supply through the influence of dominant river-fed hyperpycnal flows (Mulder and Alexander, 2001; Mulder et al., 2003; Zavala and Pan, 2018). The freshwater input —causing salinity fluctuations— carrying the continental sediments, plus the associated turbidity, created an unfavorable environment for the marine macrobenthic community.

Above these fluvial-dominated prodelta deposits, fluvial-dominated delta front environments were reestablished during the early Maastrichtian. Their deposits resemble those accumulated during the early Campanian, but the upper part offers evidence of mouth bars and levels whose high organic debris content signal fluvial flows generated during sudden floods (flood deposits), which are overlain by highly bioturbated deposits (interflood deposits). Overall, there was a strong interaction between fluvial- and marine-dominated processes in the delta front environments. To the south, Section 16 provides evidence of shoreface environments (FA3e) during the Campanian and early Maastrichtian, suggesting limited delta influence. During the late Maastrichtian there was no deposition in the region surrounding this section as it was a zone of positive relief (<500 m; Carvajal-Torres et al., 2022).

5. Discussion

5.1. Sedimentary system dynamics: western vs central-eastern zones

5.1.1. Sedimentology and stratigraphy

From its beginnings, the studied NNE-SSW oriented basin bounds different geologic domains on either side. To the west, a volcanic arc was active since Jurassic times, whereas stable areas to the east were linked to the Amazonian Craton (Cooper et al., 1995; Sarmiento-Rojas, 2001; Guerrero et al., 2020). Campanian-Maastrichtian deposits beyond the eastern side of the Eastern Cordillera Basin (within the Eastern Llanos Basin, Fig. 1), and beyond the western side, toward the north of the Middle Magdalena Valley Basin (i.e., east and west of the studied eastern and western section), are identified only from borehole studies. Thus, in order to establish the differences in the depositional processes and settings on both zones of the basin, the present research considers these easternmost and westernmost sections representative of the accumulation parameters for the eastern and western sides of the basin at that time.

According to our data, the geologic reliefs surrounding the epeiric basin bore a great influence on the basin filling processes and types of deposits of the La Luna Sea, at least in the final stages during the Campanian-Maastrichtian. Comparison among the western and central-eastern sections during the Latest Cretaceous reveals significant differences (Figs. 14 and 15). The stratigraphic and spatial variation of deposits and sedimentary environments is more diverse towards the western zone (shoreface, shelf, offshore, fan delta complex, fluvial, tidal, marsh), while the eastern and central areas show a more homogeneous distribution (shoreface-delta front, offshore-prodelta) (Fig. 13). This suggests that the western area harbored higher activity between the feeder (source) and receiver (sink) areas, perhaps in response to the dynamics of the volcanic arc, the growth of the proto-Central Cordillera and the unroofing of the sedimentary cover tied to the Caribbean Plate collision. Further influence was induced by the major fluvial inputs to the basin (see below). Another key element that may have influenced the variability of environments, deposits, and sedimentary parameters on both sides of the basin is the size and topography of the emerged areas, which are smaller in size and higher in elevation on the western side and larger and lower in elevation on the eastern side.

Within this western side, Sections 1 to 5 show the greatest paleoenvironmental variability compared to Sections 6 to 10. It is important to consider that, according to the palinspastic reconstructions (Sarmiento-Rojas, 2001; Tesón et al., 2013; Bayona, 2018; Montes et al., 2019; González et al., 2023), these southern sections were closer to the proto-Central Cordillera (today ~20 km) than the northern sections (today ~70–100 km) during the accumulation of the deposits. Therefore, it is possible to interpret that these southern sections, being closer to the western border or coastline and thus to the proto-Central Cordillera, register a greater variability in the type of deposits compared to the northern sections, which were in more distal positions.

During the Campanian-early Maastrichtian, deeper environments dominated the western area, marking the most distal parts of the basin during this period. In contrast, the central and eastern zones correspond to shallower settings associated with shoreface and deltaic deposits (Figs. 14 and 15). Accordingly, the basin was asymmetric, possibly developed as flexural response to the uplift of the proto-Central Cordillera, or perhaps related to fault front of the Central Cordillera to

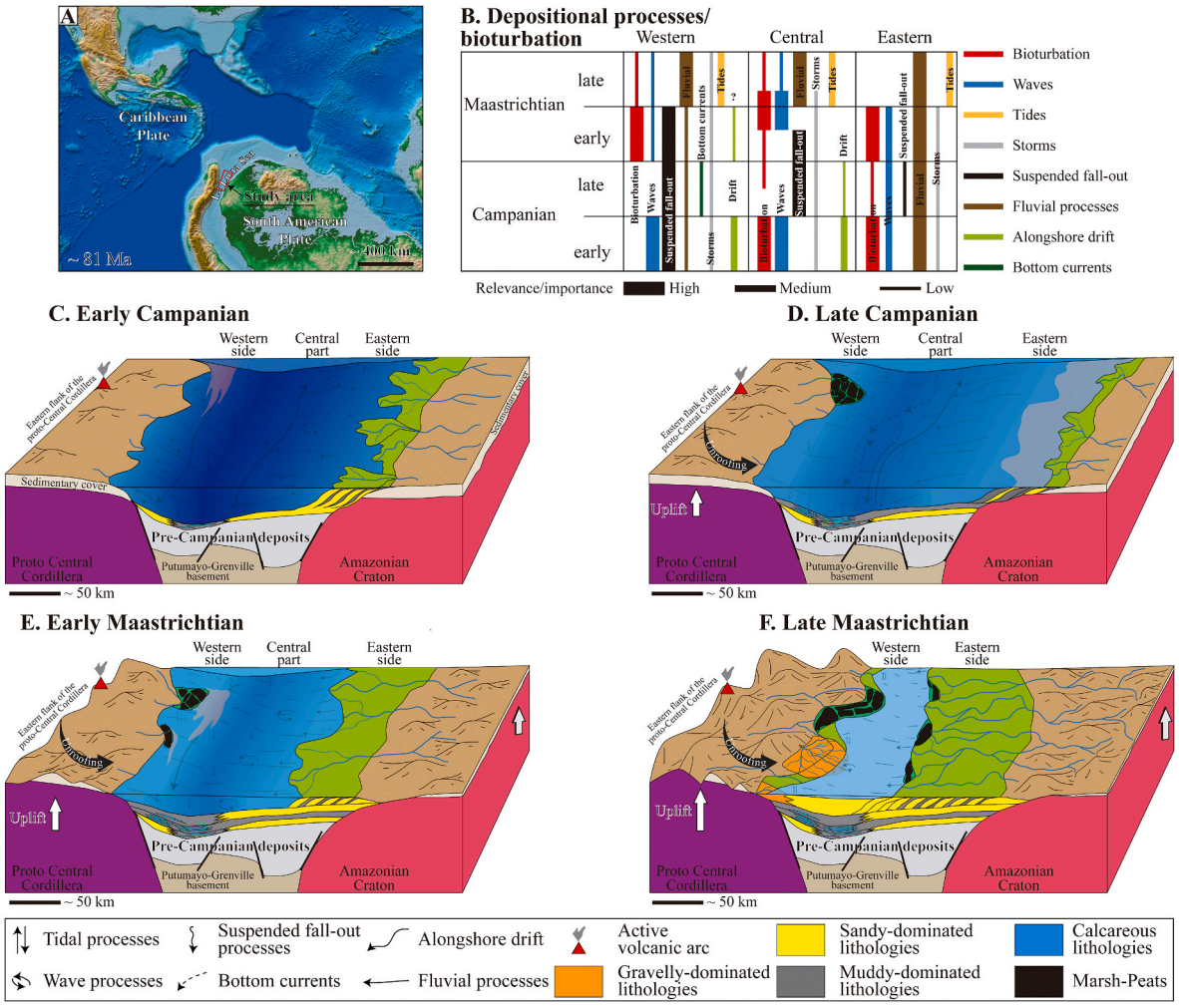

Fig. 15. Paleogeographic reconstruction of the last stages of the central part of the La Luna Sea. **A.** Paleo-tectonic configuration of the northwestern margin of South America at 81 Ma showing the La Luna epeiric sea and the approximate location of the study area (from Salles et al., 2022). **B.** Summary of depositional processes/bioturbation and their occurrence in different parts of the basin during the Campanian-Maastrichtian. **C, F.** Schematic representation of the evolution of sedimentary systems of central part of the La Luna Sea during the early Campanian-late Maastrichtian.

the west and passive tilting of the eastern zone (e.g., Mora et al., 2020; Pastor-Chacón et al., 2023), where the shallower environments of the western area were very narrow or not preserved (Fig. 15). Even though the main source of terrigenous sediments was located to the east during this period, they did not affect the calcareous sedimentation at the western zone (Fig. 13), most likely due to the distance of these sections at the time of accumulation (>40 km to the west of its current position; Tesón et al., 2013; Bayona, 2018) and a mainly north-south redistribution of sediments. The western zone was therefore relatively isolated, receiving sedimentation purely from marine processes.

Moreover, these uppermost Cretaceous successions highlight the role of fluvial systems along the eastern area of the epeiric La Luna Sea since the Campanian. In contrast, fluvial systems on the western zone developed sporadically during the late Campanian-early Maastrichtian, becoming dominant in the late Maastrichtian. Still, sandy deposits were regionally distributed towards the southwestern zone during the early Campanian (FA3w) (e.g., Upper Magdalena Valley Basin, Cooper et al., 1995; Guerrero et al., 2000; Veloza et al., 2008; Roncancio and Martínez, 2011; Sarmiento-Rojas, 2011, 2019; Garzón et al., 2012), and their provenance remains unclear. Although some of these deposits have been interpreted as originating from the proto-Central Cordillera (e.g., Cobre Formation, Caicedo et al., 2000), the associated land-ocean systems responsible for delivering this material to the basin are not yet documented for the western side in proximity to these sandy deposits.

Understanding the sedimentary environments in an integrated framework raises questions about the fluvial systems and associated deposits that transported these sediments to the basin during the early Campanian. Northward, Section 9 contains Campanian swamp environments most likely associated with fluvial systems carrying vast amounts of organic material to the coastal environments. It is therefore logical to infer that the early Campanian sandy deposits were transported by littoral drift from deltaic environments associated with well-established fluvial systems at more northerly or southerly areas. This premise would be supported by the north and south paleocurrents recorded in coeval deposits of the central part (e.g., Pérez and Salazar, 1978).

Similar processes occur during the early Maastrichtian —prior to the establishment of the river systems in the western side— when important changes in paleosalinity between the shelf limestones and overlying shelf and offshore mudrocks beds took place (Patarroyo et al., 2023), indicating an increase in the siliciclastic and freshwater input, but nearby sediment sources have not been reported. Coeval lower shoreface sandstones have been reported eastward in the Cocuy region (~130 km), towards the axial zone of the Eastern Cordillera, suggesting possible sediment sources to this area (Fabre, 1985; Bayona et al., 2021). As occurred with the Campanian deposits, these siliciclastic muddy deposits may have been transported in suspension or by longshore currents from other basin areas.

Comparable processes took place in the southern sector of the basin (Upper Magdalena Valley Basin) during the Albian. Thick sandstone deposits associated with shoreface and foreshore environments, with detrital signatures from geologic units outcropping to the west (proto-Central Cordillera; Duarte et al., 2016; Guerrero et al., 2020), show no evidence of coeval fluvial systems in proximity to these deposits sourced from westerly areas, suggesting sediment transport from other basin areas. Comparable conditions linked to deposition by littoral drift have been reported for ancient epeiric seas and present-day marine sedimentary environments (Zviely et al., 2007; Garzanti et al., 2014, 2015; Schwarz et al., 2017, 2022; Rovere et al., 2019).

Another particular case entails emerged regions that were present (proven by the detrital signal) in southerly areas during the Maastrichtian, yet apparently did not contribute sediment to the basin (e.g., Calderon-Diaz et al., 2024). This could be explained by relatively flat emerged areas, of low-elevation and not very extensive, having drainage networks close to the sea, and under particular climatic conditions unfavorable to the development of large drainage systems able to supply large sediment loads eventually preserved in the fossil record; such characteristics are more common in passive or stable tectonic settings —e.g. the eastern boundary studied here (Boggs, 2014). Another explanation could be associated with the development of small closed basins where rivers end in intracontinental lacustrine-marine systems. Nevertheless, the existence of intra-basin uplift blocks (e.g., Carvajal-Torres et al., 2022) acting as sediment traps, or the existence of very specific sedimentary pathways associated with basin floor morphology, are not excluded.

5.1.2. Ichnology

Trace fossil assemblages also show marked differences depending on location. In the Campanian, the seafloor on the western side of the central part of the La Luna Sea shows unfavorable conditions for the macrobenthic tracemaker community (Fig. 15B), e.g. low-oxygen muddy bottoms generated in response to high productivity phenomena (Föllmi et al., 1992; Villamil et al., 1999; Erlich et al., 2000, 2003). In contrast, the central and eastern parts record the activity of an abundant and diverse tracemaker community, that is favorable conditions for macrofauna in shallower settings, controlled or influenced by sediment removal processes (e.g., tides, waves) providing for bottom reoxygenation and food availability from the fluvial supply (Fig. 15B). In the Maastrichtian, although both sides of the basin harbored macrobenthic tracemaker communities, the conditions were generally less favorable than in Campanian times, probably due to increased continental input (freshwater and continental detritus) (e.g., Aumond et al., 2021). However, in the southwestern and northeastern parts of the basin, local bioturbation has been reported in the Campanian sandy deposits, even in currently producing reservoirs (e.g., Guando and Cusiana oil fields), indicating a heterogeneous distribution of environmental parameters within the basin (Warren and Pulham, 2001; Leckie et al., 2003; Rincón et al., 2003; Veloza et al., 2008; Hernández-Duran, 2021). Thus, as indicated by the depositional parameters and therefore the sedimentary environments, the behavior of the central and eastern parts is different from that of the western area (Fig. 15B).

5.2. Allogenic vs autogenic depositional controls

Allogenic and autogenic depositional parameters stratigraphically control the resulting sedimentary successions. Tectonics, subsidence and climate are the main external factors, while channel avulsion, delta lobe switching, relocation of alluvial channel belts and submarine fans are the main internal depositional controls (Catuneanu, 2022). These processes interact over time and define the filling of a sedimentary basin. The distinction between tectonics and eustasy is not straightforward; they are generally related, i.e., tectonism can lead to eustatic changes. In this case, however, scale plays an important role, both in terms of area and time. The Cretaceous epeiric basin of Colombia was tectonically controlled, as evidenced by the changes in deposit thickness (Cortés et al., 2005; Gómez et al., 2003, 2005; Sarmiento-Rojas et al., 2006; Bayona, 2018; Carvajal-Torres et al., 2022). In addition, during the Late Cretaceous-Paleocene the tectonic subsidence increased due to horizontal compressional stress from the collision of the oceanic terranes along the northwestern margin of South America (Gómez et al., 2005; Sarmiento-Rojas et al., 2006). This collision resulted in the uplift of the proto-Central Cordillera, which triggered the erosion of a sedimentary cover on its eastern flank (Gómez et al., 2003, 2005; Villagómez and Spikings, 2013; Zapata et al., 2021, 2024), leading to increased sediment input into the basin. Consequently, the filling of the La Luna Sea was driven by these tectonic processes rather than by global sea-level fall (Gómez et al., 2005).

In sedimentary terms, despite significant sediment loading through fluvio-deltaic interactions on the eastern side from the early Campanian to the late Maastrichtian, related to large drainage systems developed over extensive tectonic stables settings, the collision of the Caribbean Plate with the South American margin meant even higher sediment flux on the western margin, probably resulted from unroofing of the sedimentary cover (Gómez et al., 2003; Moreno-Sánchez and Pardo-Trujillo, 2003; Zapata et al., 2021, 2024). This may have contributed to the rapid and pronounced shift between offshore and fan delta complex deposits at the western side of the basin during the Maastrichtian, as well as the earlier development of fully fluvial environments as compared to the eastern side (Fig. 15). Such a marked change is also registered in other western parts of the basin. To the south, in the Upper Magdalena Valley Basin, coeval deposits known as La Tabla and Moserrate formations likewise overlie fine-grained shelf deposits, and their depositional settings vary between shoreface and offshore (Guerrero et al., 2000; Veloza et al., 2008; Roncancio and Martínez, 2011). La Tabla Fm. shares characteristics with the Cimarrona Fm. —previously described fan delta facies—, yet there is a notable difference in grain-size and lithological composition between the two and the Monserrate Fm., suggesting differences in depositional processes and therefore in sedimentary environments (Veloza et al., 2008), probably related to variations in accommodation space. In Ecuador, a similar stratigraphic relationship between coarse-grained fluvial deposits of the Tena Fm. sourced from western areas in the Real Cordillera, overlying fine-grained shelf successions of the Napo Fm., has been documented (Gutiérrez et al., 2019; Vallejo et al., 2021; Jaillard, 2022). There, the deposits show a wider areal distribution than the Cimarrona Fm. in Colombia —an extension 14 km to the east this unit reaches a minimum thickness of about 5–15 m (Guerrero et al., 2000; Gómez et al., 2003), confirming the local character of these deposits—. This supports the interpretation of a south-north collision of the western Caribbean terrains, generating in turn the uplift of mountain ranges (Proto-Real Cordillera in Ecuador and Proto-Central Cordillera in Colombia) along the same direction. While in Ecuador important relief was already well established during the early Maastrichtian —evidenced by the wide distribution of fluvial western derived deposits—, to the north, in Colombia, the first moments of mountain growth related to collision were recorded in the late Maastrichtian with the accumulation of these coarse-grained fan delta complex deposits. In addition, it can be inferred that the Maastrichtian coarse-grained deposits of eastern detrital signatures reported by Calderon-Diaz et al. (2024), close to the studied area, are also a response of the eastern margin basin (Amazonian Craton) to the collision of the western Caribbean terranes. This means that the response of the emerging areas did not only affect the western border or proto-Central Cordillera, with growth of the volcanic arc; but also highly stable areas of the eastern margin such as the Amazonian Craton. However, reworking of the sedimentary cover accumulated in the proto-Central Cordillera is not ruled out (Moreno-Sánchez and Pardo-Trujillo, 2003; Zapata et al., 2021, 2024).

Nonetheless, the Campanian-Maastrichtian period is represented by two sand-dominated successions separated by a mud-dominated one, interpreted as a transgressive cycle followed by a regressive one

(Guerrero, 2002). These two cycles exhibit good correspondence with the long-term curve for the Late Cretaceous (Haq, 2014), showing a maximum sea-level towards the late Campanian consistent with the accumulation of offshore deposits in the central part, and prodelta deposits in the eastern part, also consistent with the accumulation of shelf deposits on the western side.

While the previous discussion highlighted the significant sediment loading from fluvio-deltaic interactions on the eastern side and the high sediment flux on the western side due to tectonic activity, internal or autogenic depositional controls also played a less relevant role during the final stages of the La Luna Sea. The sedimentary structures associated with traction processes evident in the western side shelf deposits during the Campanian indicate the influence of bottom currents during their accumulation. This, along with the tidal signals recognized in the Maastrichtian western deposits are the clear record of internal controls.

The high productivity reported in the organic- and phosphate-rich Campanian-lower Maastrichtian deposits are further evidence of autogenic controls during sedimentation. The thick unbioturbated fine-grained successions observed in Sections 2, 4, 5, and 11, with dark colorations, evidence these processes, which also cause oxygen-deficient environments. Phosphorite beds associated with upwelling processes have also been described in other sectors of the basin, even for the Maastrichtian (Föllmi et al., 1992; Martínez, 2003; Martín Rincón et al., 2022). In some cases, the abundant phosphate fragments in the sandy deposits controlled the petrophysical properties of the producing reservoirs in the basin (Warren and Pulham, 2001).

Channel avulsion processes are reported by Giraldo-Villegas et al. (2024) in the fan delta complex deposits linked to interaction between fluvial- and marine-dominated successions during the late Maastrichtian. These avulsion processes are not excluded in the fluvio-deltaic systems of the eastern border.

The integration of sedimentologic, ichnologic and stratigraphic evidence directly related to the sedimentary environments leads us to recognize the simultaneous participation of allogenic and, to lesser extent, autogenic controls in the origin, transport and final accumulation of the sedimentary deposits described. Notwithstanding, the degree of influence and subsequent preservation of these depositional controls in the fossil record would depend on the characteristics of the sedimentary systems in different areas of the basin. In summary, the type of sedimentary environments developed in each region, and their temporal and spatial evolution, hold the key to a better understanding of the accumulation parameters and the stratigraphic evolution of the epeiric basins.

5.3. Reservoir implications

In mature sedimentary basins, the generation of new exploration ideas is essential to the search for hydrocarbons. Given that the basins in this study fall into this category, detailed analyses that provide evidence for potential exploration opportunities are particularly relevant. Sedimentary parameters associated with continent-ocean systems that supply sediments, as well as internal basin processes responsible for sediment redistribution, have a direct influence on the quality, type, and distribution of reservoirs.

Among these processes, sediment redistribution by bottom currents plays a key role in reservoir development (Viana et al., 1998; Viana and Rebesco, 2007; Rebesco et al., 2014). Unlike fluvial-marine systems (e.g., delta, submarine canyons, turbiditic fans), which typically deposit coarse-grained sediments perpendicular to the shoreline, bottom currents can redistribute these sediments parallel or oblique to the coast. In some cases, they can transport and deposit large quantities of sand far from direct the land-ocean inputs (e.g., Rovere et al., 2019), as may be the case for the Campanian sandy deposits of the El Cobre Formation in Section 1. In addition, the sustained high energy of bottom currents tends to result in well-sorted sandy deposits with minimal clay or matrix (Viana et al., 1998; Yu et al., 2020).

Bottom currents also appear to influence the Campanian shelfal facies of the La Renta Formation, a major source rock in the basin (Pastor-Chacón et al., 2023; De la Parra et al., 2024). These processes could lead to thick accumulations of coarse-grained sediments on the shelf, potentially forming source-reservoir assemblages related to unconventional hydrocarbons (Li et al., 2016). These assemblages, also know source-reservoir neighboring type, are oil and gas producers in Ordos, Junggar and Songliao basins in China (Li et al., 2016).

5.4. Comparison with other ancient and recent epeiric seas: sediment arrival and distribution in the basin

Epeiric seas have been recorded in the geologic past, and modern analogues are widespread throughout the world. The best-known Cretaceous fossil records are the Western Interior Seaway in USA and the Neuquén Sea in Argentina (Hampson, 2010; Schwarz et al., 2022). Outstanding modern records include the Baltic Sea, North Sea, Hudson Bay, the Persian Gulf, and the Adriatic Sea (Judd et al., 2020; Schwarz et al., 2022). Overall, they provide insight into the processes, conditioning factors, and the resulting sedimentary deposits generated.

The input of sediments and their dispersion pathways into the sea play a key role in the context of sedimentary deposits from epeiric seas, controlling to a significant extent the distribution of the macrobenthic communities (e.g., Walsh and Nittrouer, 2009). Sediment distribution owes to a land-ocean dispersal system —i.e., related to topographical, geomorphological and compositional (e.g., basement, sedimentary cover) features of the emerged areas, plus the efficiency and characteristics of the transport systems involved (e.g., erosive capacity)— and may entail homogeneous distribution along the bordering coastlines, or else localized (heterogeneous) distribution towards some areas of the basin (Schwarz et al., 2022). Even though land transport systems are relatively easy to characterize, the role of internal currents on the cross-shelf vs alongshore sediment distribution within the marine basin are still poorly understood (Poyatos-Moré et al., 2016; Xu et al., 2023).

The final stages of the central part of the La Luna Sea in Colombia, show continental sediment input from the east during the Campanian-early Maastrichtian, and a relatively homogeneous distribution during the late Maastrichtian, with significant fluvial entries on both sides of the basin (Fig. 15). The fluvial-dominated deltas were the main basin feeders in the eastern sectors, whereas the fan delta complex and anastomosed/meandering fine-grained fluvial systems guided the continental entry by the western side. The eastern localized distribution of the fluvial entries during the Campanian-early Maastrichtian is reflected in a heterogeneous distribution in the cross-strike deposits trends, the eastern and central parts being dominated by sandy deposits, while along the western side muddy deposits prevail (Fig. 13). During the late Maastrichtian, as the sediment input is distributed on both sides of the basin, the deposits appear more homogeneous than in the Campanian (Fig. 13). Along-strike deposit trends show similar characteristics (Figs. 11 and 12); homogeneous sandy-dominated deposits in the central and eastern parts, compared to muddy-dominated deposits in the western part —in this case for both the Campanian and early Maastrichtian— indicate a generally non-uniform along-strike deposit distribution.

The larger N-S elongated Western Interior Sea had a western-located sediment input. The continental-derived sediments were transported to the basin coast and subsequently carried to distal parts of the basin by storms and bottom currents, resulting in a relatively uniform along-strike depositional trend (Elder and Kirkland, 1994; Hampson, 2010; Hampson et al., 2014). A southeast fluvial entry point was the main supply of sediments for the SE-NW extended Neuquén Sea. In this case, however, the sediments accumulated mainly in western areas and to a lesser extent than in northern regions, resulting in non-uniform along-strike depositional trends (Schwarz et al., 2022).

Comparing the three scenarios that occurred during the Cretaceous, it can be inferred that basin size plays a very important role in the

internal along-strike redistribution of sediments. In the large Western Interior Sea, the western location of the fluvial inputs had no influence on the resulting homogeneous along-strike distribution of deposits, whereas in smaller basins, such as the Neuquén Sea (~250 km) and the central part of the La Luna Sea (~500 km), the location of the fluvial systems controlled the heterogeneous along-strike distribution of deposits (Figs. 11, 12 and 14). In the studied record, bioturbation further supports this heterogeneous sediment distribution, given the record of an abundant and diverse macrobenthic tracemaker community similarly distributed over the central and eastern parts of the basin as opposed to the western zone (Fig. 15). Perhaps longshore and bottom currents have a greater capacity to redistribute sediments in larger basins, where changes in salinity and temperature that favor current development are more pronounced (Rebesco et al., 2014). In the Central part of the La Luna Sea, though the distribution of fluvial inputs took place on both sides of the basin in the Maastrichtian, being completely different land-ocean sedimentary systems (fan delta complex vs fluvial systems), they resulted in a non-uniform distribution of deposits in this zone of the basin. In addition, although bottom and longshore currents were evident, they may not have been strong or prolonged enough to promote a homogeneous along-strike distribution of sediments. A non-uniform distribution of sediments has been reported in recent small epeiric seas with localized distribution of sediment inputs, such as the Adriatic Sea, and its associated Po Delta (Falcieri et al., 2014; Amorosi et al., 2022).

In contrast, the La Luna Sea shares characteristics with the Devonian North American Seaway, which had a supply of sediments from the east, accumulating deposits in this area, while on the opposite side marine sedimentation continued, resulting in non-uniform cross-strike deposit distribution (Schwarz et al., 2022 and references therein). In the central part of the La Luna Sea, during the Campanian-early Maastrichtian, the main fluvial entry was located along the eastern border (Figs. 13 and 14). Although the size of the basin may not be decisive in the cross-strike distribution of sediments, this is unlikely because processes such as gravity flows (important in cross-shelf transport, e.g., Wright and Friedrichs, 2006) are known to transport sediment seaward only about 100 km from the coast. Thus, in this case, we envisage other processes such as tidal currents, seasonal winds, and storm reworking as determinants for the cross-strike sediment distribution (Schieber, 2016). Although river-derived sediments have been found more than 1000 km from the coast (e.g., Talling et al., 2022; Baker et al., 2024), they are associated with submarine channels, which require sufficient gradients to sustain movement. Although synsedimentary deformation has been found on the eastern side that could be associated with high gradients, this evidence is too local to interpret steep slopes that could be conducive to the development of submarine channels.

It could be inferred from our study setting that maybe the N-S trending currents were more dominant than the E-W ones, leading to an isolation of the western side, impeding the arrival of continental sediments derived from the east. Finally, the influence of climate —not only on the origin and along- and cross-strike distribution of sediments, but also on the establishment and variability of ocean currents— cannot be ruled out. Similarly, another key factor that cannot be ignored and that may influence the arrival and subsequent distribution of sediment within the basin is the size and elevation of the emerged zones, which were different on both sides of the epeiric sea studied here (small with high elevations in the west and large with low elevations in the east).

6. Conclusions

Recent knowledge of the stratigraphic evolution of sedimentary deposits in epeiric seas contributes to better identification of the depositional controls and processes involved. The final stages of the Cretaceous epeiric sea in Colombia had two phases: one dominated by marine processes, followed by another associated with transitional and continental environments. The evolution of this basin, bounded on either side by different geologic domains, depended on the evolution of the emerged areas, the land-ocean sediment-delivery systems, and the processes of deposition and distribution of sediments within the basin. On the analyzed sections located on the western side and in the central part of the basin, a shoreface-basin profile comprising shelf, offshore, and shoreface-foreshore environments prevailed, whereas on the eastern side, prodelta and delta front environments dominated during the Campanian-Maastrichtian period. To the west, fall-out sedimentation processes were dominant during the Campanian-early Maastrichtian, reflected in the accumulation of fine-grained lithologies. In constrast, sandy and muddy deposits accumulated in the central and eastern parts of the basin: wave and fall-out sedimentation were the main parameters in the central part, while fluvial processes were mainly responsible at the eastern zone. Less important depositional processes were fluvial, bottom and longshore currents on the western side; storms, tides, and longshore currents in the central part; and suspension, wave, and storm processes on the eastern area. During the late Maastrichtian, alluvial/fluvial processes dominated the western side associated with the growth of the proto-Central Cordillera, whereas the central and eastern parts show little change. Ichnologic features suggest habitable marine bottoms during the early Campanian and the early Maastrichtian in the central and eastern parts of the basin, but paleoecological conditions on the western side (particularly oxygenation) created a challenging environment for the tracemaker community, mainly during the Campanian. During the early Maastrichtian all seafloors were colonized, suggesting favorable conditions for marine macrobenthic communities.

The sedimentologic, ichnologic and stratigraphic characteristics documented here, together with their variation in time and space, suggest that both allogenic (tectonic, subsidence, sea-level) and, to a lesser extent, autogenic processes (channel avulsion, bottom and longshore currents, tides, high productivity) simultaneously controlled the resulting sedimentary deposits. Depositional parameters provide clues as to new exploration ideas, associated with possible reservoir deposits related to longshore and bottom currents. This opens up the possibility of searching for reservoirs that are directly connected to the source rock, and in positions perpendicular to the main direction of the major fluvial systems that delivered coarse-grained sediments to the basin.

Comparison of different epeiric basins, both fossil and recent, reveals that the basin size and the emerged areas plays an important role in the internal along- and cross-strike distribution of sediments, where processes such as bottom or longshore currents, or gravity flows would play a key role.

CRediT authorship contribution statement

Carlos A. Giraldo-Villegas: Writing – review & editing, Writing – original draft, Methodology, Investigation, Formal analysis, Conceptualization. **Francisco J. Rodríguez-Tovar:** Writing – review & editing, Supervision, Methodology, Investigation, Formal analysis, Conceptualization. **Sergio A. Celis:** Writing – review & editing, Methodology, Investigation, Formal analysis, Conceptualization. **Andrés Pardo-Trujillo:** Writing – review & editing, Supervision, Methodology, Investigation, Formal analysis.

Declaration of competing interest

The authors declare that they have no known competing financial interests or personal relationships that could have appeared to influence the work reported in this paper.

Acknowledgments

This research was funded by grants TED2021-131697B-C21 and PID2019-104625RB-100, funded by MCIN/AEI/10.13039/501100011033, and by the European Union NextGenerationEU/PRTR. The National Program for Doctoral Formation provided financial

support to Giraldo-Villegas and Celis (Minciencias grants 906-2021 and 885-2020, respectively). The research was conducted within the "Ichnology and Palaeoenvironment Research Group" (UGR). Financial support for Rodríguez-Tovar was provided by the scientific projects PID2019-104625RB-100 (funded by MCIN/AEI/10.13039/501100011033), P18-RT-4074 (FEDER/Junta de Andalucía-Consejería de Economía y Conocimiento), B-RNM-072-UGR18 and A-RNM-368-UGR20 (funded by FEDER Andalucía). We thank Sebastian Echeverri, Sebastian Rosero, Alba Jiménez and Luisa Correa for their field assistance. Special thanks to Juan Betancur for his help in the preparation of Figs. 1 and 14. Thanks to the Universidad de Caldas and the Instituto de Investigaciones en Estratigrafía-IIES for their economic and logistic support, and to the ANH for encouraging the advancement of geological knowledge of the sedimentary basins of the country. We thank the editor, Luca Colombera, and the reviewers, German Bayona, Alejandro Mora Bohorquez and Juan Sebastian Carvajal Torres for their useful comments, which helped to improve the manuscript.

Appendix A. Supplementary data

Supplementary data to this article can be found online at https://doi.org/10.1016/j.marpetgeo.2025.107385.

Data availability

Data will be made available on request.

References

Ainsworth, R.B., Vakarelov, B.K., MacEachern, J.A., Nanson, R.A., Lane, T.I., Rarity, F., Dashtgard, S.E., 2016. Process-driven architectural variability in mouth-bar deposits: a case study from a mixed-process mouth-bar Complex, Drumheller, Alberta, Canada. J. Sediment. Res. 86 (5), 512–541.

Allen, J.R.L., 1982. Sedimentary Structures: Their Character and Physical Basis. Developments in Sedimentology, vol. 30. Elsevier, Amsterdam, p. 593.

Amorosi, A., Sammartino, I., Dinelli, E., Campo, B., Guercia, T., Trincardi, F., Pellegrini, C., 2022. Provenance and sediment dispersal in the Po-Adriatic source-to-sink system unraveled by bulk-sediment geochemistry and its linkage to catchment geology. Earth Sci. Rev. 234, 104202.

Archer, A.W., 1991. Modelling of tidal rhythmites using modern tidal periodicities and implications for short term sedimentation rates. In: Franseen, E.K., Kendall, W.L., Ross, W. (Eds.), Sedimentary Modelling: Computer Simulations and Methods for Improved Parameter Definition, vol. 223. Kansas Geological Survey Bulletin, pp. 185–194.

Archer, A.W., 1995. Modelling of cyclic tidal rhythmites based on a range of diurnal to semi-diurnal tidal-station data. Mar. Geol. 123, 1–10.

Arnott, R.W.C., 1993. Quasi-planar-laminated sandstone beds of the lower cretaceous bootlegger member, north-central Montana: evidence of combined-flow sedimentation. J. Sediment. Petrol. 63, 488–494.

Aumond, G.N., Kochhann, K.G.D., Netto, R.G., de Souza, L.V., Sedorko, D., Horodyski, R. S., Almeida, F.N.J., Verde, M., 2021. Paleoenvironmental conditions of the late Miocene "Entrerriense" epicontinental sea: a case study of the Camacho Formation, SW Uruguay. J. S. Am. Earth Sci. 110, 103421.

Ayala-Calvo, R.C., Bayona-Chaparro, G.A., Ojeda-Marulanda, C., Cardona, A., Valencia, V., Padrón, C.E., Yoris, F., Mesa-Salamanca, J., García, A., 2009. Estratigrafía y procedencia de las unidades comprendidas entre el Campaniano y el Paleógeno en la subcuenca de Cesar: aporte a la evolución tectónica del área. Geol. Colomb. 34, 3–33.

Baker, M.L., Hage, S., Talling, P.J., Acikalin, S., Hilton, R.G., Haghipour, N., Ruffell, S.C., Pope, E.L., Jacinto, R.S., Clare, M.A., Sahin, S., 2024. Globally significant mass of terrestrial organic carbon efficiently transported by canyon-flushing turbidity currents. Geology 52 (8), 631–636.

Bayona, G., 2018. El inicio de la emergencia en los Andes del norte: una perspectiva a partir del registro tectónico-sedimentológico del Coniaciano al Paleoceno. Rev. Acad. Colomb. Ciencias Exactas, Fis. Nat. 42, 364–378.

Bayona, G., Reyes-Harker, A., Jaramillo, C., Rueda, M., Aristizabal, J., Cortes, M., Gamba, N., 2006. Distinguishing tectonic versus eustatic flooding surfaces in the Llanos Basin of Colombia, and implications for stratigraphic correlations. In: Abstract book IX Simposio Bolivariano de Exploración Petrolera en las Cuencas Subandinas, Colombia, Asociación Colombiana de Geólogos y Geofísicos del Petróleo, p. 13.

Bayona, G., Cortes, M., Jaramillo, C., Ojeda, G., Aristizabal, J., Reyes-Harker, A., 2008. An integrated analysis of an orogen-sedimentary basin pair: latest Cretaceous–Cenozoic evolution of the linked Eastern Cordillera orogen and the Llanos foreland basin of Colombia. GSA Bulletin 120, 1171–1197.

Bayona, G., Cardona, A., Jaramillo, C., Mora, A., Montes, C., Caballero, V., Valencia, V., 2013. Onset of fault reactivation in the Eastern Cordillera of Colombia and proximal Llanos Basin; response to Caribbean – South American collision in early Paleogene time. In: Nemčok, M., Mora, A.R., Cosgrove, J.W. (Eds.), Thick-skin- Dominated Orogens: from Initial Inversion to Full Accretion, vol. 377. Geological Society of London, Special Publication, pp. 285–314.

Bayona, G., Bustamante, C., Nova, G., Salazar–Franco, A.M., 2020. Jurassic evolution of the northwestern corner of Gondwana: present knowledge and future challenges in studying Colombian Jurassic rocks. In: Gómez, J., Pinilla–Pachon, A.O. (Eds.), The Geology of Colombia, Volume 2 Mesozoic. Servicio Geológico Colombiano, vol. 36. Publicaciones Geológicas Especiales, pp. 171–207.

Bayona, G., Baquero, M., Ramírez, C., Tabares, M., Salazar, A.M., Nova, G., Duarte, E., Pardo, A., Plata, A., Jaramillo, C., Rodríguez, C., Caballero, V., Cardona, A., Montes, C., Gómez Marulanda, S., Cárdenas-Rozo, A.L., 2021. Unravelling the widening of the earliest Andean northern orogen: Maastrichtian to early Eocene intra-basinal deformation in the northern Eastern Cordillera of Colombia. Basin Res. 33 (1), 809–845.

Bertling, M., Braddy, S.J., Bromley, R.G., Demathieu, G.R., Genise, J., Mikuláš, R., Nielsen, J.K., Nielsen, K.S.S., Rindsberg, A.K., Schlirf, M., Uchman, A., 2006. Names for trace fossils: a uniform approach. Lethaia 39, 265–286.

Bertling, M., Buatois, L.A., Knaust, D., Laing, B., Mángano, M.G., Meyer, N., Mikuláš, R., Minter, N.J., Neumann, C., Rindsberg, A.K., Uchman, A., Wisshak, M., 2022. Names for trace fossils 2.0: theory and practice in ichnotaxonomy. Lethaia 55 (3), 1–19.

Bhattacharya, J.P., MacEachern, J.A., 2009. Hyperpycnal rivers and prodeltaic shelves in the Cretaceous seaway of North America. J. Sediment. Res. 79, 184–209.

Blair, T.C., 1999. Sedimentology of gravelly Lake Lahontan high-stand shoreline deposits, Churchill Butte, Nevada. Sediment. Geol. 123, 187–206.

Boggs, S., 2014. Principles of Sedimentology and Stratigraphy. Pearson Education Limited, Harlow/UK, p. 565.

Botero-Garcia, M., Vinasco, C.J., Restrepo-Moreno, S.A., Foster, D.A., Kamenov, G.D., 2023. Caribbean–South America interactions since the Late Cretaceous: insights from zircon U–Pb and Lu–Hf isotopic data in sedimentary sequences of the northwestern Andes. J. S. Am. Earth Sci. 123, 104231.

Brenchley, P.J., Pickerill, R.K., Stromberg, S.G., 1993. The role of wave reworking on the architecture of storm sandstone facies, Bell Island Group (Lower Ordovician), eastern Newfoundland. Sedimentology 40, 359–382.

Bromley, R.G., 1996. Trace Fossils. Biology, Taphonomy and Applications. Chapman & Hall, London, p. 375.

Buatois, L.A., Saccavino, L.L., Zavala, C., 2011. Ichnologic signatures of hyperpycnal flow deposits in Cretaceous river-dominated deltas, Austral Basin, southern Argentina. In: Slatt, R.M., Zavala, C. (Eds.), Sediment Transfer from Shelf to Deep Water–Revisiting the Delivery System, AAPG Studies in Geology, vol. 61, pp. 153–170.

Buatois, L.A., Santiago, N., Herrera, M., Plink-Björklund, P., Steel, R.J., Espin, M., Parra, K., 2012. Sedimentological and ichnological signatures of changes in wave, river and tidal influence along a Neogene tropical deltaic shoreline. Sedimentology 59, 1568–1612.

Caballero, V.M., Rodríguez, G., Naranjo, J.F., Mora, A., De La Parra, F., 2020. From facies analysis, stratigraphic surfaces, and depositional sequences to stratigraphic traps in the Eocene – Oligocene record of the southern Llanos Basin and northern Magdalena Basin. In: Gómez, J., Mateus–Zabala, D. (Eds.), The Geology of Colombia, Volume 3 Paleogene –Neogene, Servicio Geológico Colombiano, vol. 37. Publicaciones Geológicas Especiales, pp. 283–330.

Caicedo, J.C., Terraza, R., Mora, A., 2000. Extensión geográfica, características litoestratigráficas y posibilidades como roca almacenadora de la Arenisca del Cobre, Valle Superior del Magdalena Abstract book. Ingeominas 1–2.

Calderon-Diaz, L., Zapata, S., Cardona, A., Parra, M., Sobel, E.R., Patiño, A.M., Valencia, V., Jaramillo-Ríos, J.S., Glodny, J., 2024. Cretaceous extensional and contractional stages in the Colombian Andes unraveled by a source-to-sink geochronological and thermochronological study in the Upper Magdalena Basin. Tectonophysics 878, 230303.

Carroll, A.R., 2017. Xenoconformities and the stratigraphic record of paleoenvironmental change. Geology 45 (7), 639–642.

Carvajal-Torres, J., Catuneanu, O., Mora, A., Caballero, C., Reyes, M., 2022. First-order stratigraphic boundaries of the Late Cretaceous-Paleogene retroarc foreland basin in Colombia. Front. Earth Sci. 10, 876140.

Casero, P., Salel, J.F., Rossato, A., 1997. Multidisciplinary correlative evidences for polyphase geological evolution of the foot–hills of the Cordillera Oriental (Colombia). In: Abstract book VI Simposio Bolivariano Exploración Petrolera en las Cuencas Subandinas, Colombia, Asociación Colombiana de Geólogos y Geofísicos del Petróleo, pp. 100–118.

Catuneanu, O., 2022. Principles of Sequence Stratigraphy, second ed. Elsevier, Amsterdam/Netherlands, p. 496.

Cediel, F., Shaw, R.P., Cáceres, C., 2003. Tectonic assembly of the northern andean block. In: Bartolini, C., Buffer, R.T., Blickwede, J. (Eds.), The Circum-Gulf of Mexico and the Caribbean: Hydrocarbon Habitats, Basin Formation, and Plate Tectonics, vol. 79. AAPG Memoir, pp. 815–848.

Cediel, F., Leal-Mejía, H., Shaw, R.P., Melgarejo, J.C., Restrepo-Pace, P.A., 2011. Petroleum Geology of Colombia. Regional Geology of Colombia. Fondo Editorial Universidad EAFIT, p. 225.

Cooper, M.A., Addison, F.T., Alvarez, R., Coral, M., Graham, R.H., Hayward, A.B., Howe, S., Martínez, J., Naar, J., Peñas, R., Pulham, A.J., Taborda, A., 1995. Basin development and tectonic history of the Llanos Basin, Eastern Cordillera and Middle Magdalena Valley, Colombia. AAPG (Am. Assoc. Pet. Geol.) Bull. 79, 1421–1443.

Cortés, M., Angelier, J., Colleta, B., 2005. Paleostress evolution of the northern Andes (Eastern Cordillera of Colombia): Implications on plate kinematics of the South Caribbean region. Tectonics 24, TC1008.

Dalrymple, R.W., 1992. Tidal depositional system. In: Waters, C.N., James, N.P. (Eds.), Facies Models. Geological Association of Canada, pp. 195–218.
Davis, R.A., Dalrymple, R.W., 2012. Principles of Tidal Sedimentology. Springer, New York, p. 621.
De la Parra, F., Higuera, C., Ramírez, R., Maya, L., Céspedes, S., Marfissi, N., Carreño, A., Juliao, T., Forero, S., 2024. Chronostratigraphy of the Upper Cretaceous succession in the Middle Magdalena Valley of Colombia (northern south America). Cretac. Res. 157, 105824.
De Porta, J., 1966. Geología del extremo sur del Valle Medio del Magdalena entre Honda y Guataquí (Colombia). Bol. Geol. 22–23, 5–347.
Duarte, E., Cardona, A., Lopera, S., Valencia, V., Estupiñan, H., 2016. Provenance and diagenesis from two stratigraphic sections of the Lower Cretaceous Caballos Formation in the Upper Magdalena Valley: geological and reservoir quality implications. CT&F 8 (1), 5–29.
Dumas, S., Arnott, R.W.C., Southard, J.B., 2005. Experiments on oscillatory-flow and combined flow bed forms: implications for interpreting parts of the shallow marine rock record. J. Sediment. Res. 75, 501–513.
Dunham, R.J., 1962. Classification of carbonate rocks according to depositional texture. In: Ham, W.E. (Ed.), Classification of Carbonate Rocks, vol. 1. AAPG Memoir, pp. 108–121.
Einsele, G., 2000. Sedimentary Basins: Evolution, Facies, and Sediment Budget. Springer-Verlag, Berlin, p. 795.
Ekdale, A.A., Mason, T.R., 1988. Characteristic trace-fossil associations in oxygen poor sedimentary environments. Geology 16, 720–723.
Elder, W.P., Kirkland, J.I., 1994. Cretaceous paleogeography of the southern Western Interior region. In: Caputo, M.V., Peterson, J.A., Franczyk, K.J. (Eds.), Mesozoic Systems of the Rocky Mountain Region, USA: Rocky Mountain Section. SEPM, pp. 415–440.
Erlich, R.N., Macsotay, O., Nederbragt, A.J., Lorente, M.A., 2000. Birth and death of the Late Cretaceous "La Luna Sea'', and origin of the tres esquinas phosphorites. J. S. Am. Earth Sci. 13, 21–45.
Erlich, R.N., Villamil, T., Keens-Dumas, J., 2003. Controls on the deposition of Upper Cretaceous organic carbon– rich rocks from Costa Rica to Suriname. In: Bartolini, C., Buffler, R.T., Blickwede, J. (Eds.), The Circum-Gulf of Mexico and the Caribbean: Hydrocarbon Habitats, Basin Formation and Plate Tectonics, vol. 79. AAPG Memoir, pp. 1–45.
Etayo-Serna, F., 2019. Basin development and tectonic history of the middle Magdalena Valley. In: Etayo-Serna, F. (Ed.), Estudios geológicos y paleontológicos sobre el Cretácico en la región del embalse del río Sogamoso, Valle Medio del Magdalena, Compilación de los Estudios Geológicos Oficiales en Colombia, pp. 413–423.
Etayo-Serna, F., Barrero, D., Lozano, H., Espinosa, A., González, H., Orrego, A., Ballesteros, I., Forero, H., Ramírez, C., Zambrano, F., Duque, H., Vargas, R., Núñez, A., Alvarez, J., Ropán, C., Cardozo, E., Galvis, N., Sarmiento, L., Albers, J., Case, J., Singer, D., Bowen, R., Berger, B., Cox, D., Hodges, C., 1983. Mapa de Terrenos Geológicos de Colombia. Publicaciones Geol. Espec. del INGEOMINAS 14, 235.
Fabre, A., 1985. Estratigrafía de la Sierra Nevada del Cocuy, Boyacá y Arauca. Cordillera Oriental (Colombia). Geol. Norandina 4, 3– 2.
Falcieri, F.M., Benetazzo, A., Sclavo, M., Russo, A., Carniel, S., 2014. Po River plume pattern variability investigated from model data. Cont. Shelf Res. 87, 84–95.
Ferreira, L.O., Chagas, V.E., Bobco, F.E.R., de Souza, D.C., Salgado-Campos, V.M.J., Sedorko, D., Neves, M., Silveira, L.F., Filho, J.G.M., Araújo, B.C., Borghi, L., 2025. Tracking environmental changes in an Early Cretaceous epicontinental sea: sedimentology and geochemistry of the Romualdo Formation (Araripe Basin, NE Brazil). Cretac. Res. 166, 105986.
Flemming, B.W., 2000. The role of grain size, water depth and flow velocity as scaling factors controlling the size of subaqueous dunes. Marine Sandwave Dynamic, International Workshop 55–60.
Flügel, E., 2010. Microfacies of Carbonate Rocks, second ed. Springer-Verlag, Berlin, p. 984.
Föllmi, K., Garrison, R., Ramírez, P., Zambrano, F., Kennedy, W., Lehner, B., 1992. Cyclic phosphate- rich successions in the Upper Cretaceous of Colombia. Paleogeography, Paleoclimatology, Paleoecology 93 (3–4), 151–182.
García-García, F., 2004. Sedimentary models of coarse-grained deltas in the Neogene basins of the Betic Cordillera (SE Spain): Tortonian and Pliocene examples. Bol. Geol. Min. 115 (3), 469–494.
Garzanti, E., Vermeesch, P., Andò, S., Lustrino, M., Padoan, M., Vezzoli, G., 2014. Ultra-long distance littoral transport of Orange sand and provenance of the Skeleton Coast Erg (Namibia). Mar. Geol. 357, 26–36.
Garzanti, E., Andò, S., Padoan, M., Vezzoli, G., El Kammar, A., 2015. The modern Nile sediment system: processes and products. Quat. Sci. Rev. 130, 9–56.
Garzón, S., Warny, S., Bart, P.J., 2012. A palynological and sequence-stratigraphic study of Santonian–Maastrichtian strata from the Upper Magdalena Valley basin in central Colombia. Palynology 36, 112–133.
Giraldo-Villegas, C.A., Rodríguez-Tovar, F.J., Celis, S.A., Pardo-Trujillo, A., Duque-Castaño, M.L., 2023. Paleoenvironmental conditions over the Caribbean Large Igneous Province during the Late Cretaceous in NW of South American margin: a sedimentological and ichnological approach. Cretac. Res. 142, 105407.
Giraldo-Villegas, C.A., Rodríguez-Tovar, F.J., Celis, S.A., Pardo-Trujillo, A., 2024. Variable *Ophiomorpha* ichnofabric: improving the understanding of mouth bar environments in fan-delta complex depositional settings from the Upper Cretaceous of NW South America. Cretac. Res. 154, 205730.
Glenn, C., Föllmi, K.B., Riggs, S.R., Baturin, G.N., Grimm, K.A., Trappe, J., Abed, A.M., Galli-Olivier, C., Garrison, R.E., Ilyin, A.V., Jehl, C., Rohrlich, V., Sadaqah, R.M.Y., Schidlowski, M., Sheldon, R.E., Siegmund, H., 1994. Phosphorus and phosphorites: sedimentology and environments of formation. Eclogae Geol. Helv. 87 (3), 747–788.
Gómez, E., Pedraza, P., 1994. El Maastrichtiano de la región de Honda - Guaduas, límite norte del Valle Superior del Magdalena: Registro sedimentario de un delta dominado por ríos trenzados. In: Etayo-Serna, F. (Ed.), Estudios geológicos del Valle Superior del Magdalena. Universidad Nacional de Colombia, pp. III1–III20.
Gómez, E., Jordan, T.E., Allmendinger, R.W., Hegarty, K., Kelley, S., Heizler, M., 2003. Controls on architecture of the Late Cretaceous to Cenozoic southern Middle Magdalena Valley Basin, Colombia. GSA Bulletin 115 (2), 131–147.
Gómez, E., Jordan, T.E., Allmendinger, R.W., Cardozo, N., 2005. Development of the Colombian foreland-basin system as a consequence of diachronous exhumation of the northern Andes. GSA Bulletin 117 (9–10), 1272–1292.
González, R., Oncken, O., Faccena, C., Le Breton, E., Bezada, M., Mora, A., 2023. Kinematics and convergent tectonics of the northwestern south American plate during the cenozoic. Geochem. Geophys. Geosys. 24 (7), e2022GC010827.
Guerrero, J., 2002. A proposal on the classification of systems tracts: the allostratigraphy and sequence stratigraphy of the Colombian basin. Part 2: Barremian to Maastrichtian. Geol. Colomb. 27, 27–49.
Guerrero, J., Sarmiento, G., 1996. Estratigrafía física, palinológica, sedimentológica y secuencial del Cretácico Superior y Paleoceno del Piedemonte Llanero. Implicaciones en exploración petrolera. Geol. Colomb. 20, 3–66.
Guerrero, J., Sarmiento, G., Navarrete, R., 2000. The stratigraphy of the W side of the Cretaceous Colombian basin in the Upper Magdalena Valley. Reevaluation of selected areas and type localities including aipe, Guaduas, Ortega, and Piedras. Geol. Colomb. 25, 45–110.
Guerrero, J., Mejía–Molina, A., Osorno, J., 2020. Detrital U–Pb provenance, mineralogy, and geochemistry of the Cretaceous Colombian back–arc basin. In: Gómez, J., Pinilla–Pachon, A.O. (Eds.), The Geology of Colombia, Volume 2 Mesozoic. Servicio Geológico Colombiano, vol. 36. Publicaciones Geológicas Especiales, pp. 261–297.
Guerrero, J., Montes, L., Jaillard, E., Kammer, A., 2021. Seismic interpretation of the Cretaceous unconformities and sequences in the Middle Magdalena Valley and the western margin of the Eastern Cordillera, Colombia. C. R. Geosci. 353 (1), 155–172.
Gutiérrez, E.G., Horton, B.K., Vallejo, C., Jackson, L.J., George, S.W.M., 2019. Provenance and geochronological insights into Late Cretaceous-Cenozoic foreland basin development in the subandean zone and oriente basin of Ecuador. Andean Tectonics 237–268.
Hampson, G.J., 2010. Sediment dispersal and quantitative stratigraphic architecture across an ancient shelf. Sedimentology 57, 96–141.
Hampson, G.J., Duller, R.A., Petter, A.L., Robinson, R.A.J., Allen, P.A., 2014. Mass-balance constraints on stratigraphic interpretation of linked alluvial-coastal–shelfal deposits: example from Cretaceous Western Interior Basin, Utah and Colorado, USA. J. Sediment. Res. 84, 935–960.
Haq, B.U., 2014. Cretaceous eustasy revisited. Global Planet. Change 113, 44–58.
Hein, F.J., Walker, R.G., 1977. Bar evolution and development or stratification in the gravelly, braided Kicking Horse River, British Columbia. Can. J. Earth Sci. 14, 562–570.
Hernández-Duran, S., 2021. Litogeoquímica de las unidades del Cretácico Superior, su relación con las áreas de aporte y evolución de los medios sedimentarios, Cuenca del Valle Superior del Magdalena, Colombia (MSc thesis). Universidad Nacional de Colombia, p. 227.
Horton, B.K., Saylor, J.E., Nie, J., Mora, A., Parra, M., Reyes-Harker, A., Stockli, D.F., 2010. Linking sedimentation in the northern Andes to basement configuration, Mesozoic extension, and Cenozoic shortening: evidence from detrital zircon U-Pb ages, Eastern Cordillera, Colombia, Colombia. GSA Bulletin 122, 1423–1442.
Horton, B.K., Anderson, V.J., Caballero, V., Saylor, J.E., Nie, J., Parra, M., Mora, A., 2015. Application of detrital zircon U-Pb geochronology to surface and subsurface correlations of provenance, paleodrainage and tectonics of the Middle Magdalena Valley Basin of Colombia. Geosphere 11 (6), 1790–1811.
Horton, B.K., Parra, M., Mora, A., 2020. Construction of the Eastern Cordillera of Colombia: insights from the sedimentary record. In: Gómez, J., Mateus–Zabala, D. (Eds.), The Geology of Colombia, Volume 3 Paleogene – Neogene, Servicio Geológico Colombiano, vol. 37. Publicaciones Geológicas Especiales, pp. 67–88.
Ingram, R.L., 1954. Terminology for the thickness of stratification and parting units in sedimentary rocks. GSA Bulletin 65, 937–938.
Irastorza, A., Zavala, C., Campetella, D.M., Turienzo, M., Olivera, D., Peralta, F., Irastorza, M., Martz, P., 2021. Hyperpycnal littoral deltas: a case of study from the Lower Cretaceous Agrio Formation in the Neuquén basin, Argentina. J. Palaeogeogr. 10 (4), 550–570.
Jaillard, E., 2022. Late Cretaceous-Paleogene orogenic build-up of the Ecuadorian andes: review and discussion. Earth Sci. Rev. 230, 104033.
Jiménez, G., Speranza, F., Faccenna, C., Bayona, G., Mora, A., 2014. Paleomagnetism and magnetic fabric of the Eastern Cordillera of Colombia: evidence for oblique convergence and nonrotational reactivation of a Mesozoic intracontinental rift. Tectonics 33, 2233–2260.
Jiménez, G., García-Delgado, H., Geissman, J.W., 2021. Magnetostratigraphy and magnetic properties of the Jurassic to Lower Cretaceous Girón Group (northern Andes, Colombia). Geosphere 17 (6), 2172–2196.
Jiménez, G., Geissman, J.W., Bayona, G., 2022. Unraveling tectonic inversion and wrench deformation in the Eastern Cordillera (Northern Andes) with paleomagnetic and AMS data. Tectonophysics 834, 229356.
Johnson, H.D., Baldwin, C.T., 1996. Shallow clastic seas. In: Reading, H.G. (Ed.), Sedimentary Environments: Processes, Facies and Stratigraphy. Blackwell, Oxford, p. 687.
Judd, E.J., Bhattacharya, T., Ivany, L.C., 2020. A dynamical framework for interpreting ancient sea surface temperatures. Geophys. Res. Lett. 47 (15), 1–10.
Kidwell, S.M., 1991. The stratigraphy of shell concentrations. In: Allison, P.A., Briggs, D. E.G. (Eds.), Taphonomy: Releasing the Data Locked in the Fossil Record. Plenum Press, pp. 211–289.

Kleinspehn, K.L., Steel, R.J., Johannessen, E., Netland, A., 1984. Conglomeratic fan delta sequences, late Carboniferous - early Permian, western Spitsbergen. In: Koster, E.H., Steel, R.J. (Eds.), Sedimentology of Gravels and Conglomerates, vol. 10. Canadian Society of Petroleum Geologists, pp. 279–294.
Leal-Mejía, H., Shaw, R.P., Melgarejo i Draper, J.C., 2019. Spatial-temporal migration of granitoid magmatism and the Phanerozoic tectono-magmatic evolution of the Colombian andes. In: Cediel, F., Shaw, R.P. (Eds.), Geology and Tectonics of Northwestern South America. The Pacific-Caribbean-Andean Junction. Frontiers in Earth Sciences. Springer, pp. 253–410.
Leckie, D.A., De Armas, J.M., Du Toit, C., Glazebrook, K., Fomez, E., Kroshko, P., Norris, B., Parsons, A., Peñas, R., 2003. Paleogeographic implications of the Lower Guadalupe (Dura) Formation in the Guando oil field, Colombia. In: Abstract book VIII Simposio Bolivariano - Exploración Petrolera en las Cuencas Subandinas, Colombia, Asociación Colombiana de Geólogos y Geofísicos del Petróleo, pp. 68–80.
León, S., Jiménez-Rodríguez, S., Piraquive, A., Florez-Amaya, S., Muñoz-Rocha, J., Peña-Urueña, M.L., Bonilla, A., Lince, I.F., Contreras-Fayad, D., Jiménez, C., 2023. Sediment provenance signal of the discontinuous retroarc topography in the northern Andes during the Early Cretaceous. Terra Nova 35, 440–449.
Li, J., Zhen, M., Chen, X., Li, D., Wang, S., Song, T., 2016. Connotation analysis, source-reservoir assemblage types and development potential of unconventional hydrocarbons in China. Petroleum Research 1 (2), 135–148.
Longhitano, S.G., 2008. Sedimentary facies and sequence stratigraphy of coarse-grained gilbert-type deltas within the Pliocene thrust-top Potenza basin (southern Apennines, Italy). Sediment. Geol. 210, 87–110.
Longhitano, S.G., Nemec, W., 2005. Statistical analysis of bed-thickness variation in a Tortonian succession of biocalcarenitic tidal dunes, Amantea Basin, Calabria, southern Italy. Sediment. Geol. 179, 195–224.
Longhitano, S.G., Mellere, D., Steel, R.J., Ainsworth, R.B., 2012. Tidal depositional systems in the rock record: a review and new insights. Sediment. Geol. 279, 2–22.
Lowe, D.R., 1982. Sediment-gravity flows II: depositional models with special reference to the deposits of high-density turbidity currents. J. Sediment. Petrol. 52, 279–297.
MacEachern, J.A., Bann, K.L., 2008. The role of ichnology in refining shallow marine facies models. In: Hampson, G.J., Steel, R.J., Burgess, P.M., Dalrymple, R.W. (Eds.), Recent Advances in Models of Siliciclastic Shallow-Marine Stratigraphy, vol. 10. SEPM Special Publication, pp. 73–116.
MacEachern, J.A., Bann, K.L., 2023. Departures from the archetypal deltaic ichnofacies. In: Cónsole-Gonella, C., de Valais, S., Díaz-Martínez, I., Citton, P., Verde, M., Mcllroy, D. (Eds.), Ichnology in Shallow-Marine and Transitional Environments, vol. 522. Geological Society of London, Special Publications, pp. 175–214.
MacEachern, J.A., Bann, K.L., Bhattacharya, J.P., Howell, C.D., 2005. Ichnology of deltas, organism responses to the dynamic interplay of rivers, waves, storms, and tides. In: Giosan, L., Bhattacharya, J.P. (Eds.), River Deltas; Concepts, Models and Examples, vol. 83. SEPM Special Publications, pp. 49–85.
MacEachern, J., Gingras, M., Bann, K.L., Pemberton, G., 2007. The ichnofacies paradigm: high-resolution palaeoenvironmental interpretation of the rock record. In: MacEachern, J.A., Bann, K.L., Gingras, M.K., Pemberton, S.G. (Eds.), Applied Ichnology, Short Course Notes, vol. 52. Society for Sedimentary Geology, pp. 27–64.
Makaske, B., 2001. Anastomosing rivers: a review of their classification, origin and sedimentary products. Earth Sci. Rev. 53 (3–4), 149–196.
Martín Rincón, C.L., Terraza Melo, R., Rojas Parra, N.R., Martínez Aparicio, G.A., Rojas Jiménez, S., Hernández González, J.S., 2022. The Upper Cretaceous (Santonian-Maastrichtian) phosphate deposits in the west of the Neiva subbasin, Upper Magdalena Valley, Colombia. Bol. Geol. 49 (2), 75–96.
Martínez, J.I., 2003. The paleoecology of Late Cretaceous upwelling events from the Upper Magdalena Basin, Colombia. Palaios 18 (4–5), 305–320.
Maze, W.B., 1984. Jurassic La Quinta Formation in the Sierra de Perijá, northwestern Venezuela: geology and tectonic environment of red beds and volcanic rocks. In: Bonini, W.E., Hargraves, R.B., Shagam, R. (Eds.), The Caribbean–South American Plate Boundary and Regional Tectonics, vol. 162. Geological Society of America Memoir, pp. 263–282.
Miall, A.D., 1996. The geology of fluvial deposits: sedimentary facies. Basin Analysis and Petroleum Geology. Springer, Berlín, p. 509.
Montaño, P.C., Nova, G., Bayona, G., Mahecha, H., Ayala, C., Jaramillo, C., De La Parra, F., 2016. Análisis de secuencias y procedencia en sucesiones sedimentarias de grano fino: un ejemplo de la Formación Umir y base de la Formación Lisama, en el sector de Simacota (Santander, Colombia). Bol. Geol. 38 (1), 51–72.
Montes, C., Rodríguez-Corcho, A.F., Bayona, G., Hoyos, N., Zapata, S., Cardona, A., 2019. Continental margin response to the multiple arc-continent collisions: the northern Andes-Caribbean margin. Earth Sci. Rev. 198, 102903.
Mora, A., Parra, M., Strecker, M.R., Kammer, A., Dimaté, C., Rodriguez, F., 2006. Cenozoic contractional reactivation of Mesozoic extensional structures in the Eastern Cordillera of Colombia. Tectonics 25, 1–19.
Mora, A., Mantilla, M., de Freitas, M., 2010. Cretaceous paleogeography and sedimentation in the Upper Magdalena and Putumayo basins, southwestern Colombia. In: Extended Abstract AAPG International Conference and Exhibition. Rio de Janeiro, Brazil.
Mora, A., Reyes-Harker, A., Rodriguez, G., Tesón, E., Ramírez-Arias, J.C., Parra, M., Caballero, V., Mora, J.P., Quintero, I., Valencia, V., Ibáñez, M., Horton, B.K., Stockli, D.F., 2013. Inversion tectonics under increasing rates of shortening and sedimentation: Cenozoic example from the Eastern Cordillera of Colombia. Geological Society of London, Special Publications 377, 411–442.
Mora, A., Casallas, W., Ketcham, R.A., Gomez, D., Parra, M., Namson, J., Stockli, D., Almendral, A., Robles, W., Ghorbal, B., 2015a. Kinematic restoration of contractional basement structures using thermokinematic models: a key tool for petroleum system modeling. AAPG (Am. Assoc. Pet. Geol.) Bull. 99, 1575–1598.
Mora, A., Parra, M., Forero, G., Blanco, V., Moreno, N., Caballero, V., Stockli, D., Duddy, I., Ghorbal, B., 2015b. What drives orogenic asymmetry in the Northern Andes?: a case study from the apex of the Northern Andean Orocline. In: Bartoline, C., Mann, P. (Eds.), Petroleum Geology and Potential of the Colombian Caribbean Margin, vol. 108. AAPG Memoir, pp. 547–586.
Mora, A., Tesón, E., Martínez, J., Parra, M., Lasso, Á., Horton, B.K., Ketcham, R.A., Velásquez, A., Arias–Martínez, J.P., 2020. The eastern foothills of Colombia. In: Gómez, J., Mateus–Zabala, D. (Eds.), The Geology of Colombia, Volume 3 Paleogene – Neogene, Servicio Geológico Colombiano, vol. 37. Publicaciones Geológicas Especiales, pp. 123–142.
Mora-Páez, H., Kellogg, J.N., Freymueller, J.T., Mencin, D., Fernandes, R.M.S., Diederix, H., LaFemina, P., Cardona-Piedrahita, L., Lizarazo, S., Peláez-Gaviria, J.-R., Díaz-Mila, F., Bohórquez-Orozco, O., Giraldo-Londoño, L., Corchuelo- Cuervo, Y., 2019. Crustal deformation in the northern Andes – A new GPS velocity field. J. South Am. Earth Sci. 89, 76–91.
Moreno-Sánchez, M., Pardo-Trujillo, A., 2002. Western Colombia geological history. Geo-Eco-Trop. 26, 91–113.
Moreno-Sánchez, M., Pardo-Trujillo, A., 2003. Stratigraphical and sedimentological constraints on Western Colombia: implications on the evolution of the Caribbean Plate. In: Bartolini, C., Buffler, R.T., Blickwede, J.F. (Eds.), The Circum-Gulf of Mexico and the Caribbean: Hydrocarbon Habitats, Basin Formation and Plate Tectonics, vol. 79. AAPG Memoir, pp. 891–924.
Mulder, T., Alexander, J., 2001. The physical character of subaqueous sedimentary density flows and their deposits. Sedimentology 48, 269–299.
Mulder, T., Syvitski, J.P.M., Migeon, Faugeres, S.J.C., Savoye, B., 2003. Marine hyperpycnal flows: initiation, behavior and related deposits. A review. Mar. Petrol. Geol. 20, 861–882.
Myrow, P.M., Southard, J.B., 1996. Tempestite deposition. J. Sediment. Res. 66, 875–887.
Nemec, W., Postma, G., 1993. Quaternary Alluvial Fans in Southwestern Crete: Sedimentation Processes and Geomorphic Evolution, vol. 17. IAS Special Publication, pp. 235–276.
Nemec, W., Steel, R.J., 1984. Alluvial and coastal conglomerates: their significant features and some comments of gravelly mass-flow deposits. In: Koster, E.H., Steel, R.J. (Eds.), Sedimentology of Gravels and Conglomerates, vol. 10. Canadian Society of Petroleum Geologists, pp. 1–31.
Nemec, W., Steel, R.J., 1988. Fan Deltas: Sedimentology and Tectonic Settings. Blackie & Son, London, p. 444.
Nichols, G., 2009. Sedimentology and Stratigraphy. Wiley-Blackwell, United Kingdom, p. 419.
Nittrouer, C.A., Wright, L.D., 1994. Transport of particles across continental shelves. Rev. Geophys. 32 (1), 85–113.
Oboh-Ikuenobe, F.E., Holbrook, J.M., Scott, R.W., Akins, S.L., Evetts, M.J., Benson, D.G., Pratt, L.M., 2008. Anatomy of epicontinetal flooding: late Albian-early Cenomanian of the southern U.S. Western interior Basin. In: Pratt, B.R., Holmden, C. (Eds.), Dynamics of Epeiric Seas. Geological Association of Canada, pp. 2021–2207. Special Paper 48.
Orton, G.J., Reading, H., 1993. Variability of deltaic processes in terms of sediment supply, with particular emphasis on grain size. Sedimentology 40, 475–512.
Osorio-Afanador, D., Velandia, F., 2021. Late Jurassic syn-extensional sedimentary deposition and Cenozoic basin inversion as recorded in the Girón Formation, northern Andes of Colombia. Andean Geol. 48 (2), 237–266.
Paez-Reyes, M., Carvajal-Ortiz, H., Sahoo, S.K., Varol, O., Miller, B.V., Hughes, G.W., Gaona-Narvaez, T., Patarroyo, G.D., Curtis, J.H., Lerma, I., Copeland, P., 2021. Assessing the contribution of the La Luna Sea to the global sink of organic carbon during the Cenomanian-Turonian Oceanic Anoxic Event 2 (OAE2). Global Planet. Change 199, 103424.
Pardo-Trujillo, A., Cardona, A., Giraldo, A.S., León, S., Vallejo, D.F., Trejos-Tamayo, R., Plata, A., Ceballos, J., Echeverri, S., Barbosa-Espitia, A., Slattery, J., Salazar-Rios, A., Botello, G.E., Celis, S.A., Osorio-Granada, E., Giraldo-Villegas, C.A., 2020. Sedimentary record of the Cretaceous-Paleocene arc-continent collision in the northwestern Colombian Andes: insights from stratigraphic and provenance constraints. Sediment. Geol. 401, 105627.
Parra, M., Mora, A., Jaramillo, C., Torres, V., Zeilinger, G., Strecker, M., 2010. Tectonic controls on Cenozoic foreland basin development in the north-eastern Andes, Colombia. Basin Res. 22, 874–903.
Pastor-Chacón, A., Aguilera, R., Triana, J.L., Paez-Reyes, M., Cantisano, M., Bravo, L., Gamba, N., Niño, M., Delgado, A., Mendoza, G., Rodriguez, J.D., Romero-Bellén, O., Ruiz, M.C., Buitrago, H., Fuenzalida, H., 2023. Sweet spot areas for shale oil and shale gas plays in the Upper Cretaceous rocks of the Middle Magdalena Valley, Colombia: insights from basin modeling. Front. Earth Sci. 11, 1146126.
Patarroyo, P., Bengtson, P., Guerrero, J., 2010. *Sphenodiscus pleurisepta* (conrad, 1857) from the Maastrichtian La Tabla Formation in the Upper Magdalena Valley, Tolima, Colombia. J. S. Am. Earth Sci. 30 (2), 104–110.
Patarroyo, G.D., Torres, G.A., Rincón, D.A., Cárdenas, C.P., Márquez, R.E., 2017. Bioestratigrafía e inferencias paleoambientales de las asociaciones de foraminíferos en las Formaciones Cretácicas La Luna-Colón (Cuenca del Catatumbo, Colombia). Bol. Geol. 39 (3), 25–40.
Patarroyo, G.D., Alarcón, C.M., Torres, J.M., Díaz, J.S., Gómez, J.S., Márquez, J.J., Pontón, L.A., Barragán, D.M., 2021. Reconocimiento geológico de la Formación La Luna en el sector de Matanza (Oeste del Macizo de Santander, Colombia). Bol. Geol. 43 (1), 35–51.
Patarroyo, G.D., Kochhann, K., Ceolin, D., Guerra, R.M., Alegret, L., Bom, M., 2022. Paleoenvironmental changes recorded at a late Maastrichtian marine succession of northern South America. J. S. Am. Earth Sci. 119, 104015.

Patarroyo, G.D., Kochhann, K., Guerra, R.M., Alegret, L., Ceolin, D., Torres, J.M., 2023. Maastrichtian microfossils of the shallow marine Umir Formation, northeastern Colombia. Ameghiniana 60, 297–311.
Pérez, G., Salazar, A., 1978. Estratigrafía y facies del Grupo Guadalupe. Geol. Colomb. 10, 6–85.
Perillo, M.M., Best, J.L., García, M.H., 2014. A new phase diagram for combined-flow bedforms. J. Sediment. Res. 84, 301–313.
Petters, V., 1955. Development of Upper Cretaceous foraminiferal faunas in Colombia. J. Paleontol. 29 (2), 212–225.
Pindell, J.L., Kennan, L., 2009. Tectonic evolution of the Gulf of Mexico, Caribbean and northern South America in the mantle reference frame: an update. In: James, K.H., Lorente, M.A., Pindell, J.L. (Eds.), The Origin and Evolution of the Caribbean Plate, vol. 328. Geological Society, London, Special Publications, pp. 1–55.
Ponce, J.J., Carmona, N., Jait, D., Cevallos, M., Rojas, C., 2022. Sedimentological and ichnological characterization of delta front mouth bars in a river-dominated delta (Upper Cretaceous) from the La Anita Formation, Austral Basin, Argentina. Sedimentology 71 (1), 27–53.
Potter, P.E., Maynar, J., Depetris, P., 2005. Mud and Mudstones: Introduction and Overview. Springer, Berlin, p. 305.
Poyatos-Moré, M., Jones, G.D., Brunt, R.L., Hodgson, D.M., Wild, R.J., Flint, S.S., 2016. Mud-dominated basin-margin progradation: processes and implications. J. Sediment. Res. 86 (8), 863–878.
Pratt, B.P., Holmden, C., 2008. Epeiric Seas: introduction. Geological Association of Canada. Special Papers 48, 1–5.
Reading, H.G., 1996. Sedimentary Environments: Processes, Facies and Stratigraphy. Blackwell Publishing Company, Malden, USA, p. 704.
Rebesco, M., Hernández-Molina, F.J., Van Rooij, D., Wåhlin, A., 2014. Contourites and associated sediments controlled by deep-water circulation processes: state-of-the-art and future considerations. Mar. Geol. 352, 111–154.
Reineck, H.E., Singh, I.B., 1973. Depositional Sedimentary Environments. Springer-Verlag, Heidelberg, p. 439.
Restrepo, J.J., Toussaint, J.F., 2020. Tectonostratigraphic terranes in Colombia: an update. First part: continental terranes. In: Gómez, J., Mateus–Zabala, D. (Eds.), The Geology of Colombia, Volume 1 Proterozoic – Paleozoic, Servicio Geológico Colombiano, Publicaciones Geológicas Especiales, vol. 35, pp. 37–63.
Reyes, M., Kley, J., Mora, A., Dunkl, I., Carvajal-Torres, J., 2024. Age and tectonic setting of Mesozoic extension constrained by the first volcanic events in the Eastern Cordillera and Middle Magdalena Valley, Colombia. Int. J. Earth Sci. 113 (4), 1–27.
Rincón, G., Garzón, J.C., De Moraes, J.J., 2003. Campo Guando, primer descubrimiento de la antesala del Siglo XXI en el Valle Superior del Magdalena, Colombia. In: Abstract Book VIII Simposio Bolivariano - Exploración Petrolera en las Cuencas Subandinas, Colombia, Asociación Colombiana de Geólogos y Geofísicos del Petróleo, pp. 111–122.
Rodríguez, E., Ulloa, C., 1994. Memoria explicativa del mapa geológico de la Plancha 189 -La Palma, escala 1:100000. Internal report. Ingeominas.
Roncancio, J., Martínez, M., 2011. Upper Magdalena Valley Basin. In: Cediel, F., Colmenares, F. (Eds.), Petroleum Geology of Colombia Geology and Hydrocarbon Potential. Fondo Editorial Universidad EAFIT, p. 183.
Rovere, M., Pellegrini, C., Chiggiato, J., Campiani, E., Trincardi, F., 2019. Impact of dense bottom water on a continental shelf: an example from the SW Adriatic margin. Mar. Geol. 408, 123–143.
Salles, T., Husson, L., Lorcery, M., Boggiani, B.H., 2022. Paleo-physiography Maps 0 Ma to 127 Ma. HydroShare. http://www.hydroshare.org/resource/bbf65a3ba448456b8a7f2e2bb5e59733.
Sarmiento, G., 1992. Estratigrafía y medios de depósito de la Formación Guaduas. Bol. Geol. 32 (1–3), 3–44.
Sarmiento, G., Guerrero, J., 2000. Palinología del Santoniano Tardío al Maastrichtiano del Piedemonte L1anero Colombia. Correlación con el paleocinturon tropical. Geol. Colomb. 25, 111–147.
Sarmiento, G., Puentes, J., Sierra, C., 2015. Evolución geológica y estratigrafía del sector norte del Valle Medio del Magdalena. Geol. Norandina 12, 51–82.
Sarmiento-Rojas, L.F., 2001. Mesozoic Rifting and Cenozoic Basin Inversion History of the Eastern Cordillera, Colombian Andes. Inferences from Tectonic Models (PhD Thesis), p. 320. Vrije Universiteit Amsterdam.
Sarmiento-Rojas, L.F., 2011. Middle Magdalena Valley Basin. In: Cediel, F., Colmenares, F. (Eds.), Petroleum Geology of Colombia Geology and Hydrocarbon Potential. Fondo Editorial Universidad EAFIT, p. 193.
Sarmiento-Rojas, L.F., 2019. Cretaceous stratigraphy and PaleoFacies maps of northwestern south America. In: Cediel, F., Shaw, R.P. (Eds.), Geology and Tectonics of Northwestern South America. The Pacific-Caribbean-Andean Junction. Frontiers in Earth Sciences. Springer, pp. 673–747.
Sarmiento-Rojas, L.F., Van Wess, J.D., Cloetingh, S., 2006. Mesozoic transtensional basin history of the Eastern Cordillera, Colombian Andes: inferences from tectonic models. J. S. Am. Earth Sci. 21, 383–411.
Savrda, C.E., Bottjer, D.J., 1991. Oxygen-related biofacies in marine strata: an overview and update. In: Tyson, R.V., Pearson, T.H. (Eds.), Modern and Ancient Continental Shelf Anoxia, vol. 58. Geological Society of London, Special Publications, pp. 201–219.
Scherer, C.M.S., Goldberg, K., Bardola, T., 2015. Facies architecture and sequence stratigraphy of an early post-rift fluvial succession, Aptian Barbalha Formation, Araripe Basin, northeastern Brazil. Sediment. Geol. 322, 43–62.
Schieber, J., 2016. Mud re-distribution in epicontinental basins – exploring likely processes. Mar. Petrol. Geol. 71, 119–133.
Schieber, J., Southard, J., Thaisen, K., 2007. Accretion of mudstone beds from migrating floccule ripples. Science 318, 1760–1763.
Schwarz, E., Veiga, G.D., Álvarez Trentini, G., Isla, M.F., Spalletti, L.A., 2017. Expanding the spectrum of shallow-marine, mixed carbonate–siliciclastic systems: processes, facies distribution and depositional controls of a siliciclastic-dominated example. Sedimentology 65, 1558–1589.
Schwarz, E., Remírez, M., Lazo, D.G., Veiga, G.D., Isla, M.F., Echevarria, C., Toscano, A. G., Garberoglio, R.M., 2022. A review on depositional systems, bioevents and paleogeography of the Valanginian-Hauterivian Neuquén Sea: refining sedimentary and biological signals linked to the dynamics of epeiric seas. Earth Sci. Rev. 234, 104224.
Scotese, C.R., Vérard, C., Burgener, L., Elling, R.P., Kocsis, A.T., 2024. The Cretaceous World: Plate Tectonics, Palaeogeography, and Paleoclimate. Geological Society of London, Special Publications 544, 1–289.
Seilacher, A., 1969. Fault-graded beds interpreted as seismites. Sedimentology 13, 155–159.
Siggerud, E.I.H., Steel, R.J., 1999. Architecture and trace-fossil characteristics of a 10,000-20,000 year, fluvial-to-marine sequence, SE Ebro Basin, Spain. J. Sediment. Res. 69, 365–383.
Siravo, G., Faccena, C., Gérault, M., Becker, T., Giuditta, F., Herman, F., Molin, P., 2019. Slab flattening and the rise of the Eastern Cordillera, Colombia. Earth Planet Sci. Lett. 512, 100–110.
Sohn, Y.K., Rhee, C.W., Kim, B.C., 1999. Debris flow and hyperconcentrated flood-flow deposits in an alluvial fan, northwestern part of the Cretaceous Yongdong Basin, Central Korea. J. Geol. 107, 111–132.
Spalletti, L.A., Poiré, D.G., Pirrie, D., Matheos, S.D., Doyle, P., 2001. Respuesta sedimentológica a cambios en el nivel de base en una secuencia mixta clástica-carbonática del Cretácico de la Cuenca Neuquina, Argentina. Rev. Soc. Geol. Espana 14 (1–2), 57–74.
Spikings, R., Cochrane, R., Villagómez, D., Van der Lelij, R., Vallejo, C., Winkler, W., Beate, B., 2015. The geological history of northwestern South America: from Pangaea to the early collision of the Caribbean Large Igneous Province (290-75Ma). Gondwana Res. 27, 95–139.
Steel, R.J., Plink-Bjorklund, P., Aschoff, J., 2012. Tidal deposits of the Campanian Western Interior Seaway, Wyoming, Utah and Colorado, USA. In: Davis, R.A., Dalrymple, R.W. (Eds.), Principles of Tidal Sedimentology, pp. 437–472.
Stow, D.A.V., 1985. Fine-grained sediments in deep water: an overview of processes and facies models. Geo Mar. Lett. 5, 17–23.
Stow, D.A., Smillie, Z., 2020. Distinguishing between deep-water sediment facies: turbidites, contourites and hemipelagites. Geosciences 10, 1–43.
Stow, D.A.V., Tabrez, A., 1998. Hemipelagites: processes, facies and model. In: Stoker, M. S., Evans, D., Cramp, A. (Eds.), Geological Processes on Continental Margin: Sedimentation Mass-Wasting and Stability, vol. 129. Geological Society of London, Special Publications, pp. 317–337.
Sumner, E.J., Amy, L.A., Talling, P.J., 2008. Deposit structure and processes of sand deposition from decelerating sediment suspensions. J. Sediment. Res. 78 (8), 529–547.
Talling, P.J., Baker, M.L., Pope, E.L., Ruffell, S.C., Silva Jacinto, R., Heijnen, M.S., Hage, S., Simmons, S.M., Hasenhündl, M., Heerema, C.J., McGhee, C., Apprioual, R., Ferrant, A., Cartigny, M.J.B., Parsons, D.R., Clare, M.A., Tshimanga, R.M., Trigg, M. A., Cula, C.A., Faria, C.A., Gaillot, A., Bola, G., Wallance, D., Griffiths, A., Nunny, R., Urlaub, M., Peirce, C., Burnett, R., Neasham, J., Hilton, R.J., 2022. Longest sediment flows yet measured show how major rivers connect efficiently to deep sea. Nat. Commun. 13, 4193.
Taylor, A.M., Goldring, R., 1993. Description and analysis of bioturbation and ichnofabric. Journal of the Geological Society of London 150, 141–148.
Tchegliakova, N., 1993. Los foraminíferos y los minerales antigénicos de la Formación Umir (sección Quebrada La Julia, Valle Medio del Magdalena): registro de laguna costera a finales del Cretácico Superior cuspidal (Maastrichtiano). Geol. Colomb. 18, 107–117.
Tchegliakova, N., 1995. Los Foraminíferos de la Formación Umir (Sección Quebrada La Julia): registro del Cretáceo Superior Cuspidal (Maastrichtiano) en el Valle Medio del Magdalena, Colombia. Geol. Colomb. 19, 109–130.
Tchegliakova, N., 1996. Registro de las biozonas de foraminíferos planctónicos *Gansserina gansseri* y *Abathomphalus mayaroensis* (Maastrichtiano medio y superior) en el extremo meridional del Valle Medio del Magdalena (Colombia, Suramérica). Geol. Colomb. 20, 67–90.
Tchegliakova, N., Mojica, J., 2001. El Senoniano de la barrera de Girardot-Guataquí, Valle Alto del Magdalena, Colombia: precisiones sobre la estratigrafía y establecimiento de una zonación micropaleontológica. Rev. Acad. Colomb. Ciencias Exactas, Fis. Nat. 25 (4), 37–75.
Tchegliakova, N., Sarmiento, G., Guerrero, J., 1997. Bioestratigrafía y Paleoecología de los Foraminíferos Bentónicos de la Formación Chipaque y el Grupo Guadalupe. Turoniano-Maastrichtiano del Piedemonte Llanero de los Andes Colombianos. Geol. Colomb. 22, 103–119.
Terraza, R., 2003. Origen diagenético de cherts y porcelanitas en las Formaciones Lidita Inferior y Lidita Superior (Grupo Olini), al sur de San Luis (Tolima), Valle Superior del Magdalena, Colombia. Geol. Colomb. 28, 79–94.
Terraza, R., 2019. "Formación La Luna": expresión espuria en la geología colombiana. In: Etayo-Serna, F. (Ed.), Estudios geológicos y paleontológicos sobre el Cretácico en la región del embalse del rio Sogamoso, Valle Medio del Magdalena, Compilación de los Estudios Geológicos Oficiales en Colombia, pp. 303–362.
Tesón, E., Mora, A., Silva, A., Namson, J., Teixell, A., Castellano, J., Casallas, W., Julivert, M., Taylor, M., Ibáñez-Mejía, M., Valencia, V.A., 2013. Relationship of Mesozoic graben development, stress, shortening magnitude, and structural style in the Eastern Cordillera of the Colombian Andes. In: Nemčok, M., Mora, A., Cosgrove, J.W. (Eds.), Thick-Skin-Dominated Orogens: from Initial Inversion to Full Accretion, vol. 377. Geological Society, London, Special Publications, pp. 257–283.

Toussaint, J.F., Restrepo, J.J., 2020. Tectonostratigraphic terranes in Colombia: an update. Second part: oceanic terranes. In: Gómez, J., Pinilla–Pachon, A.O. (Eds.), The Geology of Colombia, Volume 2 Mesozoic. Servicio Geológico Colombiano, vol. 36. Publicaciones Geológicas Especiales, pp. 237–260.
Tyson, R.V., Pearson, T.H., 1991. Modern and ancient continental shelf anoxia: an overview. In: Tyson, R.V., Pearson, T.H. (Eds.), Modern and Ancient Continental Shelf Anoxia, vol. 58. Geological Society of London, Special Publications, pp. 1–24.
UCaldas-ANH, 2021. Estudio geológico en la parte sur de la cuenca Valle Medio del Magdalena con el fin de actualizar el modelo de evolución geológica, definir los sistemas petrolíferos y evaluar la prospectividad del crudo y gas-Fase 2. Internal Report.
Valencia-Gómez, J.C., Cardona, A., Bayona, G., Valencia, V., Zapata, S., 2020. Análisis de procedencia del registro sin-orogénico Maastrichtiano de la Formación Cimarrona, flanco occidental de la Cordillera Oriental colombiana. Bol. Geol. 42 (3), 171–204.
Vallejo, C., Romero, C., Horton, B., Spikings, R., Gaibor, J., Winkler, W., Esteban, J.L., Thomsen, T.B., Mariño, E., 2021. Jurassic to early Paleogene sedimentation in the Amazon region of Ecuador: implications for the paleogeographic evolution of northwestern South America. Global Planet. Change 204, 103555.
van Yperen, A.E., Poyatos-Moré, M., Holbrook, J.M., Midtkandal, I., 2020. Internal mouth-bar variability and preservation of subordinate coastal processes in low-accommodation proximal deltaic settings (Cretaceous Dakota Group, New Mexico, USA). Depositional Record 6, 431–458.
Varejão, F.G., Warren, L.V., Simões, M.G., Buatois, L.A., Mángano, M.G., Bahniuk Rumbelsperger, A.M., Assine, M.L., 2021. Mixed siliciclastic–carbonate sedimentation in an evolving epicontinental sea: Aptian record of marginal marine settings in the interior basins of north-eastern Brazil. Sedimentology 68, 2125–2164.
Veloza, G.E., Mora, A., De Freitas, M., Mantilla, M., 2008. Dislocación de facies en el tope de la secuencia Cretácica de la subcuenca de Neiva, Valle Superior del Magadalena, y sus implicaciones en el modelo estratigráfico secuencial colombiano. Bol. Geol. 30 (1), 29–44.
Vergara, L.S., 1997. Stratigraphy, foraminiferal assemblages and paleoenvironments in the Late Cretaceous of the Upper Magdalena Valley, Colombia (Part I). J. S. Am. Earth Sci. 10 (2), 111–132.
Vergara, L.E., Rodriguez, G., 1997. The Upper Cretaceous and lower Paleocene of the eastern Bogotá plateau and Llanos thrustbelt, Colombia: alternative appraisal to the nomenclature and sequence stratigraphy. Geol. Colomb. 22, 51–79.
Viana, A.R., Rebesco, M., 2007. Economic and Paleoceanographic Significance of Contourite Deposits, vol. 276. Geological Society of London, Special Publications, p. 356.
Viana, A.R., Faugères, J.C., Stow, D.A.V., 1998. Bottom-current-controlled sand deposits—a review of modern shallow- to deep-water environments. Sediment. Geol. 115, 53–80.
Villagómez, D., Spikings, R., 2013. Thermochronology and tectonics of the Central and Western Cordilleras of Colombia: Early cretaceous–Tertiary evolution of the northern Andes. Lithos 160–161, 228–249.
Villamil, T., 1998. Chronology, relative sea-level history and a new sequence stratigraphic model for basinal Cretaceous of Colombia. In: Pindell, J., Drake, C. (Eds.), Eustacy and Tectonostratigraphic Evolution of Northern South America, vol. 58. Society for Sedimentary Geology (SEPM), Special Publication, pp. 161–216.
Villamil, T., Pindell, J., 1998. Mesozoic paleogeographic evolution of northern South America. In: Pindell, J., Drake, C. (Eds.), Paleogeographic Evolution and Non-glacial Eustacy, Northern South America, vol. 58. Society for Sedimentary Geology (SEPM), Special Publications, pp. 283–318.
Villamil, T., Arango, C., Hay, W.W., 1999. Plate tectonic paleoceanographic hypothesis for Cretaceous source rocks and cherts of northern South America. Geological Society of America, Special Papers 332, 191–202.
Vinasco, C., 2019. The Romeral shear zone. In: Cediel, F., Shaw, R.P. (Eds.), Geology and Tectonics of Northwestern South America. The Pacific-Caribbean-Andean Junction. Frontiers in Earth Sciences. Springer, pp. 833–876.
Walker, R., Plint, G., 1992. Wave- and storm-dominated shallow marine systems. In: Walker, R., James, N. (Eds.), Facies Models Response to Sea Level Change. Geological association of Canada, pp. 219–238.
Walsh, J.P., Nittrouer, C.A., 2009. Understanding fine-grained river-sediment dispersal on continental margins. Mar. Geol. 263, 34–45.
Warren, E.A., Pulham, A.J., 2001. Anomalous porosity and permeability preservation in deeply buried tertiary and Mesozoic sandstones in the Cusiana field, Llanos foothills, Colombia. J. Sediment. Res. 71, 2–14.
Weimer, R.J., Howard, J.D., Lindsay, D.R., 1982. Tidal flats. In: Scholle, P.A., Spearing, D. (Eds.), Sandstone Depositional Environments, American Association of Petroleum Geologist, vol. 31, pp. 191–245.
Wilson, R.D., Schieber, J., 2014. Muddy prodeltaic hyperpycnites in the Lower Genesee Group of central New York, USA: implications for mud transport in epicontinental seas. J. Sediment. Res. 84, 866–874.
Wright, L.D., Friedrichs, C.T., 2006. Gravity-driven sediment transport on continental shelves: a status report. Cont. Shelf Res. 26 (17–18), 2092–2107.
Wright, L.D., Nittrouer, C.A., 1995. Dispersal of river sediments in coastal seas—six contrasting cases. Estuarines 18 (3), 494–508.
Xu, G., Bi, S., Gugliotta, M., Liu, J., Liu, J.P., 2023. Dispersal mechanism of fine-grained sediment in the modern mud belt of the East China Sea. Earth Sci. Rev. 240, 104388.
Yawar, Z., Schieber, J., 2017. On the origin of silt laminae in laminated shales. Sediment. Geol. 360, 22–34.
Yeste, L.M., Henares, S., McDougall, N., García-García, F., Viseras, C., 2019. Towards the multi-scale characterization of braided fluvial geobodies from outcrop, core, ground-penetrating radar and well log data. Geological Society of London, Special Publications 488 (1), 73–95.
Yeste, L.M., Varela, A., Viseras, C., Mcdougall, N., García-García, F., 2020. Reservoir architecture and heterogeneity distribution in floodplain sandstones: key features in outcrop, core and wireline logs. Sedimentology 67, 3355–3388.
Yu, X., Stow, D., Smillie, Z., Esentia, I., Brackenridge, R., Xie, X., Bankole, S., Ducassou, E., Llave, E., 2020. Contourite porosity, grain size and reservoir characteristics. Mar. Petrol. Geol. 117, 104392.
Zapata, S., Cardona, A., Jaramillo, J.S., Patiño, A., Valencia, V., León, S., Mejía, D., Pardo-Trujillo, A., Castañeda, J.P., 2019. Cretaceous extensional and compressional tectonics in the Northwestern Andes, prior to the collision with the Caribbean oceanic plateau. Gondwana Res. 66, 207–226.
Zapata, S., Cardona, A., Jaramillo-Ríos, J.S., Siachoque, A., Peverelli, V., Chew, D., Wemmer, K., Rodríguez, M.C., Valencia-Gomez, J.C., Sobel, E.R., Calderon-Diaz, L. C., Valencia, V.A., Patiño, A.M., Parra, M., Botello, G.E., Glodny, J., 2024. Repeated structural reworking in the basement of the Central Colombian Andes unraveled by a multi-chronometric approach. Tectonics 43, e2024TC008340.
Zapata, S., Zapata-Henao, M., Cardona, A., Jaramillo, C., Silvestro, D., Oboh-Ikuenobe, F., 2021. Long-term topographic growth and decay constrained by 3D thermo-kinematic modeling: Tectonic evolution of the Antioquia Altiplano, Northern Andes. Glob. Planet. Change 203, 103553.
Zapata-Villada, J.P., Cardona, A., Serna, S., Rodríguez, G., 2021. Late Cretaceous to Paleocene magmatic record of the transition between collision and subduction in the Western and Central Cordillera of northern Colombia. J. S. Am. Earth Sci. 112, 103557.
Zavala, C., Pan, S., 2018. Hyperpycnal flows and hyperpycnites: origin and distinctive characteristics. Lithologic Reservoirs 30 (1), 1–27.
Zavala, C., Arcuri, M., Blanco-Valiente, L., 2012. The importance of plant remains as diagnostic criteria for the recognition of ancient hyperpycnites. Revue de Paléobiologie, Genève 11, 457–469.
Zviely, D., Kit, E., Klein, M., 2007. Longshore sand transport estimates along the Mediterranean coast of Israel in the Holocene. Mar. Geol. 238, 61–73.